INFORMATION TO USERS

This manuscript has been reproduced from the microfilm master. UMI films the text directly from the original or copy submitted. Thus, some thesis and dissertation copies are in typewriter face, while others may be from any type of computer printer.

The quality of this reproduction is dependent upon the quality of the copy submitted. Broken or indistinct print, colored or poor quality illustrations and photographs, print bleedthrough, substandard margins, and improper alignment can adversely affect reproduction.

In the unlikely event that the author did not send UMI a complete manuscript and there are missing pages, these will be noted. Also, if unauthorized copyright material had to be removed, a note will indicate the deletion.

Oversize materials (e.g., maps, drawings, charts) are reproduced by sectioning the original, beginning at the upper left-hand corner and continuing from left to right in equal sections with small overlaps. Each original is also photographed in one exposure and is included in reduced form at the back of the book.

Photographs included in the original manuscript have been reproduced xerographically in this copy. Higher quality 6" x 9" black and white photographic prints are available for any photographs or illustrations appearing in this copy for an additional charge. Contact UMI directly to order.

UMI®

A REAL TIME SELF-TUNING ALGORITHM FOR PI CONTROL

OF THE HEATING AND COOLING COILS IN BUILDINGS

A Dissertation

by

QIANGHUA ZHOU

Submitted to the Office of Graduate Studies of
Texas A&M University
in partial fulfillment of the requirements for the degree of

DOCTOR OF PHILOSOPHY

August 1999

Major Subject: Mechanical Engineering

UMI Number: 9943591

A REAL TIME SELF-TUNING ALGORITHM FOR PI CONTROL

OF THE HEATING AND COOLING COILS IN BUILDINGS
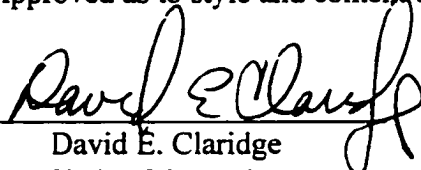
A Dissertation

by

QIANGHUA ZHOU

Submitted to Texas A&M University
in partial fulfillment of the requirements
for the degree of

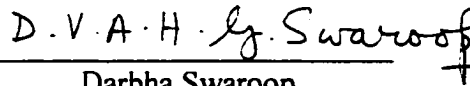DOCTOR OF PHILOSOPHY

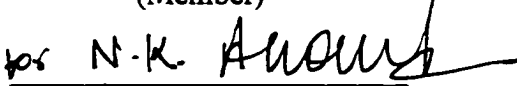Approved as to style and content by:

David E. Claridge
(Chair of Committee)

Larry O. Degelman
(Member)

Darbha Swaroop
(Member)

W. D. Turner
(Member)

for N-K. Anand
Suhada Jayasuriya
(Department Head)

August 1999

Major Subject: Mechanical Engineering

ABSTRACT

A Real Time Self-tuning Algorithm for PI Control of the Heating and Cooling Coils in

Buildings. (August 1999)

Qianghua Zhou, B.S., Hunan University; M.S., Tsinghua University

Chair of Advisory Committee: Dr. David E. Claridge

Proportional and Integral (PI) controllers are used widely in HVAC applications. It is necessary to choose suitable values for PI gains for PI control of the heating and cooling coils in buildings. Consequently, suitable indoor comfort can be maintained; the energy efficiency of the heating and cooling systems will be maximized; and the lifetime of heating and cooling valves will be prolonged.

A self-tuning algorithm is developed in this dissertation to find the good P and I gains. The proposed algorithm evaluates the controller performance by the integral square error (ISE) of the coil supply air temperature. The controller operation will be considered as not suitable when the ISE is too big. The P and I gains are required to change at this condition. The algorithm uses the 'iteration' concept to find better values for P and I gains. It first changes the P and I gains to certain values to decrease the ISE. The iteration then will stop if the ISE is small enough; otherwise the change of the P and I gains will continue until optimal values are found. Further, the new algorithm determines the iteration direction by observing the spectrum distribution of the ISE. P

and I gains will be increased if the low frequency content is the dominant part in the coil supply air temperature; P and I gains will be decreased if high frequency content is the dominant part.

The new algorithm can be realized on-line without interrupting the coil normal operation. It functions as a watchdog to be sure the PI controller maintains smooth and rapid tracking properties. The new algorithm only requires about forty lines of program code in the current Direct Digital Control (DDC) systems used for HVAC control. The basic concept of the algorithm will be developed by theoretically analyzing the dynamic behavior and frequency characteristics of the cooling and heating coils in buildings. The whole algorithm is then demonstrated by controlling a coil in a building, thus proving its feasibility.

ACKNOWLEDGMENTS

I would like to express my sincere gratitude and appreciation to Prof. David E. Claridge and Dr. Mingsheng Liu. I have benefited greatly, on numerous occasions, from their timely advice, continuous encouragement and generous support over the years. I also would like to thank the members of my advisory committee, Professor Larry O. Degelman, Professor Darbha Swaroop, and Professor Dan Turner for their helpful comments and constructive criticism. I thank Professor John Leggett for serving as the Graduate Council Representative on my doctoral committee. I thank Professor John Bryant for serving as the substitute of Professor Larry O. Degelman in my defense. Also, thanks to you, my friends and office-mates here for your kindly friendship and generous help.

I thank Professor Yi Jiang, who was my advisor for my Master of Science degree. He led me into the HVAC field six years ago. I especially thank for my wife Rong Zong for her love and encouragement. I would like to respectfully dedicate this dissertation to my beloved parents and sister, who looked after me for the past 28 years.

This research is sponsored by Texas A&M University. Special thanks are given to Mr. Mustafa Abbas, and Mr. Homer Bruner, who helped me to test the algorithm developed in this dissertation.

TABLE OF CONTENTS

TABLE OF CONTENTS (continued)

LIST OF FIGURES

LIST OF FIGURES (continued)

LIST OF FIGURES (continued)

LIST OF FIGURES (continued)

NOMENCLATURE

C is the control signal into the valve. It has units of % valve range.

E represents the difference between the coil air discharge temperature and its setpoint in the frequency domain. It has units of °F.

e is the difference between the coil air discharge temperature and its setpoint. It has units of °F.

el is the difference between the coil air discharge temperature and its setpoint in low frequency. It has units of °F.

ISE is the integral square error between the coil discharge air temperature and its setpoint. It has units of °F².sec.

ISE_L is the ISE in low frequency part. It has units of °F².sec.

ISE_T is the same as ISE. The subscript T is used to discern from the ISE_L.

J the cost function to evaluate the PI controller. It has units of °F².sec.

k_i is the integral gain. It has units of % valve range per °F per second.

k_p is the proportional gain. It has units of % valve range per °F.

k_s is the DC gain which is the ratio of the output of a system to its input. It is non-dimensional.

N is the total number of samples from the signal.

T is the time constant. It has units of seconds.

T_d is the sampling duration. It has units of seconds.

T_s is the sampling time. It has units of seconds.

NOMENCLATURE (continued)

t_{ao} is the coil output air temperature. It has units of °F.

$t_{ao,set}$ is the setpoint of output air temperature. It has units of °F.

w is the frequency. It has units of radians/second.

τ_d is the delay time. It has units of seconds.

ΔC is the change of the valve position. It has units of % valve range.

Δf is the discretion of the signal in frequency domain. It has units of sec^{-1}.

Δt_{ao} is the change of output air temperature. It has units of °F.

CHAPTER I

INTRODUCTION AND LITERATURE REVIEW

Heating and cooling coils are key components of an air conditioning system. Their operation is introduced principally in this chapter. Coils can be simplified to be a single input, single output, linear, and time-invariant system such as, a first order system with time delay, though they are inherently multiple input, multiple output, nonlinear, and time-variant systems. Consequently, PI controllers are applied to control the coil operation instead of predictive controllers. Then the PI tuning is introduced and current PI tuning methods are reviewed. There are two categories of tuning methods: the manual tuning and the auto tuning. Their concept and implementation are discussed in detail and disadvantages are pointed out.

THE HEATING AND COOLING COILS

In response to a control signal, a control valve adjusts the flow rate of chilled water, through a cooling coil to achieve a discharge air temperature close to the setpoint (Figure 1-1). A heating coil achieves a discharge air temperature near its setpoint through an analogous process. The output air temperature (t_{ao}) of the coils is effected by multiple factors, including the air flow rate (G), input air temperature (t_{ai}), input water temperature (t_{wi}), valve position (C), and the characteristics of the coil and valve. A

This dissertation follows the style and format of *ASHRAE Transactions*.

Control signal to the
valve

Control valve

Return chilled/hot
water

Supply chilled/hot
water

Cooling/heating
coil

Entering air

Discharge air
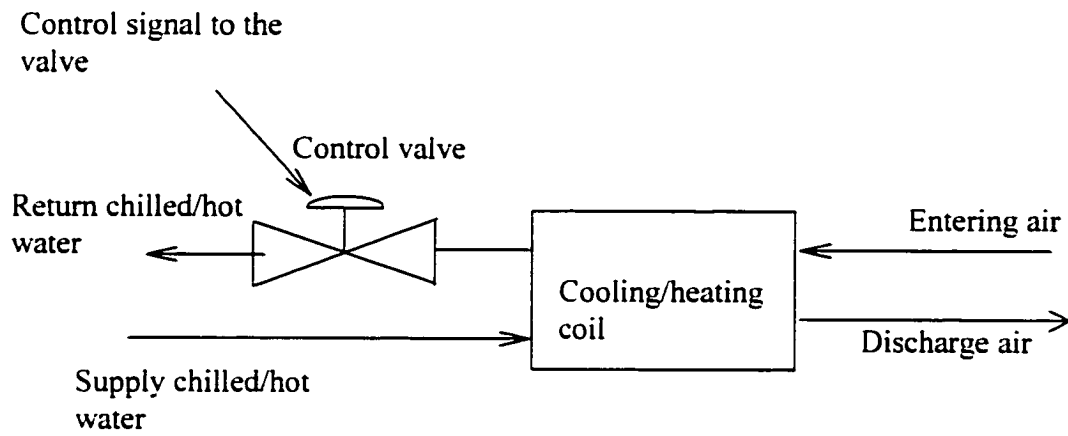
Figure 1-1 Schematic diagram of a cooling/heating coil.

precise model may be obtained based on extensive experiments for a specific coil. It will have the form,

$$f(t_{ao},t_{ai},t_{wi},G,C,t_{ao}{}^0 t_{ai}{}^0,t_{wi}{}^0,G^0,C^0,\tau) = 0 \qquad (1\text{-}1)$$

where,

f is a nonlinear function determined by characteristics of the coil and valve.

τ is time.

The superscript 0 represents the initial values of variables.

Such models are difficult to obtain and expensive to apply to HVAC systems in the field. First, the function f, is different for different coils. It is too expensive to obtain such a model for each coil experimentally. In addition, measurements of air flow rate (G), input air temperature (t_{ai}), and input water temperature (t_{wi}) are not available in most air conditioning systems.

Practically, the coil model can be simplified as shown in Equation 1-2:

$$g(t_{ao},C,t_{ao}{}^0,C^0,\tau) = 0 \qquad (1\text{-}2)$$

where g is typically determined as the solution of a linear differential equation.

Compared with Equation 1-1, the function g above is itself a function of G, t_{ai} and t_{wi}. However, the change of g will be relatively small if the change in system operation is very small. The coil is then assumed to be a single input, single output (SISO) and time-invariant system.

A typical coil exhibits a process reaction curve like that shown in Figure 1-2. The control valve position has undergone a step change, for example from 50% open to 60% open. (The curve shown corresponds to an input air temperature of 70°F, air flow rate of 2000 cfm and chilled water input temperature of 40°F.) First, the coil discharge air temperature remains at its initial value for a period of time, which is called the delay time, τ_d. Then the discharge air temperature begins to increase toward a new value. The speed of this temperature change can be evaluated by a time constant, T. The magnitude of the final temperature change can be evaluated by DC gain, k_s. (These parameters will be defined later.) Therefore, the dynamic model of a coil can be approximated as a first order system with delay. This provides a good approximation of higher order systems. This model has been applied widely in the HVAC field and gets very good results (Dexter and Jota 1985; Franklin et al. 1995; Zhang 1992; Marshall 1992; Ziegler and Nichols 1942a).

Mathematically, such a dynamic process can be approximated in the time domain by,
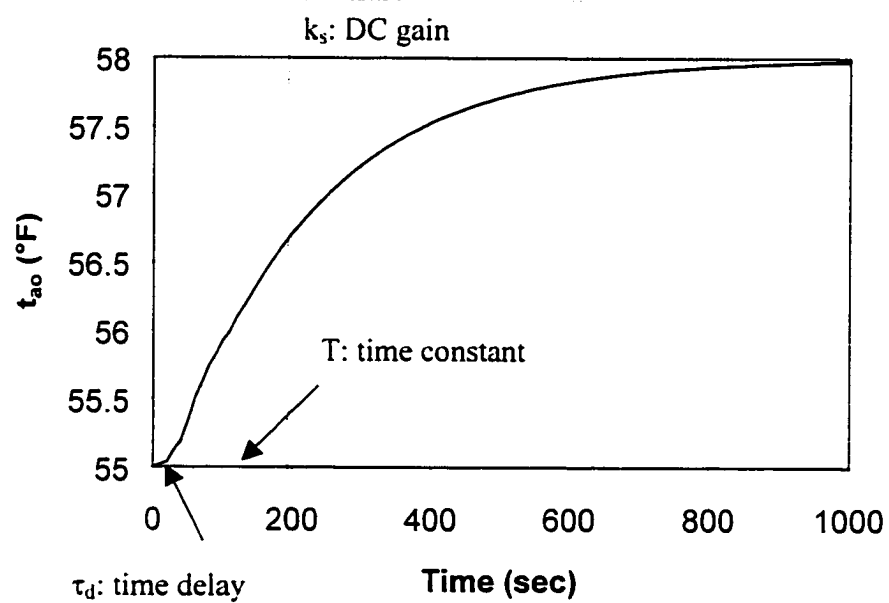
Figure 1-2 *The process reaction curve of the coil discharge air temperature after a step change of the valve position. This curve can be described by three parameters: time constant (T), time delay (τ_d) and DC gain (k_s).*

$$T \frac{d\Delta t_{ao}}{d\tau} + \Delta t_{ao} = k_s \Delta C(\tau - \tau_d) \tag{1-3}$$

And in the transform domain by,

$$\frac{\Delta t_{ao}}{\Delta C} = \frac{k_s e^{-\tau_d s}}{Ts + 1} \tag{1-4}$$

Δt_{ao} is the change of output air temperature in response to ΔC;

ΔC is the change in the valve position;

T is the time constant, which is the time it takes for the output air temperature to reach 63% of its final change in temperature. This response time is caused by multiple factors: water flow rate, water volume inside the coil, and the coil heat transfer coefficient. (This is discussed in detail in Appendix A.)

τ_d is the delay time, and is the time it takes the system before it responds the disturbance. There are two reasons for the existence of the delay time. One reason is the inherent higher order of the coil dynamics (Franklin et al. 1995). The discharge air temperature does not change immediately after the control signal to the valve has changed. The coil shell needs to be warmed up first before heat can be transferred from water to air. The discharge air temperature then begins to change. Although the change is initially slow, it gradually becomes faster and faster. Eventually, the change will

gradually become slower and slower, until the discharge air temperature reaches its final value (Figure 1-2). Mathematically, this process exhibits a dynamic behavior with higher order. A first order model with delay is an approximation of the higher order system, and the impact of the higher order dynamics is included in the time delay term. If the temperature sensor is not installed immediately behind the coil, it will then take some time for the temperature change in the coil to be transferred to the sensor. This time period will also add to the time delay (Bekker et al. 1992). Expressions for the time delay as a function of factors such as water flow rate, coil size etc. are not available at present. Time delay is evaluated by model identification, which may be carried out using the least square error method (Franklin et al. 1995; Dexter and Jota 1985).

k_s is the DC gain, which is the ratio of the output of a system to its input (presumed constant) after all transients have decayed. It depends on water flow rate, air flow rate, coil heat transfer coefficient, differential pressure across the water side of the coil, and the valve characteristic (Appendix A).

Equation 1-3 presents the coil model in the time domain, where τ is the variable. Equation 1-4 presents the coil model in a transform domain, where s is the transform variable.

Practically, the method demonstrated in Figure 1-2 is used to determine the time constant, the delay time, and the DC gain. A straight line is drawn tangential to the system reaction curve at its steepest point. This line intersects the initial and final output

temperatures of the system. The delay time is approximated as the time between the change in valve position and the first intersection. The time constant is approximated as the time between the two intersection points. The DC gain is the ratio of the difference between the final and initial coil discharge air temperatures to the change of the valve position. Thus, the delay time of the coil is 30 sec, the time constant of the coil is 200 sec and the DC gain of the coil is 3°F for 10% valve position change in the example.

The model in Equation 1-3 can be expressed for discrete times as:

$$\Delta t_{ao}(k+1) = a * \Delta t_{ao}(k) + b1 * \Delta C(k-n+1) + b2 * \Delta C(k-n) \tag{1-5}$$

where,

$\Delta t_{ao}(k)$ is the change of the measured coil discharge air temperature.

$\Delta C(k)$ is the change of the control signal into the valve.

n depends on the magnitude of sampling interval and time delay. It may be 1, 2, or 3 when the sampling interval is 10 second and time delay is lower than 30 second.

The three model alternatives, n =1, 2, and 3, correspond to different relations between the process time delay, τ_d, and the sampling interval, h:

$$n=1 \iff 0 < \tau_d < h \tag{1-6}$$

$$n=2 \iff h < \tau_d < 2h \qquad (1\text{-}7)$$

$$n=3 \iff 2h < \tau_d < 3h \qquad (1\text{-}8)$$

Comparing Equation 1-3 with Equation 1-5, the continuous time model parameters corresponding to the three discrete time models are

$$T = -h/\ln(a) \qquad (1\text{-}9)$$

$$\tau_d = h*(n\text{-}1) + T*\ln((b1 + b2/a)/(b1 + b2)) \qquad (1\text{-}10)$$

$$k_s = (b1 + b2)/(1\text{-}a) \qquad (1\text{-}11)$$

where n=1, 2, 3.

Applying the least square error method to Equation 1-5 can identify the DC gain, delay time, and time constant of a coil. This approach gives the same results, graphically obtained for the system of Figure 1-2: a DC gain of 3°F for 10% valve position change, a time constant of 200 sec, and a delay time of 30 sec.

These constants are different for different coils, or even for the same coil under different working conditions. Based on the experience of the continuous commissioning

group of the Energy Systems Laboratory, in more than 100 buildings, the following

ranges are typical for heating and cooling coils (shown also in Equations 1-12, -13 and -

14): time constants between 30 sec and 300 sec; delay times between 0 sec and 30 sec;

DC gains between 0°F and 20°F for a 10 % valve position change.

$$30 \text{ sec} < T < 300 \text{sec} \tag{1-12}$$

$$0 \text{ sec} < \tau_d < 30 \text{sec} \tag{1-13}$$

$$0 < K_s < 20°F \text{ for } 10\% \text{ valve position change} \tag{1-14}$$

THE PI CONTROL OF COILS

Optimal control of coils must be implemented to maintain suitable indoor

comfort and maximize the energy efficiency of heating and cooling systems.

Theoretically, the coil discharge air temperature can be controlled to track its

setpoint exactly and reject disturbances totally. This ideal controller can be realized in a

predictive controller form. First, a precise physical model (Equation 1-1) for the coil is

developed. Then, the coil discharge air temperature is calculated once the inputs to the

model, including the control signal into the control valve, the input water temperature,

the air flow rate, and the input air temperature, are obtained. Conversely, the required

control signal is calculated once the discharge air temperature setpoint, the input water

temperature, the air flow rate and the input air temperature are obtained. This control signal is sent to the coil valve. The exact output of the coil discharge air temperature is obtained (Shown in Figure 1-3).

This predictive controller cannot be realized in practice. First of all, it is too hard or too expensive to measure all the model inputs accurately. For example, it is not easy to accurately determine the change of the air flow rate due to the time delay of flow meters. Furthermore, there is no flow rate meter available in most cases, and in the rare cases where the sensors are available, it is common for flow rate sensors to have a bias of up to 50%. Second, the precise model of the coils is hard to develop, due to its inherent non-linearity and the variation of the model with coil operating parameters. The model may be obtained by means of extensive experimentation for a specific coil. However, this approach is too expensive for use in the HVAC field.

Currently, single input and single output (SISO) feedback controllers are often applied to control the coil discharge air temperature. They use the coil discharge air temperature as the feedback signal, then send the bias between discharge air temperature and its setpoint to the controller. The controller then calculates how much the valve position needs to be adjusted. Take a cooling coil as an example (shown in Figure 1-4); more cooling water will be required to cool the supply air if the coil setpoint is decreased. Reducing the setpoint creates a bias between the discharge air temperature and the setpoint. When the bias appears at the controller, the controller will signal the
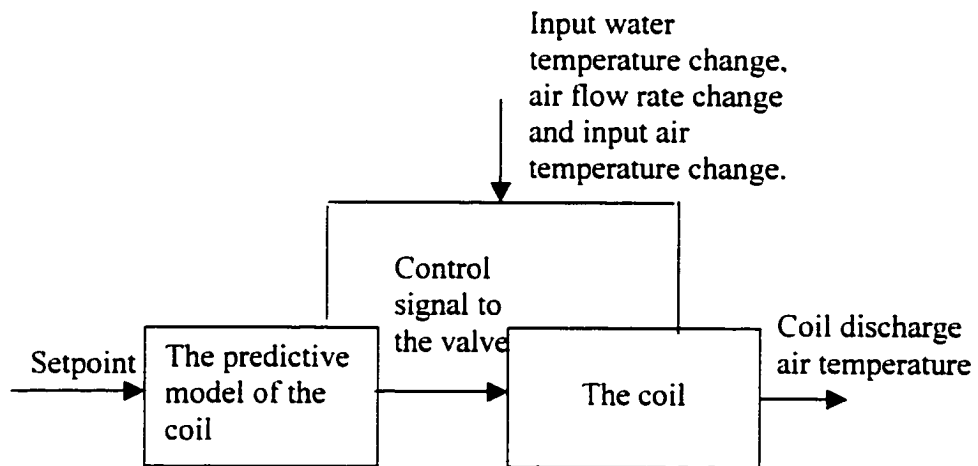
Figure 1-3 *The ideal predictive controller for coils.*
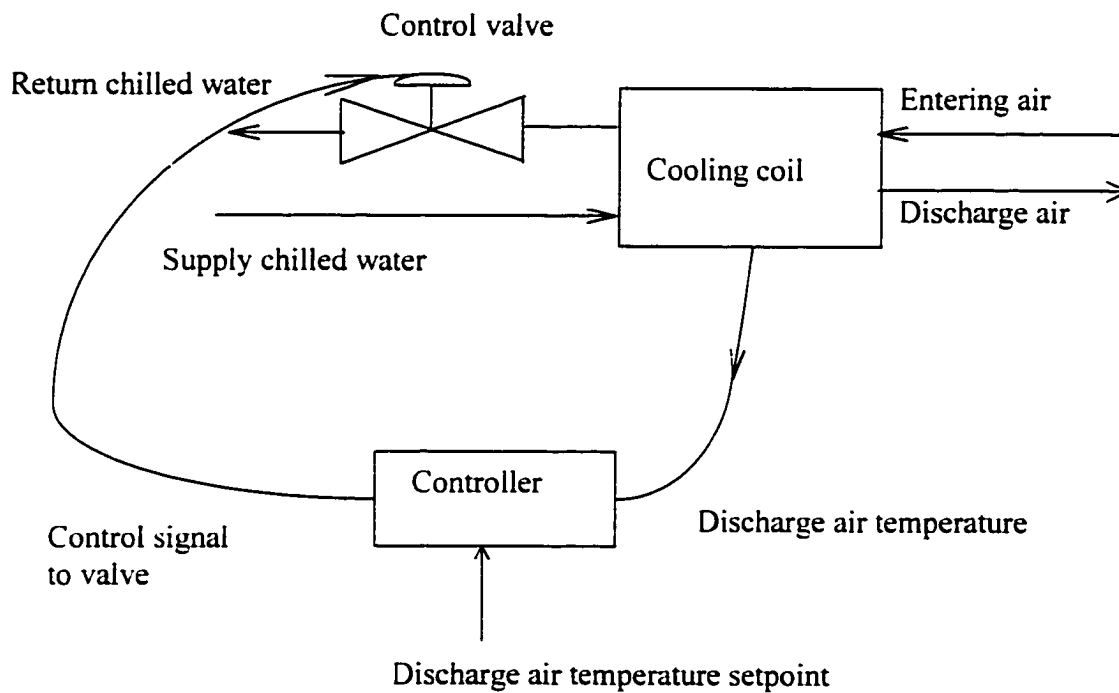
Figure 1-4 *Schematic diagram for the cooling coil with a feedback controller. The objective of the control system is to maintain the coil discharge air temperature at its setpoint.*

valve to open further. Then, more cooling water will flow through the coil and the air will be cooled to a lower temperature.

The concept of feedback has been applied in industry for a long time. The earliest example of feedback control was the control of liquid level for a wine vessel in the first century AD (Mayr 1970). In this feedback control process, as the liquid level falls, so does the float, allowing the flow into the tank to increase; as the level rises the flow is reduced and, if necessary, cut off (Figure 1-5). This is a type of proportional feedback control, which means the feedback control signal is made to be linearly proportional to the bias or error in the measured output. We can view the Proportional (P) controller as an amplifier with a "knob" to adjust the gain up or down. It can reduce error responses to disturbances and has an adjustable response speed. However, a system with proportional control may have a steady-state offset (or droop) in response to a constant reference input, and may not be entirely capable of rejecting a constant disturbance. Take the proportional controller in the cooling coil with a normally open valve as an example:

$$C = k_p \left(t_{ao} - t_{ao\_set} \right)$$
(1-15)

where

C is the control signal into the valve;

t_{ao} is the coil output air temperature;

t_{ao_set} is the setpoint of output air temperature; and
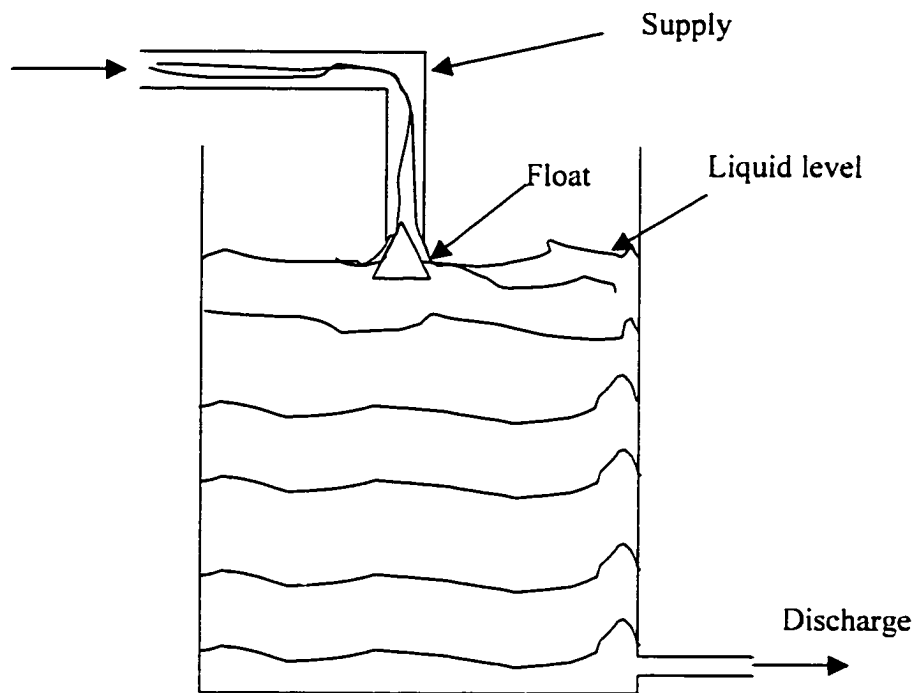
Figure 1-5 *Early historical feedback control of liquid level*

and flow.

k_p is the proportional gain;

When the discharge air temperature is higher than the setpoint, we can see from Equation 1-15 that the valve will open further when the bias between the discharge air temperature and its setpoint increases. More cooling water will flow through the coil, and the discharge air temperature will then be decreased. The response speed of the controller can be adjusted by changing the value of the proportional gain. However, there will always be a steady-state bias between the discharge air temperature and its setpoint. Equation 1-1 shows that the control signal will be zero when the bias goes to zero. Therefore, it may be noted that the feedback process will not cause the coil discharge air temperature to precisely reach the setpoint with a proportional controller.

This drawback of the pure proportional controller may be overcome by adding an Integral (I) term to the proportional controller and the controller evolves into a PI controller. The PI control equation is:

$$C = k_p \left(t_{ao} - t_{ao,set} \right) + k_i \int \left(t_{ao} - t_{ao,set} \right) d\tau \tag{1-16}$$

where

k_i is the integral gain; and

τ is time.

This feedback system has the virtue that it can provide a finite control signal with no bias-signal input, and it retains the adjustable response speed to the bias, which is a desirable property of the proportional controller. This comes about because the control signal from the second term of the equation is a function of all past values of bias. Therefore, past bias "charges up" the integrator to some value which remains, even if the bias decreases to zero; the bias no longer has to be finite to produce a control signal that will counteract the disturbance.

The PI controller has been used widely in the HVAC field due to its robustness, zero steady-state offset and simplicity (Haines 1988).

WHY USE PI TUNING

The coil discharge air temperature can reach its setpoint within 5 minutes after a step change in the setpoint with a properly set PI controller. However, a system with improper P gain and I gain will respond poorly to disturbances and setpoint changes. The result will be oscillation of the discharge air temperature around the setpoint or a drift away from the setpoint. These phenomena should be avoided in HVAC systems in order to maintain suitable indoor comfort with maximum energy efficiency of the heating and cooling systems.

In reality, PI gains are often tuned in the factory or in the field when the system is installed. Unfortunately, the tuning of P and I gain values is not a one-time job. A coil

exhibits inherent nonlinear behavior (Federspiel and Seem 1996). Also, loads on HVAC systems frequently change with the time of day, day of the week, and yearly season. Consequently, coils have time-varying dynamics. Additionally, the dynamics of systems may change because of coil fouling, wear on valves, unusual operational status during start-up, or after a component failure (Seborg et al. 1989). For example, consider a cooling coil in a building. The coil is operating under the following conditions: input air temperature is 70°F, air flow rate is 2000 cfm, chilled water input temperature is 40°F, and the valve is 10% open. A PI controller with P gain and I gain of 6 and 0.06 respectively responds very well to a step change of the coil temperature setpoint from 55°F to 57°F. (The settling time is measured as 290 sec for this case.) However, if the same PI controller is applied when the valve is 50% open, while with the other conditions remaining the same, the controller cannot achieve the same change in coil discharge air temperature from 55°F to 57°F. The discharge air temperature fluctuates more than 10°F around the setpoint, and the fluctuation never dies out as shown in Figure 1-6. This is due to inappropriate P and I gains, and will cause comfort complaints. When the P gain and I gain values of 2 and 0.02 are used, the controller maintains the process output at the setpoint, with relatively good dynamic response. The setpoint is reached in less than five minutes, when the setpoint changes from 55 °F to 57 °F (shown in Figure 1-7).
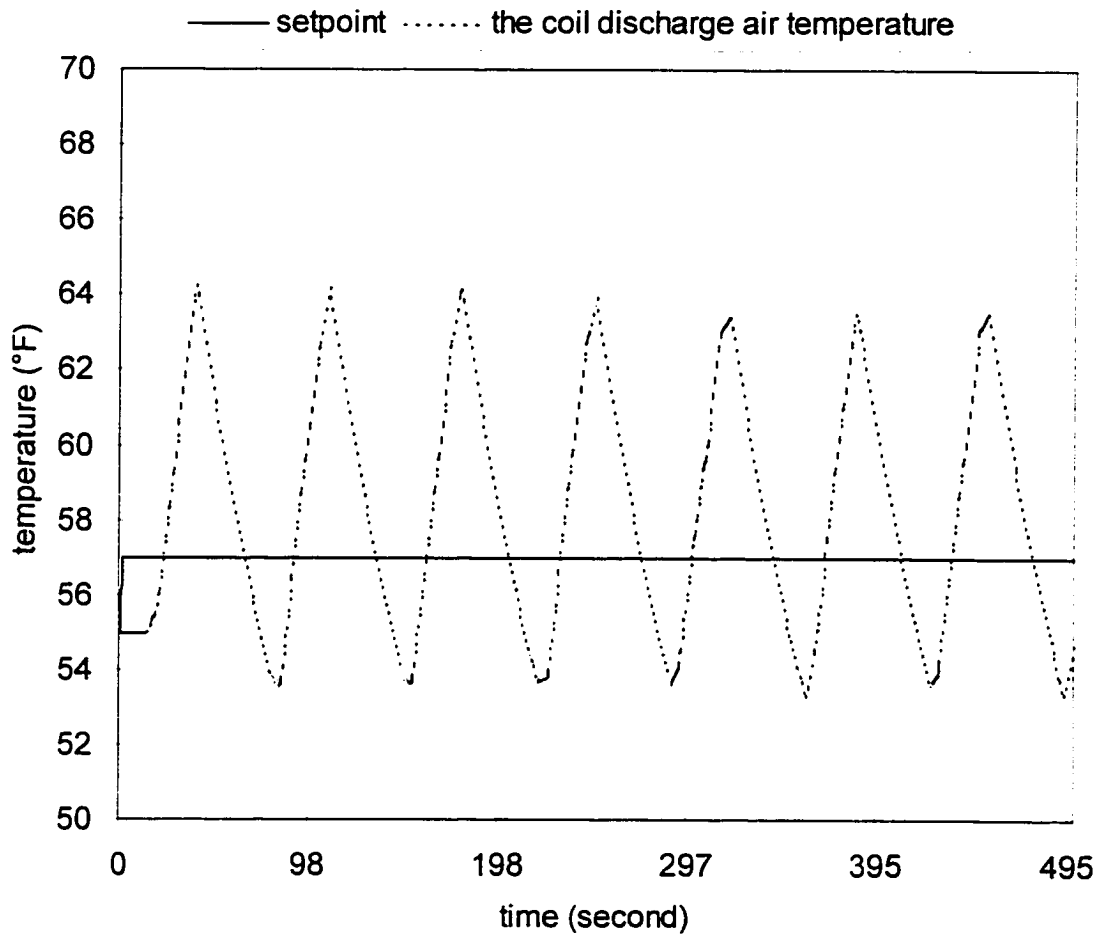
Figure 1-6 The step response of the system when incorrect P and I gain is used. The setpoint of the coil discharge air temperature can not be reached in this case. The objective of the feedback control system is not fulfilled.

setpoint ······ the coil discharge air temperature
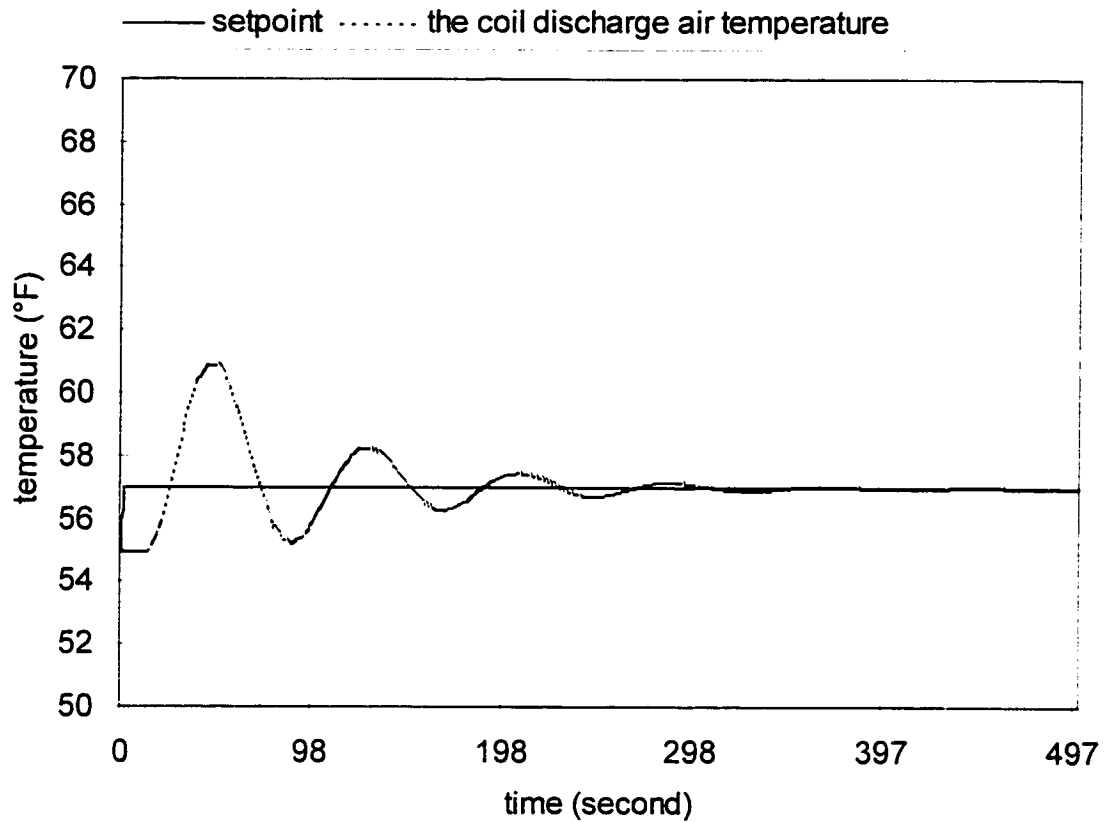
Figure 1-7 The step response of the system when the correct P and I gains

(calculated by Ziegler's rules) are used. The setpoint of the coil discharge air

temperature is reached in five minutes. The objective of the feedback system is

fulfilled.

Therefore, the P and I gains need to be adjusted at least twice a year. Fine tuning

is essential to maintain the HVAC system performance, and algorithm development is a

focus of research in the HVAC field.

CURRENT PI TUNING METHODS

The tuning of PI controllers has been investigated for decades. Generally, there

are two categories of methods to determine "good" values for the proportional gain and

integral gain of a PI controller: manual tuning and auto-tuning methods.

The operator typically follows a trial-and-error process (Seborg et al. 1989;

Corripio 1990), called manual tuning, to tune the controllers in typical engineering

applications. The operator runs different tests to determine the best values of P gain and

I gain. Simple rules are applied such as: the P gain needs to be decreased when the

system responds too quickly and I gain needs to be increased when the static bias is too

large, etc. Some more accurate empirical rules are also used, such as the Ziegler-Nichols

tuning method (1942). This method increases the proportional gain until continuous

oscillations are observed, that is, until the system becomes marginally stable. The

corresponding P gain (k_u) and the period of oscillation (T_u), which are determined by

observing the system dynamic response, are recorded for this test. They are called the

ultimate gain and ultimate period respectively. Then, the final P gain and I gain values

are calculated based on these two values (shown in Equations 1-17 and 1-18) (Ziegler

and Nichols 1942).

$$k_p = 0.4 k_u \qquad (1\text{-}17)$$

$$k_i = 0.5 \frac{k_u}{T_u} \qquad (1\text{-}18)$$

The manual tuning methods are time-consuming and experience is required to determine appropriate values of P and I gains.

Auto-tuning procedures have been developed to solve this problem. They will theoretically save engineers much time in the tuning of controllers, since they can automatically find suitable P and I gains. The basic procedure of auto tuning has two steps: identifying the system model (Equation 1-3), finding the DC gain, time constant and delay time of the system, and then calculating optimal P and I gain values based on the identified model (shown in Figure 1-8).

There are different algorithms to calculate the optimal P and I gains, based on different criteria for evaluation of the dynamic process of the system. Ziegler and Nichols (1942) claimed the P and I gains will be adequately optimal when a system has a decay ratio of 0.25, which means the second maximum value under a unit step disturbance will be a quarter of the first maximum value. The dynamic response to the disturbance will approximate good performance if this criterion is satisfied. Corresponding P and I gains are given empirically in Equations 1-19.
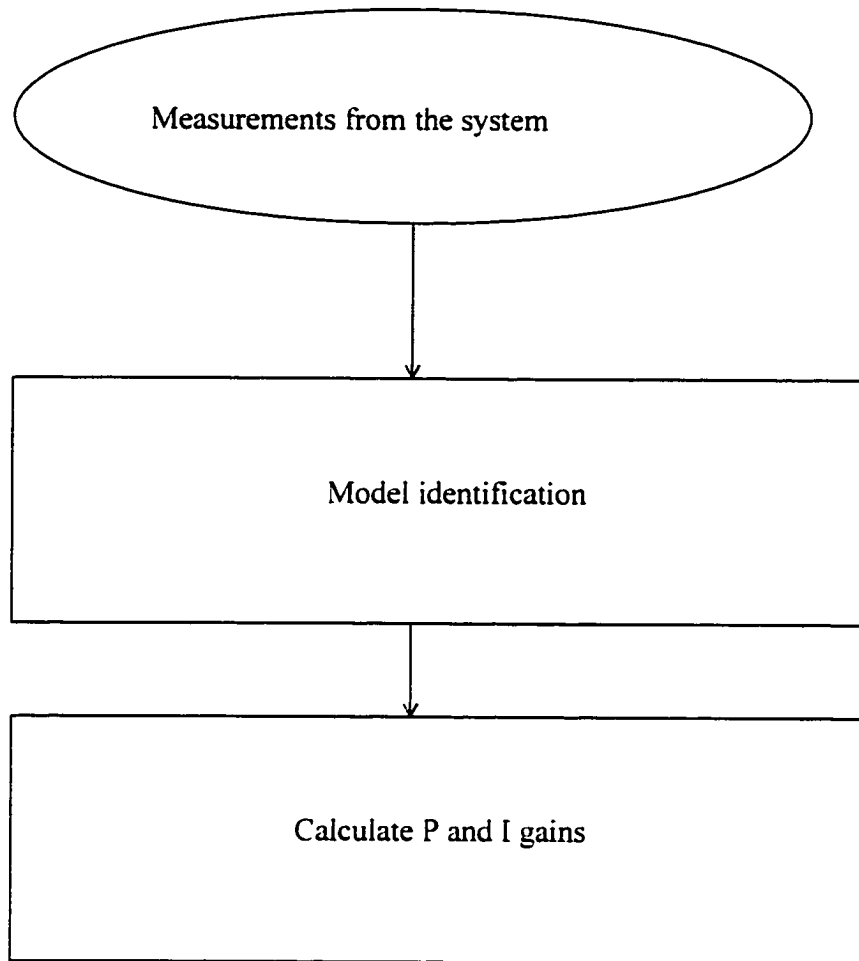
Figure 1-8 Current self-tuning procedure in HVAC application. It is based on model identification. The correct P and I gains can be obtained only after the coil model is identified.

and -20. The system in the former example has a time constant of 200 sec, delay time of 30 sec, and DC gain of 3 °F for 10% valve position change. The optimal P and I gains of 2 and 0.02 are calculated for the system based on Ziegler's rules and the dynamic response of the system is shown in Figure 1-7. (The settling time is less than 5 minutes). This algorithm has been proven successful in its fifty years' application in the HVAC field.

$$k_p = \frac{0.9T}{k_\gamma \tau_d}$$ (1-19)

$$k_i = \frac{0.27T}{k_\gamma \tau_d^2}$$ (1-20)

Recently, Bekker et al.(1992) suggested the criterion proposed by Ziegler is not good enough since it will result in too large an overshoot in the system (The overshoot in Figure 1-7 is 300% in one and a half minutes). He proposed that the critically damped response is the desired system response for the coil. Such a system will possess the most rapid gain, without having any overshoot. The algorithm (shown in Equations 1-21 and -22) has been developed based on pole-zero cancellation (MacArthur et al. 1989) and root locus techniques (Pinnella 1986; Donoghue 1977). The same system with P and I gains of 0.82 and 0.004 based on Bekker's rule, demonstrated better dynamic response (Figure 1-9). It has a settling time of 150 sec and overshoot of only 10%.
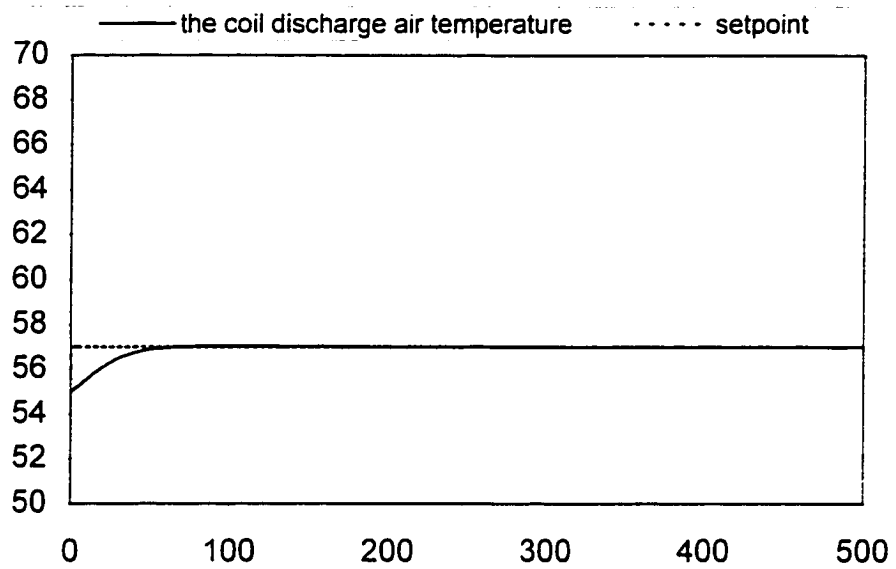
Figure 1-9 *The step response of the system with P and I gains*

calculated by Bekker's rules. An improved dynamic response is

demonstrated.

$$k_p = \frac{T}{k_s \tau_d} e^{-1}$$ (1-21)

$$k_i = \frac{1}{k_s \tau_d} e^{-1}$$ (1-22)

Current PI tuning methods for HVAC applications are built upon the assumption that the coil model can be successfully identified. In reality, the discharge air temperature and its setpoint will typically change by very small amounts during normal operation. These changes will be contaminated by noise in the field. Thus, it is necessary to apply an intentional large disturbance (For example, change the setpoint of the coil discharge air temperature by 2°F) to the coil to obtain a change large enough so that the noise in the signal can be ignored (Wallenborg 1992; Astrom and Hagglund 1984, 1988; Jota and Dexter 1988) and the model may then be identified with sufficient accuracy. This abnormal disturbance interrupts the normal operation of coils. With this in mind, the auto-tuning algorithm is not used continuously with Direct Digital Control (DDC) systems at present. Normal operation and auto tuning are separated in most current controls for HVAC systems. Auto tuning must be manually turned on when the operator finds the controller needs to be tuned.

Due to the present status of self-tuning algorithm development, most of the tuning for PI control of coils is either performed at the beginning of the operation or off line. Therefore, poor control performance (oscillation and drifting) is often observed in

HVAC systems. The continuous commissioning group in the Energy Systems Laboratory has finished commissioning projects in 30 buildings on the main campus of Texas A&M University. They found that 60% of the PI controllers examined in these buildings, about 900 PI controllers, were performing poorly. It is still an unsolved problem in the HVAC field to find an on-line self-tuning algorithm.

CHAPTER II

THE CONCEPT OF THE NEW ALGORITHM

The performance of the auto-tuning algorithm, described in the previous chapter, is seriously limited by the need to identify the model accurately. From this point, the dissertation will focus on developing an on-line algorithm that avoids this problem. First, the criterion used to evaluate the coil dynamic behavior is introduced. The application of Integral Square Error (ISE) in coils is discussed in detail. Then the proposed algorithm is introduced and the application range of the algorithm is given.

THE PERFORMANCE INDEX OF THE COIL

What criterion should we use to evaluate the dynamic behavior of the closed loop system of coils? This question is equivalent to, "what is the definition of good P and I gains, and what is the definition of bad P and I gains." Generally, there are two categories of the criteria: one is the transient criterion; the other is the steady state criterion.

There are several transient criteria currently applied in HVAC control. They are the rise time (Appendix B), the overshoot, the settling time, the peak time, a quarter decay ratio (Ziegler and Nichols 1942a), and the critically damped response (Bekker et al. 1992). All these criteria are suggested based on the assumption that a big enough step change is available for inputs of the closed loop system. Therefore, the criteria may be measured and evaluated in relatively short time on line. However, this is not the case for

air conditioning systems. The change of the coil discharge air temperature setpoint is very small when the coil is operated normally. We may assume the normal disturbance in an air conditioning system is approximately a step change. However, the resulting step input change is so small that normal air conditioning control sensors do not have the accuracy to recognize if the desired criteria are met. Therefore, the criteria mentioned above are difficult to calculate or observe on line.

When only the difference between the coil discharge air temperature and its setpoint is taken into consideration, there are three common steady state criteria, the integral of the square error (ISE) (Seem 1997), the integral of the absolute value of the error (IAE), and integral to time square error (ITSE). We also have the fourth criterion of the integral of the square bias of the coil discharge air temperature plus the square travel distance of the valve (ISS), when both the temperature bias and the valve travel are considered. The four performance indices are determined from

$$ISE = \int_0^\infty e(\tau)^2 d\tau = \int_0^\infty [t_{ao}(\tau) - t_{ao,set}(\tau)]^2 d\tau \qquad (2\text{-}1)$$

$$IAE = \int_0^\infty |e(\tau)| d\tau = \int_0^\infty |t_{ao}(\tau) - t_{ao,set}(\tau)| d\tau \qquad (2\text{-}2)$$

$$ITSE = \int_0^\infty \tau e(\tau)^2 d\tau = \int_0^\infty \tau [t_{ao}(\tau) - t_{ao,set}(\tau)]^2 d\tau \qquad (2\text{-}3)$$

$$ISS = \int_0^\infty [e(\tau)^2 + \Delta C(\tau)^2] d\tau$$

$$= \int_0^\infty \{[t_{ao}(\tau) - t_{ao,set}(\tau)]^2 + [C(\tau) - C(\infty)]^2\} d\tau \qquad (2\text{-}4)$$

Where,

C is the control signal to the valve;

$C(\infty)$ is the control signal when the closed loop system of the coil with a PI

controller is stabilized;

t_{ao} is the coil discharge air temperature and is a function of time;

$t_{ao,set}$ is the coil discharge air temperature setpoint and it is also a function of time.

Comparing the ISE to the IAE, the ISE performance index has an advantage in

that it places a larger weight on big errors, which is critical to indoor comfort.

One advantage of the ITSE performance index over the ISE and IAE

performance indices is that following a disturbance, the ITSE performance index places

little weight on the initial response when the error is large. However, for the systems that

do not have a steady-state error of zero, the ITSE performance has a disadvantage in that

a large weight is placed on the final errors. The proposed algorithm is designed for both

noise free systems and extremely noisy systems. For extremely noisy systems, the

process output continually oscillates around the setpoint and thus the ITSE performance index would place a large weight on the final errors.

Theoretically, ISS is the most comprehensive performance index. It takes both the temperature bias and the travel distance of the valve into consideration. However, the dominant frequency of the disturbance to the coil is lower than $1/3600$ sec^{-1}, and the time constant of the coil is less than 5 minutes. The transient part of the coil dynamic behavior is much less than the steady part, when the coil is in normal operation. Therefore, the valve position change is directly related to the change of coil discharge air temperature. The integral of the square error of the discharge air temperature and its setpoint can indicate the magnitude of the integral of the square of the valve travel. Practically, ISS is often replaced by ISE due to the simplicity of the ISE criterion.

Thus, the ISE performance index was used to design the algorithm. Indoor comfort and energy efficiency can be achieved as long as this criterion is in the allowed range. Also, the algorithm is simplified when ISE is applied instead of ISS.

There exists a minimum ISE for each coil and set of conditions. The performance of the coil is maximized if a minimum value of ISE can be realized. However, the minimum ISE is different for different coils or for the same coil under different conditions. For example, the minimum ISE is $30°F^2$.sec when the coil DC gain is $3°F$ per 10% valve position change, the time constant is 300 sec and the time delay is 30 sec.

However, the minimum ISE is 50°F².sec when the coil DC gain is 3°F per 10% valve position change, the time constant is 400 sec and the time delay is 30 sec (Marshall 1992). It is possible for us to predict this minimum ISE for a coil under specific conditions, if the coil model is available. However, the coil model is very difficult to obtain accurately on line as described earlier.

The air conditioning system must be controlled to keep people in a building comfortable; the comfort range in office buildings and commercial buildings is approximately 4°F based on the ASHRAE comfort chart. This may permit the use of a "sufficiently small" ISE value. This ISE value can be obtained for all practical coils by wisely choosing P and I gains; meanwhile, the coil will operate optimally enough when the actual ISE is less than this value. Indoor comfort can be achieved and energy efficiency is maximized in this case. Based on research in this dissertation, an ISE equal to 100°F².sec can be obtained for most practical coils, as demonstrated later in this chapter. The coil discharge air temperature can reach its setpoint within 5 minutes when the P and I gains are set to achieve ISE less than 100°F²sec for a unit step change in setpoint. The transients of the coil discharge air temperature for this case will not cause comfort complaints, so we consider the coil operation is optimal enough.

Some energy efficiency may be lost if the ISE less than 100°F².sec is chosen as the PI controller evaluation criterion instead of ISE equal to the optimal value. However, a general criterion is obtained for all practical coils. More importantly, we may be able

to skip the model identification step and find an on line PI tuning algorithm. Also, we may not lose any energy efficiency at all by choosing ISE less than $100°F^2$.sec as the criterion, since the sensors in a DDC system normally have an error of $±0.5$ °F. Most DDC systems for air conditioning systems will treat ISE equal to $100°F^2$.sec and ISE equal to $30°F^2$.sec as the same number.

CALCULATION OF ISE FOR THE COIL

Combining the model for PI control (Equation 1-16), and the model for the coil (Equation 1-3), the closed loop coil system is described in Figure 2-1. The controller measures the supply air temperature, and calculates the bias using P gain, I gain and setpoint. A correction signal is sent out to the control valve to modulate the water flow rate. This closed loop system can be expressed by Equation 2-5 in the transform domain where s is the transform variable.

$$\frac{t_{ao}}{t_{ao.set}} = \frac{\left(k_p + \dfrac{k_i}{s}\right)\left(\dfrac{k_s}{Ts+1}\right)e^{-\tau_d s}}{1 + \left(k_p + \dfrac{k_i}{s}\right)\left(\dfrac{k_s}{Ts+1}\right)e^{-\tau_d s}} \qquad (2\text{-}5)$$

where,

t_{ao} is the coil discharge air temperature;

$t_{ao.set}$ is the coil discharge air temperature setpoint;
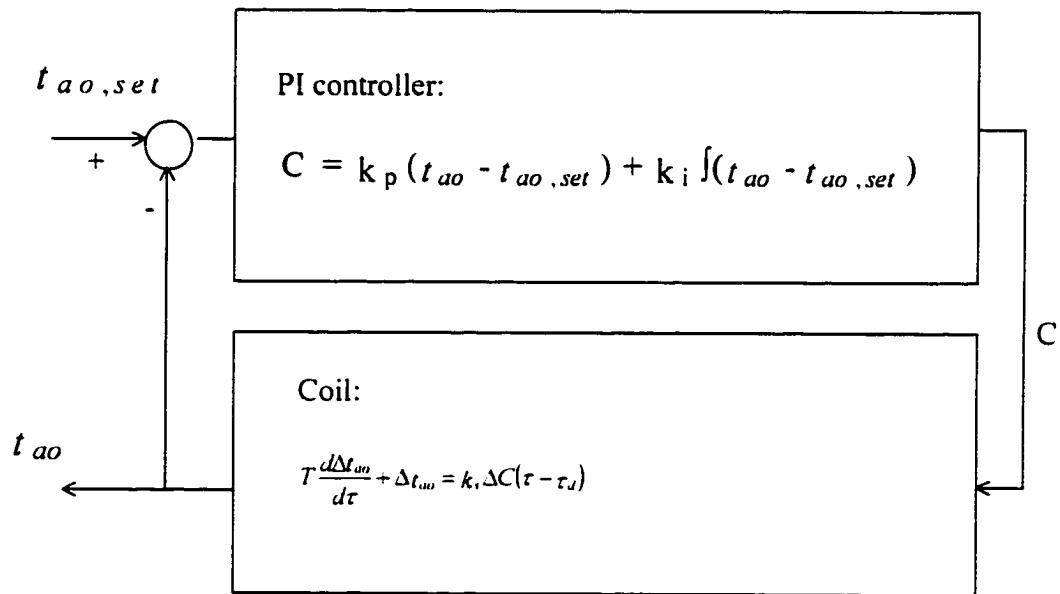
Figure 2-1 *The cooling coil with a PI controller. The coil model is*

assumed to be a first order model with time delay.

k_p is the proportional gain for the PI controller;

k_i is the integral gain for the PI controller;

k_s is the DC gain;

T is the time constant;

τ_d is the delay time.

To maintain the ISE (Equation 2-1) of the coil below some finite number, which ensures that the difference between the setpoint and the coil discharge air temperature will become zero eventually, the P and I gains must satisfy Equations 2-6, -7 and -8 according to the Nyquist criterion (Franklin et al. 1995). More detailed information can be found in Appendix C. The closed loop system will be stable for this case. The poles of the system will be in the left half plane.

$$k_p > 0 \qquad\qquad\qquad (2\text{-}6)$$

$$k_i > 0 \qquad\qquad\qquad (2\text{-}7)$$

$$\tau_d \sqrt{\frac{\sqrt{\left(\left(\frac{k_s k_p}{T}\right)^2 - \left(\frac{1}{T}\right)^2\right)^2 + 4\left(\frac{k_s k_i}{T}\right)^2} - \left(\frac{1}{T}\right)^2 + \left(\frac{k_s k_p}{T}\right)^2}{2}}$$

$$< \arccos \frac{\frac{k_s k_i}{T} - \frac{1}{T}\frac{k_s k_p}{T}}{\left(\frac{1}{T}\right)^2 + \frac{\sqrt{(\left(\frac{k_s k_p}{T}\right)^2 - \left(\frac{1}{T}\right)^2)^2 + 4\left(\frac{k_s k_i}{T}\right)^2} - \left(\frac{1}{T}\right)^2 + \left(\frac{k_s k_p}{T}\right)^2}{2}} \qquad (2\text{-}8)$$

We can express the Nyquist criterion of Equations 2-6, -7, and -8 in Figure 2-2, using the curve of ISE tending to infinity for a specific coil and specific working conditions (The example shown has a DC gain of 3°F for 10% valve position change, a time constant of 200 sec and a time delay of 30 sec.). The system will be unstable when the point representing the P and I gains is located outside (above or to the right of) the curve of ISE tending to infinity. The difference between the coil discharge temperature and its setpoint will never reach zero in this case. In contrast, the system will be considered stable when the point representing P and I gains are located inside the curve. The discharge air temperature will match the setpoint after some period of time. However, the system may oscillate for a much longer period if the P and I gains do not meet an optimal criterion. That is the reason why we introduced the criterion that requires that ISE be less than 100°F²sec.
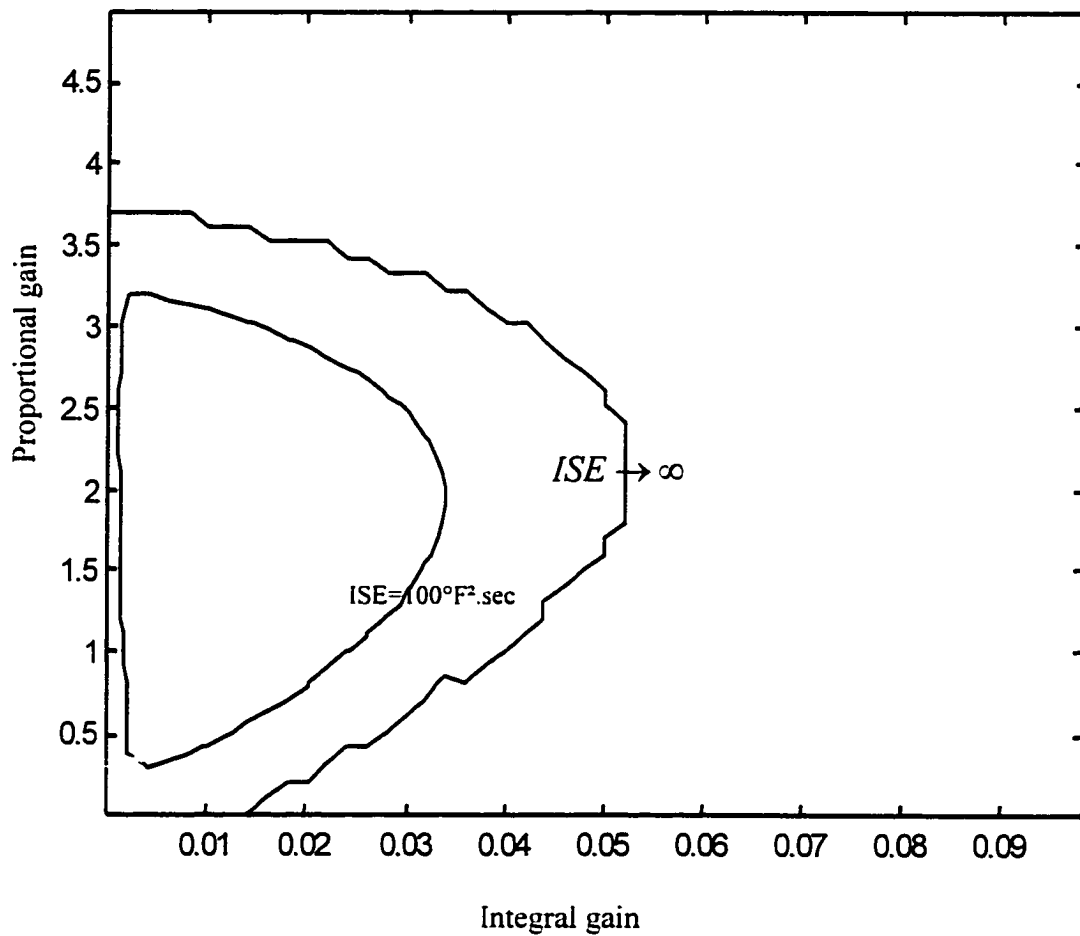
Figure 2-2 *System dynamic characteristics for different P and I gain values when*

the time constant is 200 sec, time delay is 30 sec and DC gain is 3°F for 10% valve

position change.

Any finite value of ISE can be expressed as a function of τ_J, T, k_s, k_p, and k_i as given in Equation 2-9 (Marshall 1992). This equation is plotted as the curve for ISE equals to $100°F^2sec$ in Figure 2-2. So far, the curve of ISE tending to infinity and the curve of ISE equal to $100°F^2.sec$ have divided the P and I plane into three zones. The system is not stable when the P and I gains are located outside the curve of ISE tending to infinity. The system is stable, but takes too long for the system to achieve its setpoint, when the P and I gains are located between the curve of ISE tending to infinity and the ISE equal to $100°F^2.sec$ curve. The system is optimized in practical terms when the P and I gains are located inside the curve of ISE equal to $100°F^2.sec$, which means that the system will reach its setpoint within 5 minutes.

Therefore, the self-tuning process must find a set of P and I gains which fall inside the curve of ISE equals to $100°F^2.sec$ in Figure 2-2. The system will have optimal dynamic characteristics (in practical terms) if such a pair of P and I gains can be found.

$$ISE = \begin{cases} \dfrac{1}{2\sqrt{\left(\left(\dfrac{k_s k_p}{T}\right)^2 - \left(\dfrac{1}{T}\right)^2\right)^2 + 4\left(\dfrac{k_s k_i}{T}\right)^2}} \\[6ex] \left[\left(\left(\dfrac{1}{T}\right)^2 - \rho^2\right)\dfrac{\dfrac{k_s k_i}{T} - \dfrac{1}{T}\dfrac{k_s k_p}{T} + \left(\left(\dfrac{1}{T}\right)^2 - \rho^2\right)\cosh(\rho\,\tau_d)}{\dfrac{k_s k_p}{T}\rho^2 - \dfrac{1}{T}\dfrac{k_s k_i}{T} - \rho\left(\left(\dfrac{1}{T}\right)^2 - \rho^2\right)\sinh(\rho\,\tau_d)} \\[8ex] + \left(\left(\dfrac{1}{T}\right)^2 + \sigma^2\right)\dfrac{\dfrac{k_s k_i}{T} - \dfrac{1}{T}\dfrac{k_s k_p}{T} + \left(\left(\dfrac{1}{T}\right)^2 + \sigma^2\right)\cos(\sigma\,\tau_d)}{\dfrac{k_s k_p}{T}\sigma^2 + \dfrac{1}{T}\dfrac{k_s k_i}{T} - \sigma\left(\left(\dfrac{1}{T}\right)^2 + \sigma^2\right)\sin(\sigma\,\tau_d)}\right] \quad when\ k_p \neq T\,k_i \\[8ex] \dfrac{1}{2\sigma}\dfrac{1 + \sin(\sigma\,\tau_d)}{\cos(\sigma\,\tau_d)} \quad when\ k_p = T\,k_i \quad (2\text{-}9) \end{cases}$$

where

$$\rho = \sqrt{\dfrac{\sqrt{\left(\left(\dfrac{k_s k_p}{T}\right)^2 - \left(\dfrac{1}{T}\right)^2\right)^2 + 4\left(\dfrac{k_s k_i}{T}\right)^2} + \left(\dfrac{1}{T}\right)^2 - \left(\dfrac{k_s k_p}{T}\right)^2}{2}}$$

$$\sigma = \sqrt{\dfrac{\sqrt{\left(\left(\dfrac{k_s k_p}{T}\right)^2 - \left(\dfrac{1}{T}\right)^2\right)^2 + 4\left(\dfrac{k_s k_i}{T}\right)^2} - \left(\dfrac{1}{T}\right)^2 + \left(\dfrac{k_s k_p}{T}\right)^2}{2}}$$

THE CONCEPT OF THE NEW ALGORITHM

The range of ISE tending to infinity includes the range of ISE equal to $100°F^2$.sec (shown in Figure 2-2). The contour graph of ISE is continuous and ISE will be less than $100°F^2$.sec, when the P and I gains are chosen inside the curve of ISE equal to $100°F^2$.sec. Also, we find that the straight line of $k_i = k_p /100$ crosses this range (Figure 2-3). Therefore, we can possibly use the 'iteration' concept to find an optimal P and I gains. We do not change P and I gains if the ISE is less than $100°F^2$sec. We can either increase P gain and I gain at the same time or decrease P and I gain at the same time along the straight line of $k_i=k_p/100$, when the ISE is larger than $100°F^2$sec. P and I gain are not optimal in this case. We observe the ISE of the system after the change of P and I gain. We will stop the P and I gain search if the ISE is not larger than $100°F^2$sec any more, while we will continue the search if the ISE is still too big. This iteration concept is shown in Figure 2-3, where the system has a time constant of 200 sec, time delay of 30 sec and DC gain of $3°F$ for 10% valve position change.
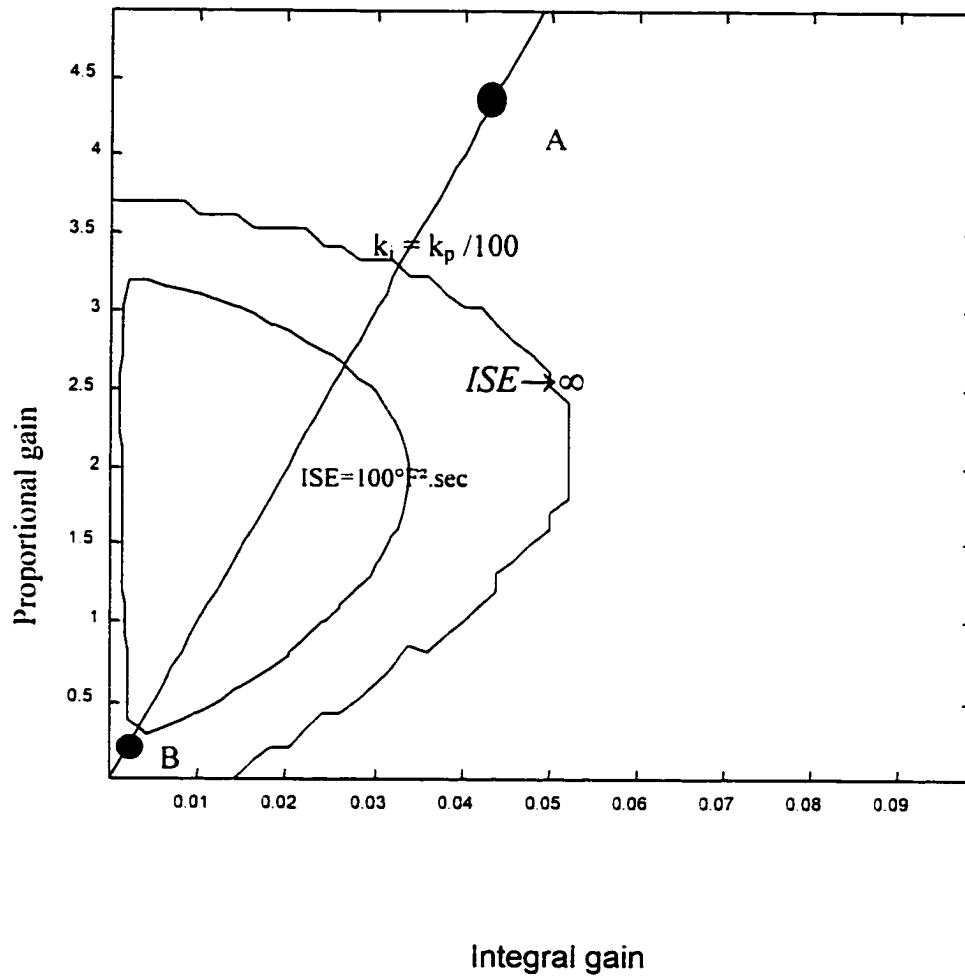
Figure 2-3 *The search strategy of the new algorithm.*

It is also found that the maximum optimal P and I gains along the straight line of $k_i = k_p/100$ are at least two times the minimum value. For example, in Figure 2-3, the maximum optimal P gain along the straight line of $k_i = k_p/100$ is 2.7, while the minimum optimal P gain along the straight line is 0.3. Therefore, it is safe to double the P and I gains when the P and I gains need to be increased, and cut the P and I gains in half when P and I gains need to be decreased. An "optimal" value will not be missed if we use this iteration step.

However, there still remains a problem to be solved. Whether the P and I gains need to be increased or decreased must be determined, since the ISE will be larger than $100°F^2sec$ under both cases. An indicator needs to be developed to discern the two cases.

The system responses are recorded in Figures 2-4 and -5, when the P and I gains stand at points A and B respectively, in Figure 2-3. The discharge air temperature oscillates around the setpoint when the P and I gains are selected at the point A, when both gains are larger than the optimal values. The period of the temperature oscillation is about 3 minutes. The discharge air temperature drifts around the setpoint when the P and I gains are at point B. Both P and I gains are smaller than the optimal values for this case. The dominant frequency of the temperature change in this case is about 1/1200

——— discharge air temperature .... plant setpoint
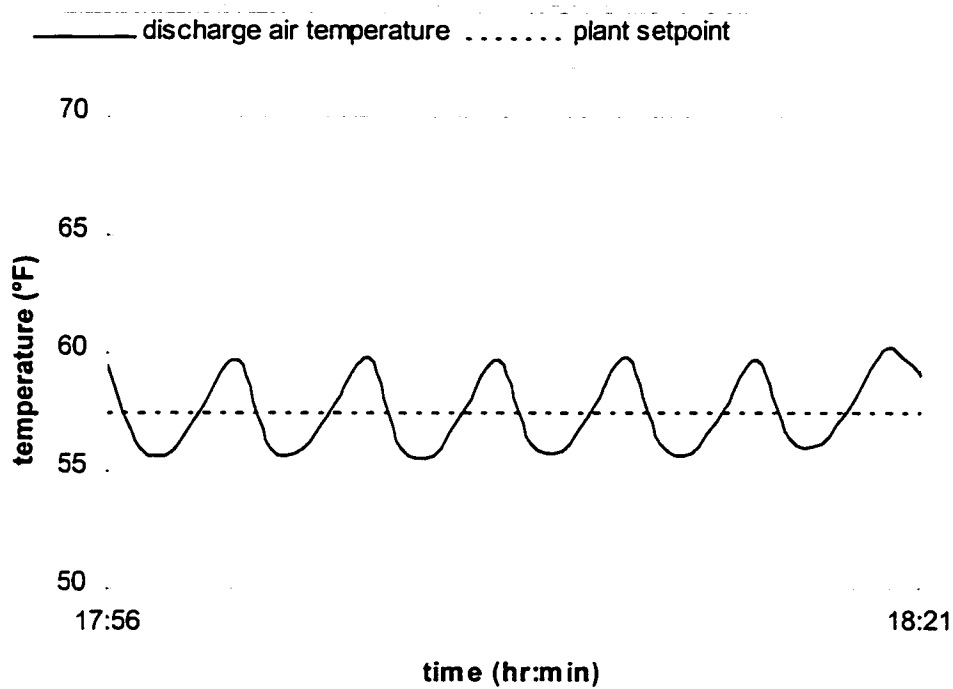
Figure 2-4 *The temperature oscillates when both P and I gains are too large. The period of the oscillation in this case is approximately three minutes.*

_____ discharge air temperature _ _ _ _ setpoint
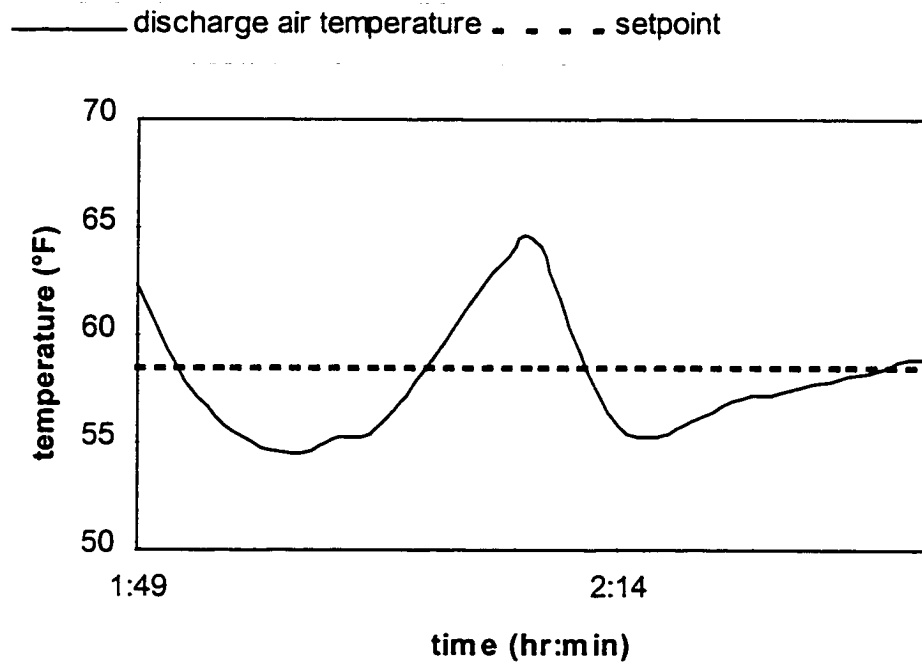
Figure 2-5 *The temperature drifts when both P and I gains are too small. The "period"*

of the drift is approximately twenty minutes for the case shown.

sec^{-1}. It has a period of 20 minutes. The spectral distribution of the coil discharge air temperature changes moves to the high frequency side when the P and I gains are too large. This is equivalent to "the low frequency proportion in total energy decreases". On the the other hand, the spectrum distribution moves to the low frequency side when the P and I gains are too small. The low frequency proportion increases in this case.

This gives us a hint that we can use the low frequency proportion (LFP, shown in Equation 2-10) as an indicator to decide whether we need to decrease P and I gains or increase P and I gains. The P and I gains will be increased if the low frequency proportion is small. The high frequency content is the dominant part of this case; the P and I gains will be decreased if the low frequency proportion is large and the low frequency content is the dominant part. "What is a low frequency?" or "what is a high frequency?" is the first question that needs to be answered if we use the low frequency proportion as the indicator. This question is the same as, "what is the value of w_c in Equation 2-10?" This question can be answered by an analysis of the coil dynamic response in the frequency domain.

$$LFP = \frac{\int_{0}^{w_c} [E(w)]^2 \, dw}{\int_{0}^{\infty} [E(w)]^2 \, dw} \qquad (2\text{-}10)$$

where w is the frequency in units of rad/sec.

w_c is a constant parameter which helps define the LFP.

E represents the difference between the coil air discharge temperature and its sepoint in the frequency domain.

The frequency distribution of the difference between the coil air discharge temperature and its setpoint can be analyzed for two different cases: one is when the system is stable; the other is when the system is not stable.

When the system is stable, the frequency distribution of the bias can be obtained from the temperature difference in the s domain, due to the similarity of the Fourier and Laplace transforms. That is,

$$E(w) = e(s)\big|_{s=jw}$$ (2-11)

where,

e(s) is the difference between the coil air discharge temperature and its sepoint in the s domain.

Deduced from Equation 2-5, the difference of the output and the reference signal under unit step input can be written in the s-domain as:

$$e(s) = \frac{Ts + 1}{Ts^2 + s + (k_p s + k_i) k_s e^{-\tau_d s}} \tag{2-12}$$

Then the magnitude of spectral energy content of the error signal at different frequencies is:

$$
\begin{aligned}
|E(w)| &= |e(s)|_{s=jw}| \\
&= \frac{\sqrt{1 + (Tw)^2}}{\sqrt{\begin{array}{l}(k_i k_s \cos(\tau_d w) + k_p k_s \sin(\tau_d w) - T w^2)^2 \\ + (w + k_p k_s \cos(\tau_d w) - k_i k_s \sin(\tau_d w))^2\end{array}}}
\end{aligned} \tag{2-13}
$$

The LFP can be calculated for a specific coil, when it is under specified conditions, by using Equation 2-13 in Equation 2-10 as long as we know the critical frequency, w_c. This critical frequency should be picked wisely so that the indicator can discern between cases with large and small P and I gains, respectively. Likewise, a critical value, LFP_c, is needed, such that if $ISE>100°F^2$.sec and $LFP>LFP_c$, the values of P and I gains must be increased, while if $ISE>100°F^2$.sec and $LFP<LFP_c$, P and I gains must be decreased. Trial and error calculations have shown that w_c values from 0.01 to 0.04 rad/sec provide LFP values which will indicate whether P and I values need to be increased or decreased. A w_c value of 0.02 rad/sec was chosen to demonstrate the algorithm in this dissertation.

Again, we choose the system with a time constant of 200 sec, time delay of 30 sec, and DC gain of 3°F for 10% valve position change as an example (Figure 2-6). The figure shows that the LFP will be substantially less than 0.4 if the P and I gains are larger than the optimal values; the LFP will be substantially larger than 0.6 if the P and I gains are smaller than the optimal values.

The system becomes unstable when the P and I gains chosen are too large (Figure 2-3). In this case, the above analysis is not valid since Equation 2-11 does not stand. However, the change of the control signal to the valve will become very fast, due to the poles in the right half of the complex plane. It may go to an infinite speed if no physical restriction is applied. However, the cooling/heating valve normally requires 30 sec for a full stroke. Therefore, the spectrum of the change of the valve position focuses on the frequency of 0.21 rad/sec. Consequently, the spectrum of the change of the discharge air temperature focuses on the same frequency, which is much higher than 0.02 rad/sec. LFP in Equation 2-10 is close to zero in this case.

Combining the above analysis, the P and I gains need to be increased when LFP is larger than 0.5, while the P and I gains need to be decreased when LFP is smaller than 0.5.
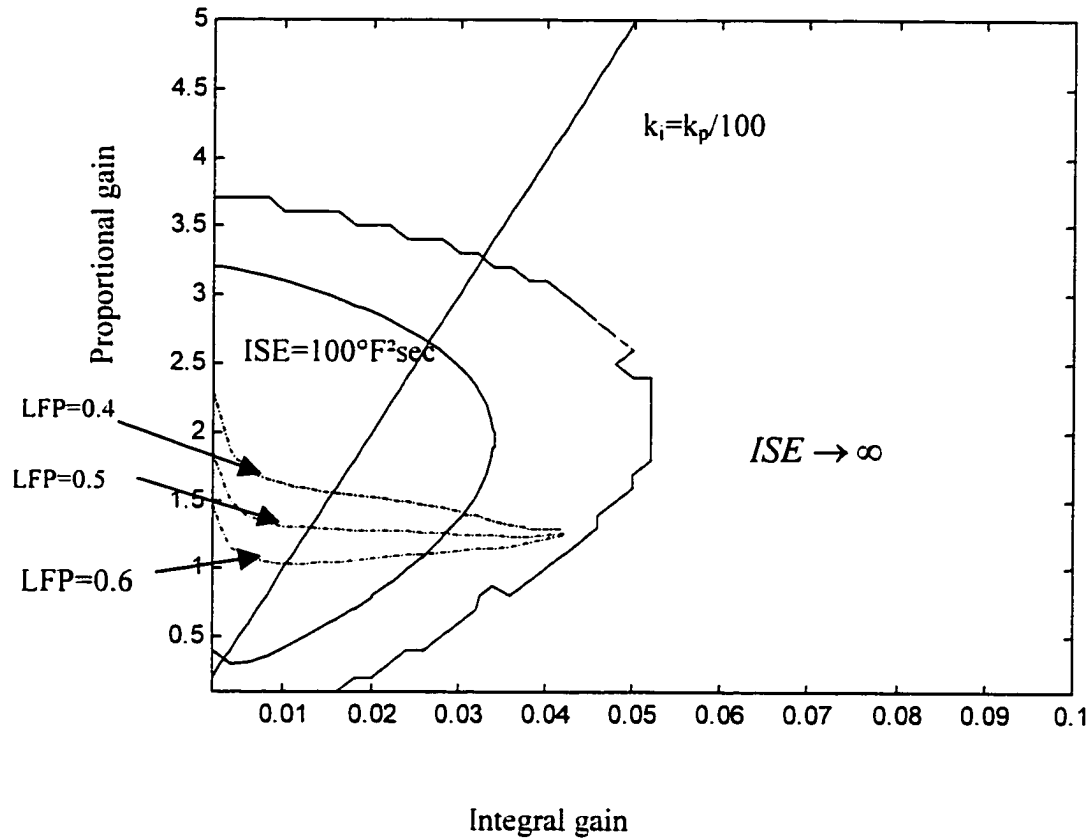
Figure 2-6 Series of constant LFPs as a function of P and I gains. This demonstration is

for the system with time constants of 200 sec, time delay of 30 sec, and DC gain of 3°F

for 10% valve change.

So far, the basic idea of the new algorithm has been developed. The new algorithm will avoid the model identification step that is indispensable in the conventional self-tuning algorithm of HVAC applications. A flow chart of the procedure for implementing the algorithm is shown in Figure 2-7. The algorithm first calculates the integral square error to see whether it is larger or smaller than 0.5. P and I gains will not be changed if the ISE is small enough, while the P and I gains need to change when the ISE is too large. The algorithm will calculate the Low Frequency Proportion, using measurements from the Direct Digital Control system, if the P and I gain needs to be changed (The procedure of calculating LFP will be discussed in Chapter III.). The values of P and I gains will both be cut in half along the straight line of $k_i = k_p/100$ if the LFP is smaller than 0.5. The values of P and I gain will be doubled along the straight line of $k_i = k_p/100$ if the LFP is larger than 0.5. The algorithm will continue doing this 'iteration' until the ISE criterion is satisfied, which means that the system has optimal P and I gains.

THE APPLICATION RANGE OF THE NEW ALGORITHM

As mentioned before, several rules are the bases of the new algorithm:

1. The range of ISE tending to infinity includes the range of ISE equal to $100°F^2$.sec. Therefore, the contour graph of ISE is continuous and ISE will be less than $100°F^2$.sec when the P and I gains are chosen inside the curve of ISE equal to $100°F^2$.sec.
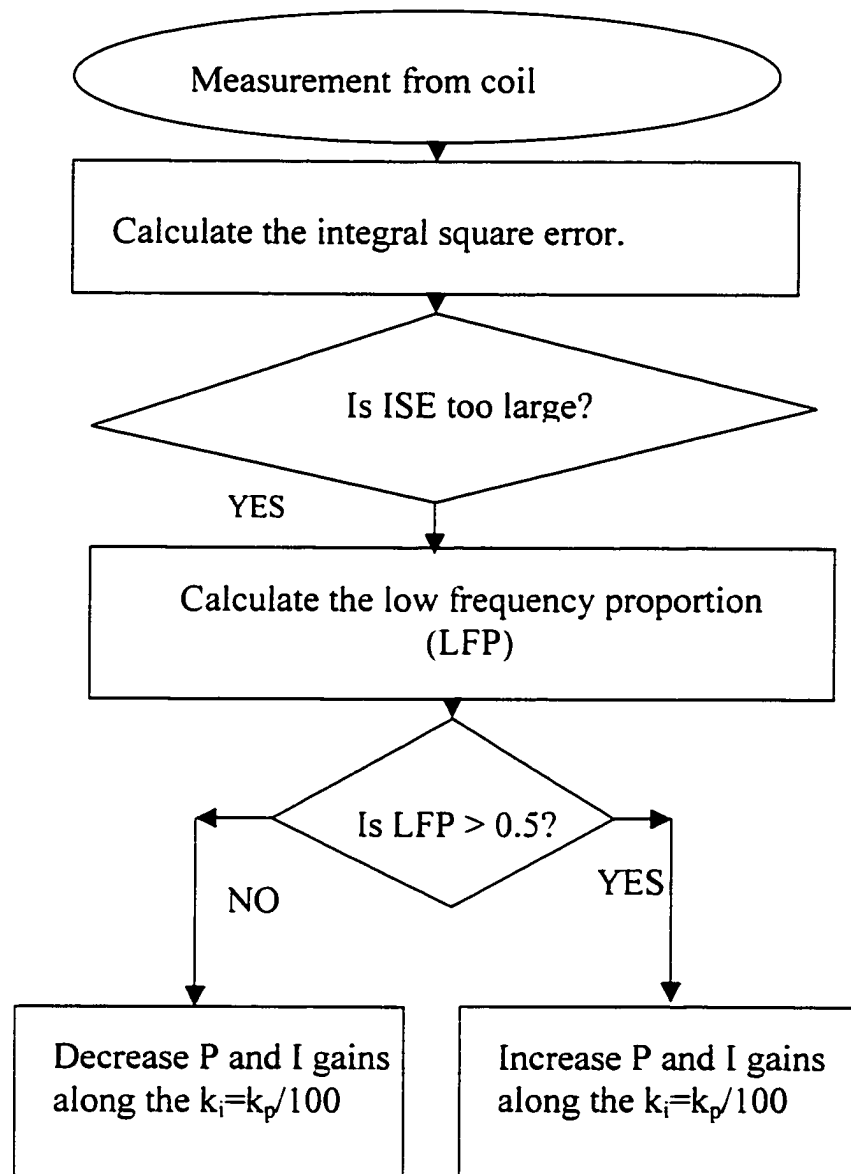
Figure 2-7 The general procedure of the new algorithm.

2. The range of ISE equal to $100°F^2.sec$ is continuous and the straight line of $k_i=k_p/100$ crosses this range. Therefore, we can possibly find the optimal P and I gain by doing an iterative search along the straight line of $k_i=k_p/100$.

3. The maximum "optimal" P and I gain along the straight line of $k_i=k_p/100$ is at least two times the minimum "optimal" value. Therefore, it is safe to double the P and I gains when they need to be increased and cut P and I gains to half when they need to be decreased. An optimal value will not be missed if we use this iterative step change.

4. The LFP will be less than 0.5 if the P and I gains are larger than the optimal values; the LFP will be larger than 0.5 if the P and I gains are smaller than the optimal values. Therefore, the P and I gains need to be increased when LFP is larger than 0.5, while the P and I gains need to be decreased when LFP is smaller than 0.5.

These rules have already been demonstrated when the system has a time constant of 200 sec, time delay of 30 sec, and DC gain of 3°F for a 10% valve position change. However, the algorithm will turn out to be useless if it is only applicable in this case. The algorithm should be applicable for the range of coils and operating conditions, which are typically encountered in HVAC systems. As noted in Chapter I (see Equations 1-12, -13, and -14), normal operating conditions for typical HVAC coils result in time constants between 30 sec and 300 sec, delay times between 0 sec and 30 sec, and DC

gains between 0°F for a 10% valve position change to 20°F for a 10% valve position change.

It can be seen from Equations 2-6, -7, -8 and -9 that k_s is always combined with k_p and k_i, and vice versa. Therefore, since we chose k_p and k_i along the straight line k_p/k_i=100 as described before, the rules can be applied for any k_s, as long as we prove that the rules apply for one specific value of k_s.

Equations 2-6, -7, -8, -9, -10, -11 and -12, from which the four rules just enumerated were developed, have been numerically evaluated for the range of time constants and time delays expressed in Equations 1-12 and 1-13, for a DC gain value of 1°F for 10% valve position change. The evaluation found that the rules are satisfied for these ranges of parameters and hence for practical coils and practical operating conditions. Results of this evaluation for 9 different systems are shown in Figures 2-8, -9, -10, -11, -12, -13, -14, -15, and -16 respectively. These systems have different combinations of the time constant (100, 200 or 300 sec) and the time delay (10, 20 or 30 sec). These figures demonstrate that the above rules are satisfied for these nine systems.
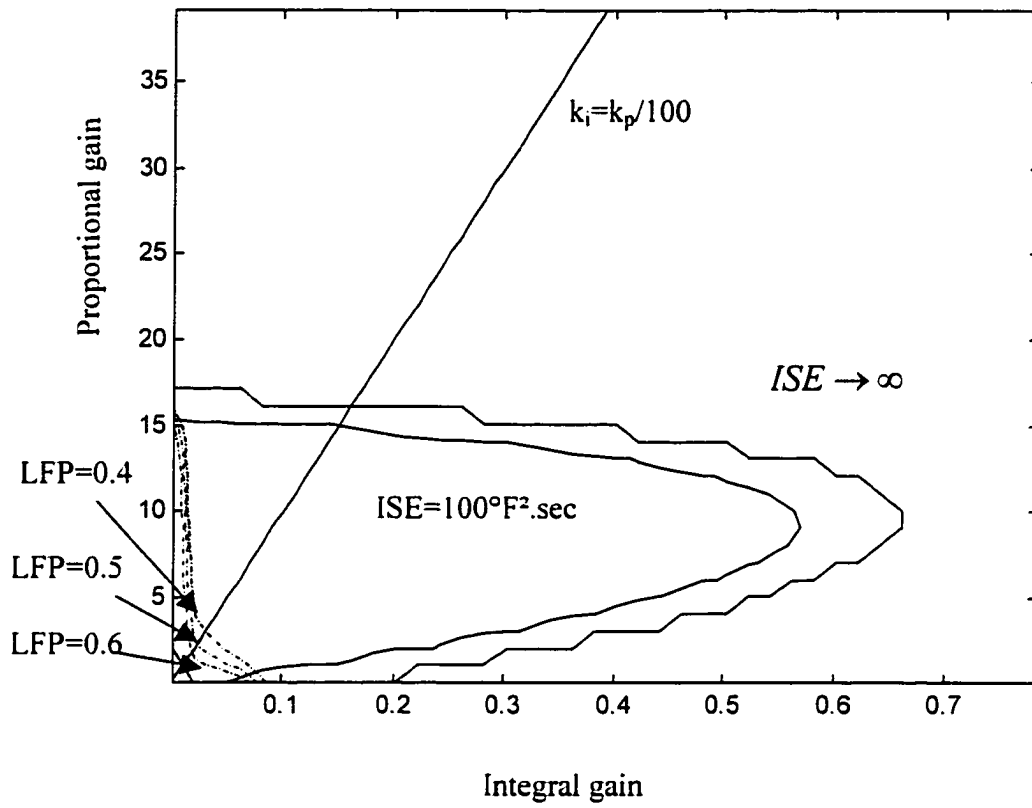
Figure 2-8 *The dynamic and frequency characteristics of a system with time constant of*

100 sec, delay time of 10 sec and DC gain of 1°F for 10% valve position change.
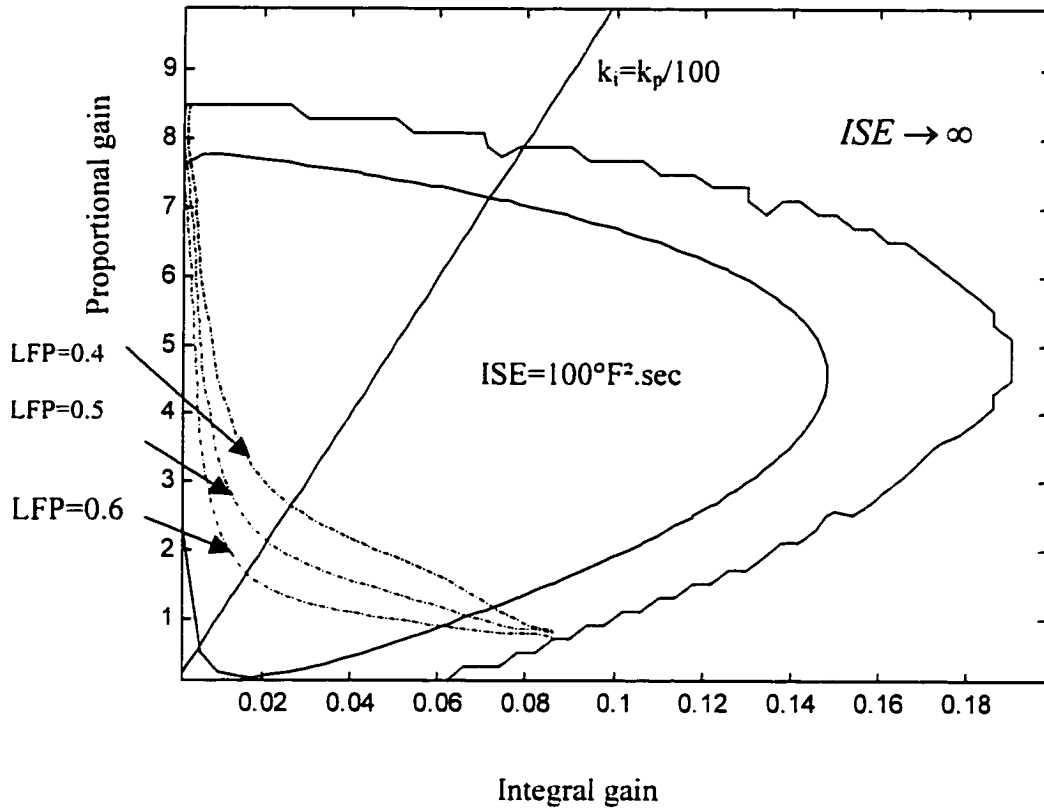
Figure 2-9 *The dynamic and frequency characteristics of a system with time constant of*

100 sec, delay time of 20 sec and DC gain of 1°F for 10% valve position change.

56
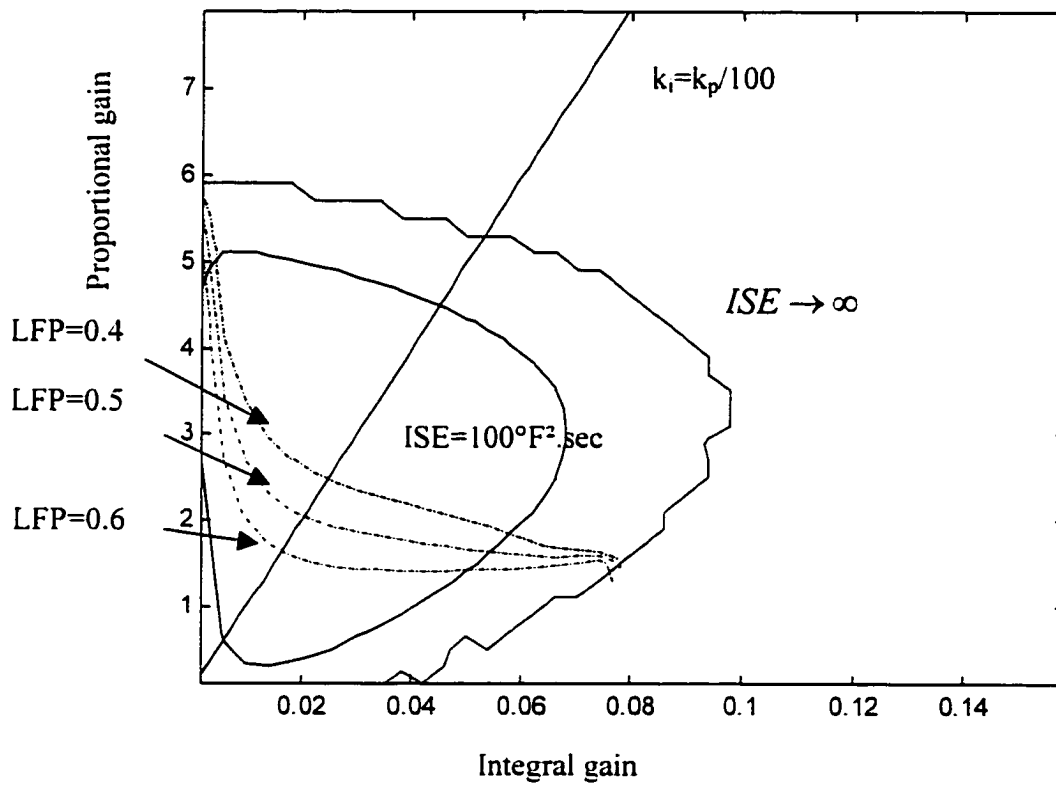
Figure 2-10 The dynamic and frequency characteristics of a system with time constant

of 100 sec. delay time of 30 sec and DC gain of 1°F for 10% valve position change.
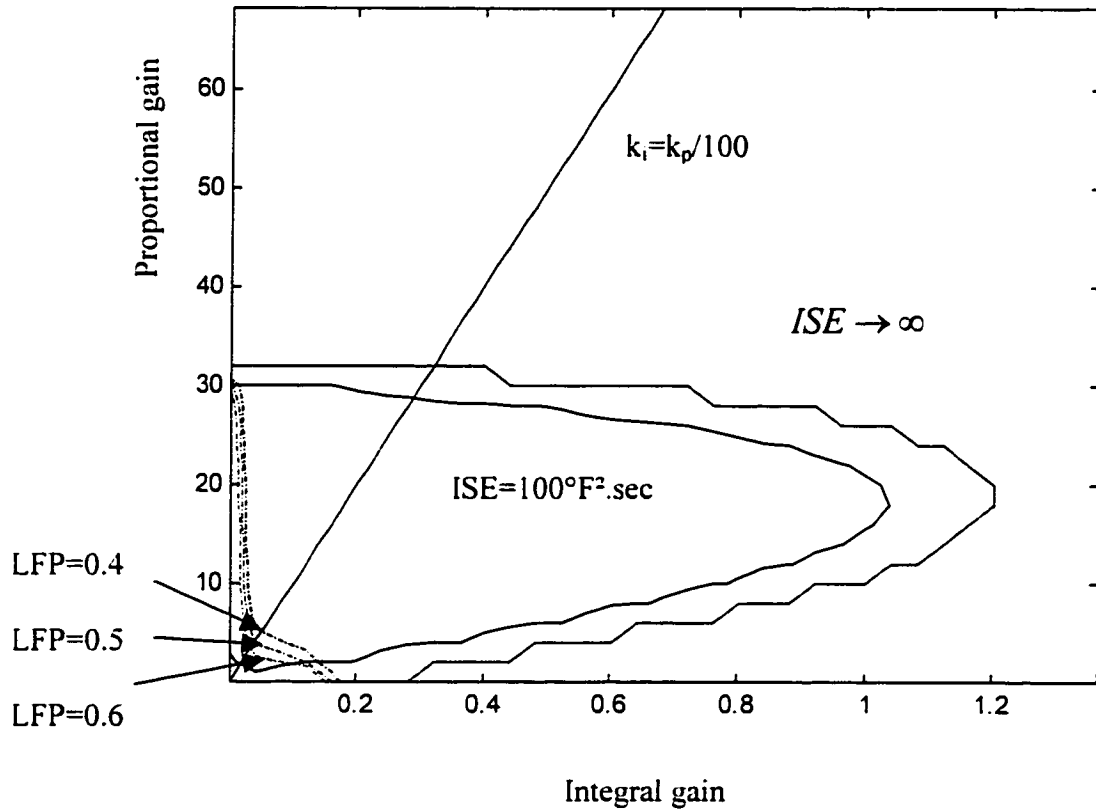
Figure 2-11 The dynamic and frequency characteristics of a system with time constant

of 200 sec. delay time of 10 sec and DC gain of 1°F for 10% valve position change.
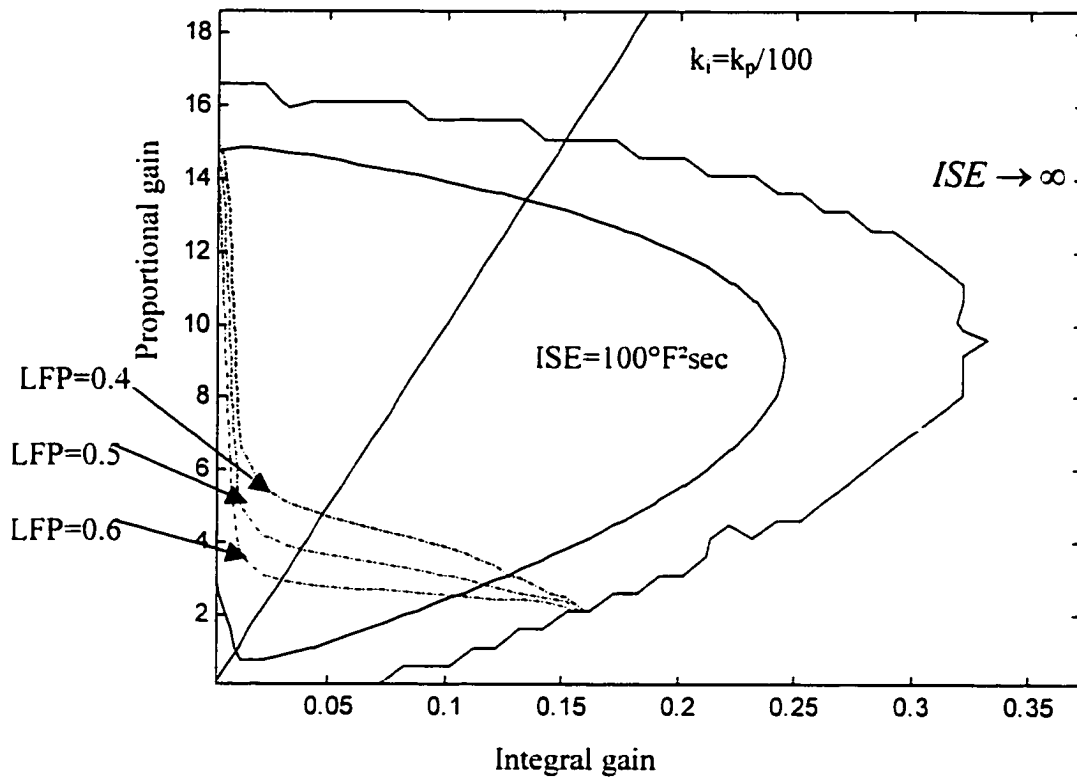
Figure 2-12 *The dynamic and frequency characteristics of a system with time constant of 200 sec. delay time of 20 sec and DC gain of 1°F for 10% valve position change.*
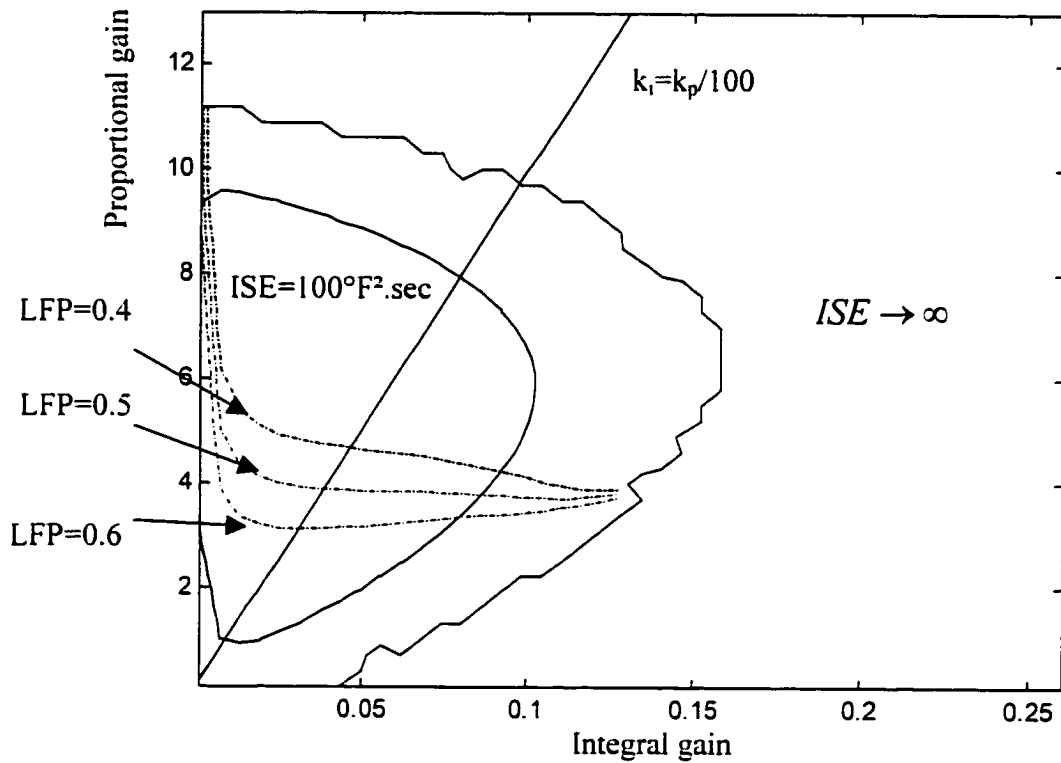
Figure 2-13 *The dynamic and frequency characteristics of a system with time constant*

of 200 sec, delay time of 30 sec and DC gain of 1°F for 10% valve position change.
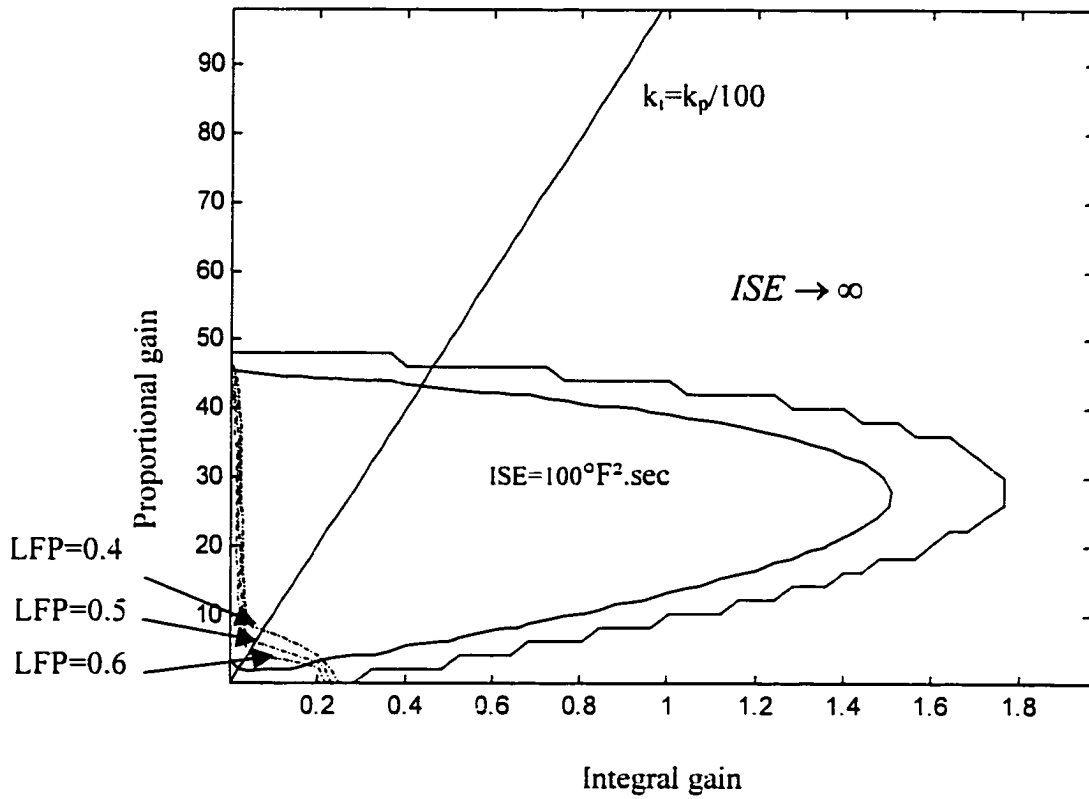
Figure 2-14 *The dynamic and frequency characteristics of a system with time constant*

of 300 sec, delay time of 10 sec and DC gain of 1 °F for 10% valve position change.
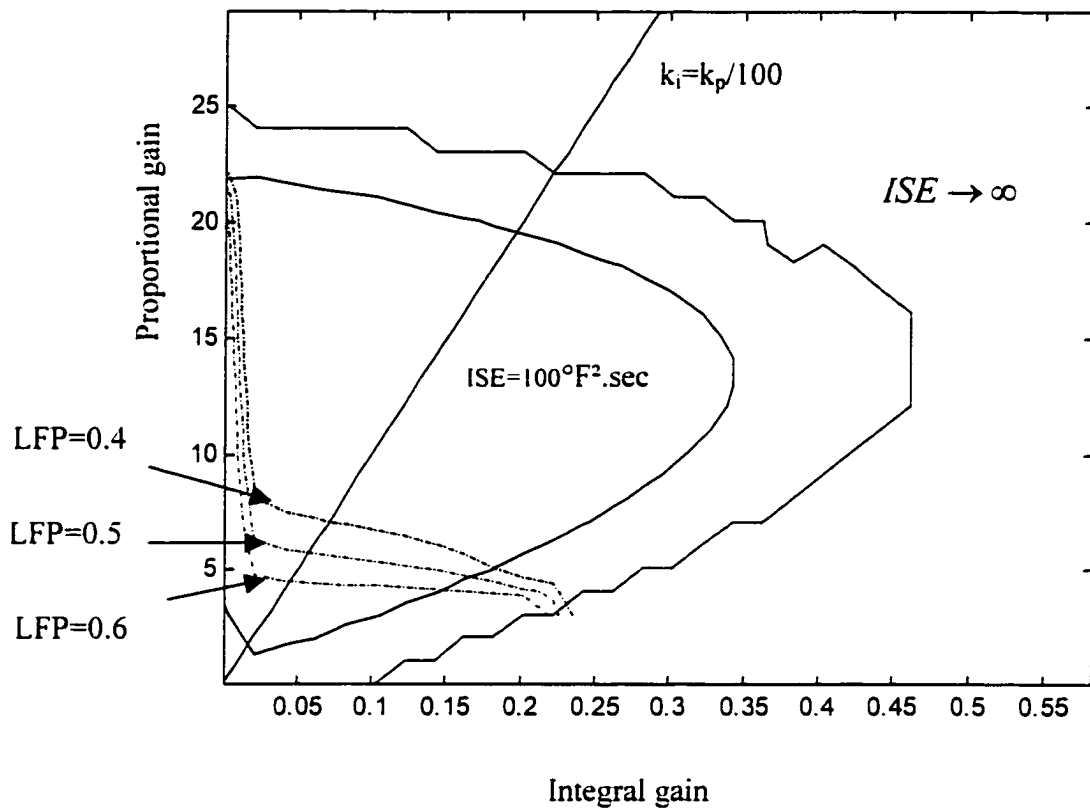
Figure 2-15 *The dynamic and frequency characteristics of a system with time constant of 300 sec, delay time of 20 sec and DC gain of 1 °F for 10% valve position change.*
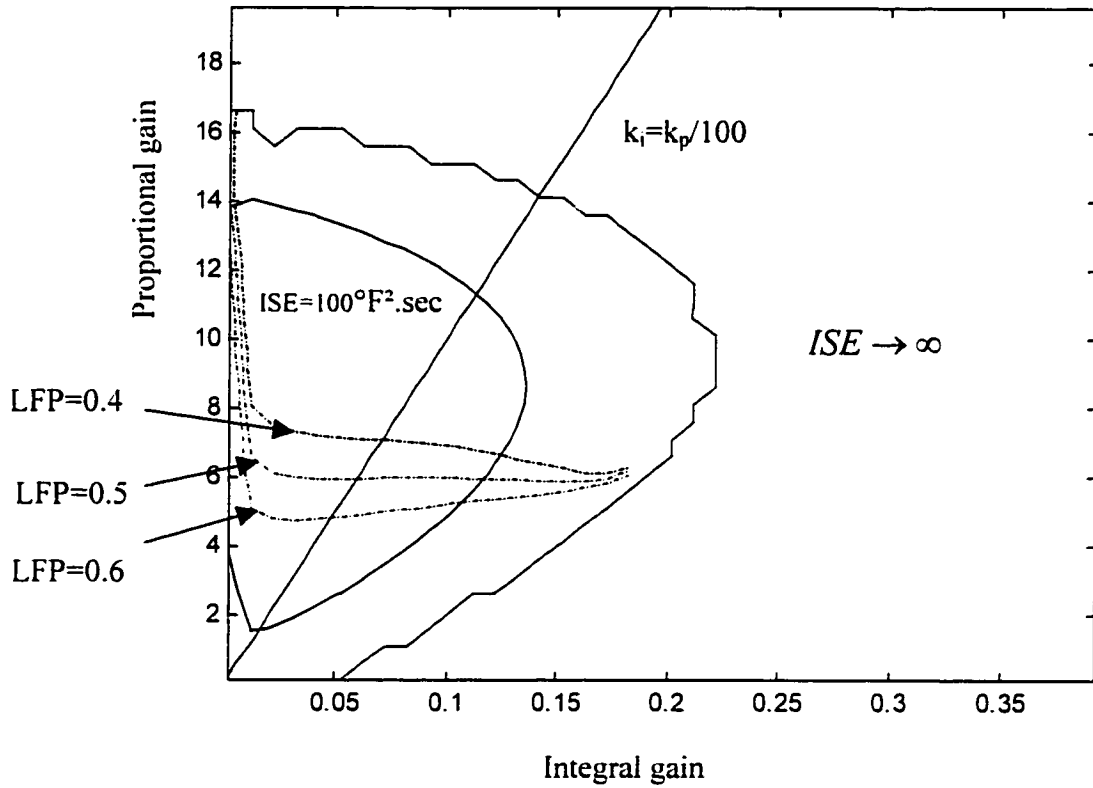
Figure 2-16 *The dynamic and frequency characteristics of a system with time constant*

of 300 sec, delay time of 30 sec and DC gain of 1°F for 10% valve position change.

Further, Equations 2-6, -7, -8, -9, -10, -11 and -12 are then evaluated for fictitious systems, which have parameters well beyond the practical range, namely time constants from 1 sec to 100,000 sec; time delays from 0 sec to 100 sec and a DC gain of 1°F for 10% valve position change, to test the limits of the algorithm (Figure 2-17). This evaluation showed that the new algorithm is feasible when the time constant and delay time of systems are on the left side of the curve in Figure 2-17.

The limits of the new algorithm
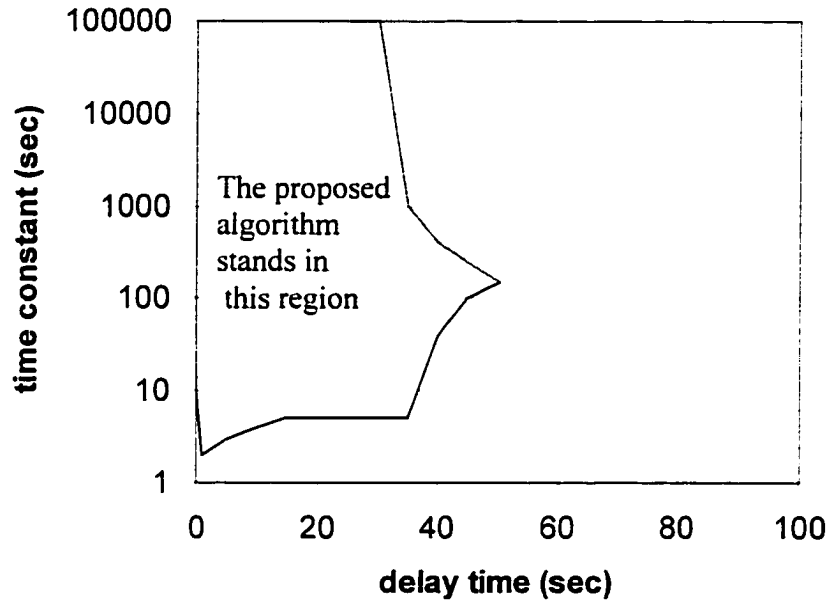
Figure 2-17 The application range of the new algorithm. (The DC gain is chosen as

1°F for 10% valve position change.)

CHAPTER III

THE CALCULATION OF LFP

The tuning algorithm developed requires that the output signal of the coil be separated into two frequency ranges: one includes the frequencies less than the critical frequency w_c, and the other includes the frequencies larger than the critical frequency. This is necessary to calculate the Low Frequency Proportion in Equation 2-7, and then determine the search direction of the P and I gains. We need to analyze the signal in the frequency domain instead of in the time domain to solve this problem. Therefore, the basic frequency analysis concept and the special technique for our algorithm are developed in this chapter.

INTRODUCTION TO FREQUENCY ANALYSIS

It is well known that a prism can be used to break up white light (sunlight) into the colors of the rainbow. In a paper submitted in 1672 to the Royal Society, Isaac Newton used the term spectrum to describe the continuous bands of colors produced by this apparatus. To demonstrate this phenomenon, Newton placed another prism upside-down with respect to the first, and showed that the colors blended back into white light (Figure 3-1). By inserting a slit between the two prisms and blocking one or more colors from hitting the second prism, he showed that the remixed light is no longer white. Hence, the light passing through the first prism is simply analyzed into its component colors without any other change. However, only if we again mix all of these colors do we obtain the original white light.

Violet
Indigo
Blue
Green
Yellow
Orange
Red
Spectrum

(a)

White light

(b)
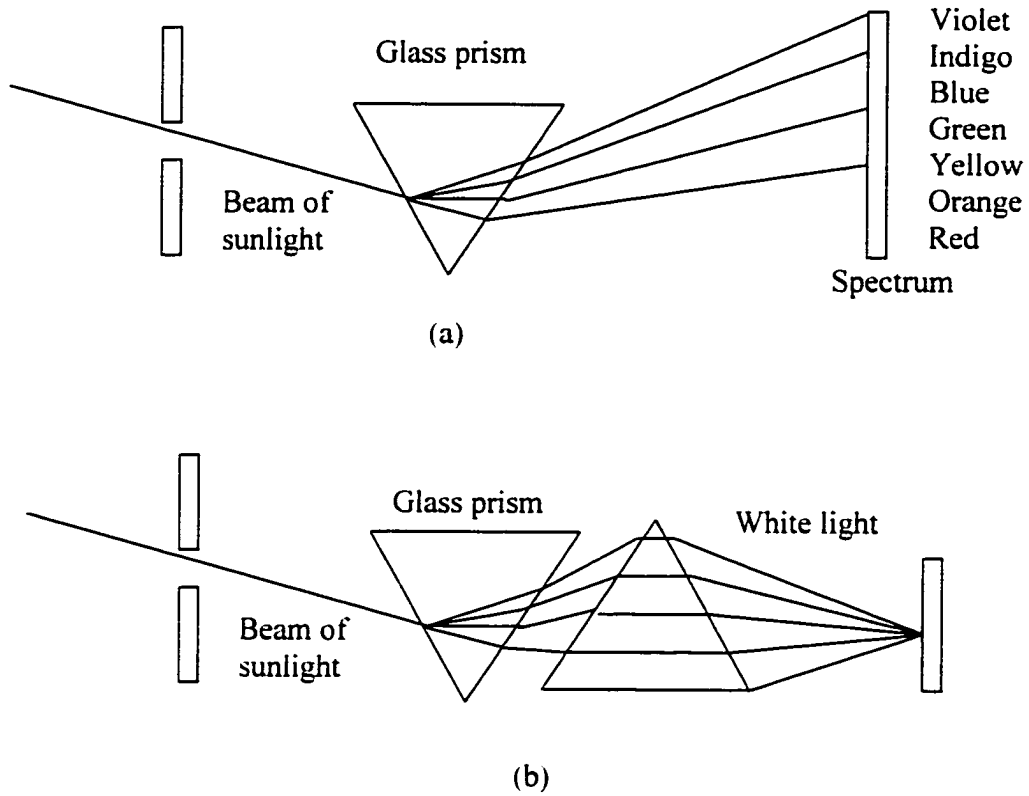
Figure 3-1 *(a) Analysis and (b) synthesis of white light (sunlight) using glass prisms. The prisms have the same function as a Fourier transform. The continuous bands of colors are the signature of the sunlight.*

Later, Joseph Fraunhofer (1787-1826), while making measurements of light emitted by the sun and stars, discovered that the spectrum of the observed light consists of distinct color lines. A few years later (mid-1800s) Gustav Kirchhoff and Robert Bunsen found that each chemical element, when heated to incandescence, radiated its own distinct color of light. As a consequence, each chemical element can be identified by its own line spectrum.

From physics we know that each color corresponds to a specific frequency of the visible spectrum. Hence the splitting of light into colors is actually a form of frequency analysis. Frequency analysis of a signal involves the resolution of the signal into its frequency (sinusoidal) components. Instead of light, our signal waveforms are basically functions of time. The role of the prism is played by the Fourier analysis tool – the Fourier transform. The problem of signal analysis is basically the same for the case of a signal waveform as for the case of the light from heated chemical compositions. Just as in the case of chemical compositions, different signal waveforms have different spectra. Thus the spectrum provides an "identity" or a signature for the signal in the sense that no other signal has the same spectrum. This attribute is the same as the mathematical treatment of frequency domain techniques. If we decompose a waveform into sinusoidal components, in much the same way that a prism separates white light into different colors, the sum of these sinusoidal components results in the original waveform. On the other hand, if any component is missing, the result is a different signal.

Frequency analysis can be processed for both continuous-time signals and discrete-time signals. Among them, frequency analysis of discrete-time signals is usually and most conveniently performed on digital signal processors, which may be general-purpose digital computers or specially designed hardware.

We can sample the difference, e(t), between the coil discharge air temperature and its setpoint at a certain sampling rate to get a discrete-time signal {e (n)}. To perform frequency analysis on a discrete-time signal {e (n)}, we convert the time-domain sequence to an equivalent frequency-domain representation. We know that such a representation is given by the Fourier transform E (w) of the sequence {e (n)}.

$$E(w) = \sum_{n=0}^{N-1} e(n) \exp(-jwn) \qquad 0 \le w \le 2\pi \qquad (3\text{-}1)$$

N is the total number of measurements from the signal.

w is the frequency of interest.

e is the signal in time domain.

E is the representation of the signal in the frequency domain.

n is the order of samples. It is an integer between 0 and N-1.

However, E (w) is a continuous function of frequency and therefore, it is not a computationally convenient representation of the sequence {e (n)}. We represent the sequence {e (n)} by samples of its spectrum E (w) (shown in Equation 3-2). Such a

frequency-domain leads to the Discrete Fourier Transform (DFT), which is a powerful computational tool for performing frequency analysis of discrete-time signals.

$$E_1(k) = E(\frac{2\pi k}{N}) = \sum_{n=0}^{N-1} e(n) \exp(-j2\pi kn / N) \quad k=0, 1, 2... N-1 \qquad (3-2)$$

This transformation is based on two assumptions: one is that the sample duration is adequate which means that "N" is significantly large; the other is that the sampling rate is sufficiently high. The selection of the sampling rate and sample duration for coils is discussed in detail in Chapter IV.

The signal e(t) needs to be separated into the low frequency part and high frequency part in the algorithm. Then we calculate the integral square error of both parts and compare them to get the value of LFP. We repeat the equation of the LFP for convenience.

$$LFP = \frac{\int_{0}^{W_c} [E(w)]^2 dw}{\int_{0}^{\pi} [E(w)]^2 dw} \qquad (3-3)$$

The calculation of LFP in Equation 3-3 can be transformed to the discrete format given in Equation 3-4 based on the DFT technique in Equation 3-2.

$$LFP = \frac{\sum_{k=0}^{k_c} |E_1(k)|^2}{\sum_{k=0}^{N-1} |E_1(k)|^2}$$

(3-4)

Where $k_c = w_c N / 2\pi$ and $E_1(k) = E(w)|_{w=2\pi k / N}$.

So far, a procedure for calculating the LFP has been developed (Figure 3-2). It first converts the signal in time domain to its representation in the frequency domain with Equation 3-2; then the integral square error in different frequency intervals is calculated, and we get the value of LFP as given by Equation 3-4. Significant computer memory and CPU time are required to calculate Equation 3-2, and this luxury is generally not available in field applications. Therefore, the digital filter is introduced to solve this problem.

CALCULATE THE LFP BY DIGITAL FILTER

A filter is a system, which only permits a part of the signal go through, while the remaining frequency content is blocked. For example, a piece of red glass is a filter. It will only let the red light go through, while all other colors included in the original white light are blocked. Mathematically, a filter is a transfer function (H(s) in Equation 3-5). It has a special frequency response, and the magnitude of its response is equal to 1 in certain frequency ranges, while the magnitude is nearly equal to zero in other frequency ranges. A filter is an "ideal" low pass filter if the magnitude of its frequency response is

e (n): the difference between
the coil discharge air
temperature and its setpoint.

Fourier transform

$$E_1(k) = E(\frac{2\pi k}{N}) = \sum_{n=0}^{N-1} e(n)\exp(-j2\pi kn/N)$$

E (k): the representation of e (n)
in frequency domain.

$$LFP = \frac{\sum_{k=0}^{k_c}|E_1(k)|^2}{\sum_{k=0}^{N-1}|E_1(k)|^2}$$

LFP
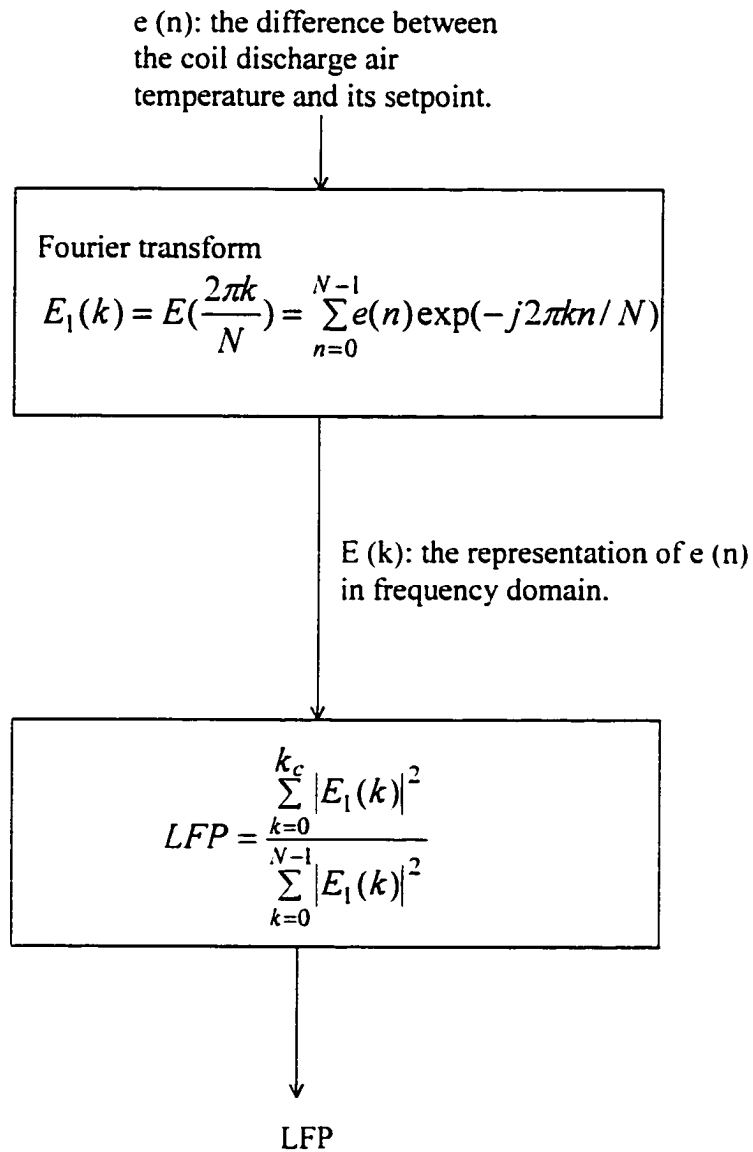
Figure 3-2 The calculation of LFP using Fourier transform.

identically one for all frequencies less than or equal to a cutoff frequency and is zero for all frequencies greater than the cutoff frequency. It is an "ideal" high pass filter if the magnitude of its frequency response is identically one for all frequencies greater than or equal to a cutoff frequency and is zero for all frequencies less than the cutoff frequency. It is called an "ideal" band pass filter if the magnitude of the frequency response is equal to one when the frequency is in the filter's pass-band and is zero for other frequencies.

$$H(s) = \frac{Y(s)}{X(s)} = \frac{a_0 s^n + a_1 s^{n-1} + ... + a_n}{s^n + a_1 s^{n-1} + ... + b_n} \qquad (3-5)$$

X is the input to the filter, which is the original signal.

Y is the output of the filter, which is the filtered signal.

a_i, i=1,2,...,n are constants;

b_i, i=1,2,...,n are constants;

n is the order of the filter.

Basically, the LFP is the ratio of ISE below the cutoff frequency to ISE of the original signal. Therefore, we can pass the discharge air temperature signal through a low pass filter to get the signal content in the low frequency interval, and then divide the ISE at low frequencies by the ISE of the original data to get LFP. This method uses a digital filter instead of a Fourier transform, and it saves CPU time and memory. This procedure is shown in Figure 3-3.
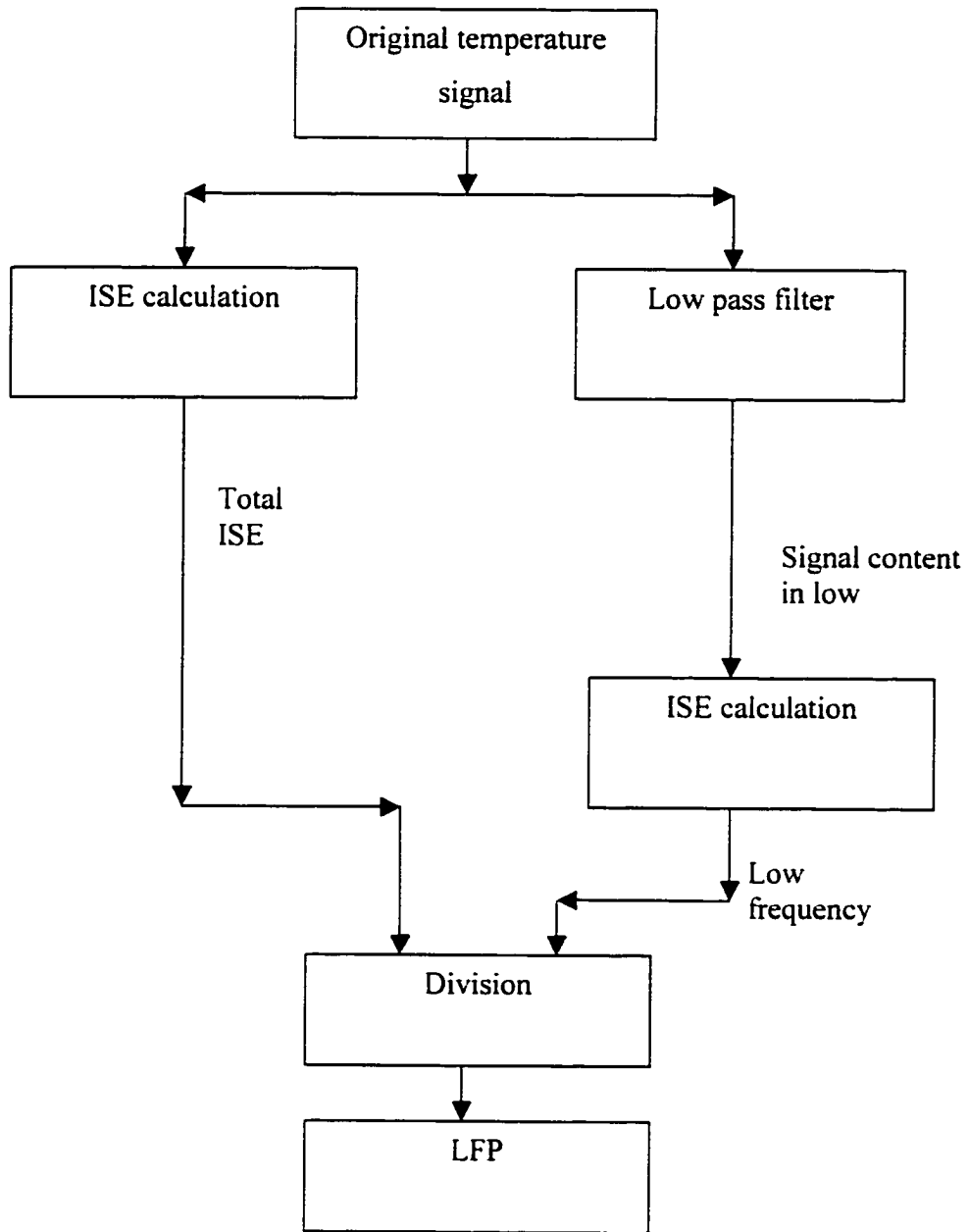
Figure 3-3 A digital filter is used to calculate LFP.

SELECTION OF DIGITAL FILTERS

There are several types of commonly used filters such as: Butterworth filters, Chebyshev filters, and Elliptic filters, etc. A normalized low pass analog filter, having a cutoff frequency of 1 rad/sec and amplitude response of -20dB at the normalized frequency of 1.2, is designed in the format of Butterworth filters, Chebyshev filters and Elliptic filters respectively. The frequency responses of the three filters are shown in Figures 3-4, -5 and -6 respectively.

The magnitude response of the three filters is higher than 0.9 when the system is in the low frequency range. It is lower than 0.1 when the system is in the high frequency range. From the analysis in Chapter II, the LFP is smaller than 0.4 when P and I gains are too large, and the LFP is larger than 0.6 when P and I gains are too small. Therefore, when these three filters are used to calculate LFP, the minimum LFP will be 0.54 when P and I gains are too large, and the maximum LFP will be 0.46 when P and I gains are too small. The calculated LFP is sufficiently accurate to serve as an indicator. It can discern between P and I gains that are too large, and P and I gains that are too small. However, the order of filters is different: the order of the Butterworth filter is 19, the order of the Chebyshev filter is 6, and the order of the Elliptic filter is 4. The Elliptic filter is the most efficient filter among the three due to its low order. We use it in the algorithm and its transfer function is shown in Equation 3-6.
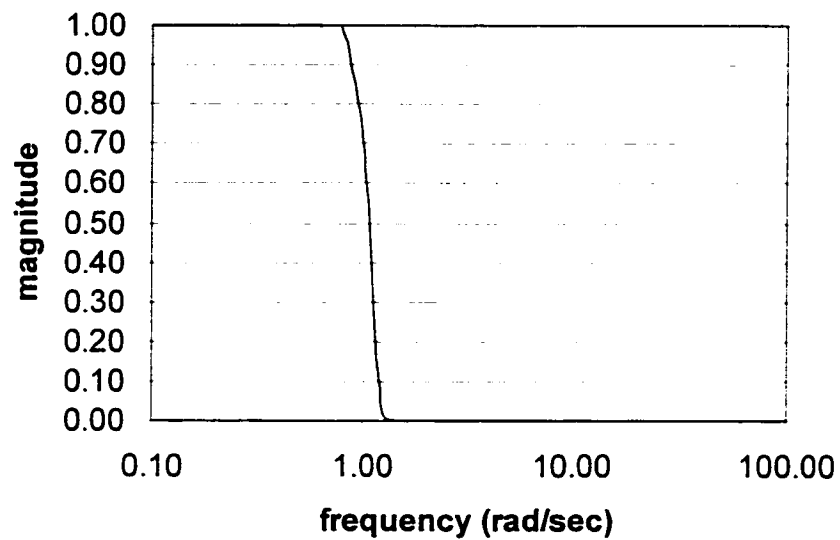
Figure 3-4 *Normalized Butterworth filter with the order of 17. The magnitude is larger than -1db when frequency < 1.0 rad/sec and less than -20 dB when frequency >1.2 rad/sec.*
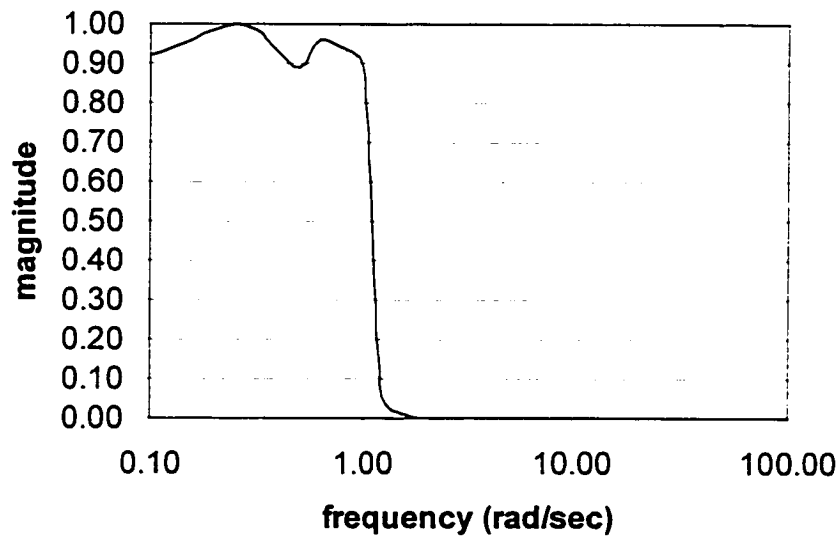
Figure 3-5 *Normalized Chebyshev filter with the order of 6. The magnitude is*

larger than -1db when frequency < 1.0 rad/sec and less than -20 dB when

frequency > 1.2 rad/sec.
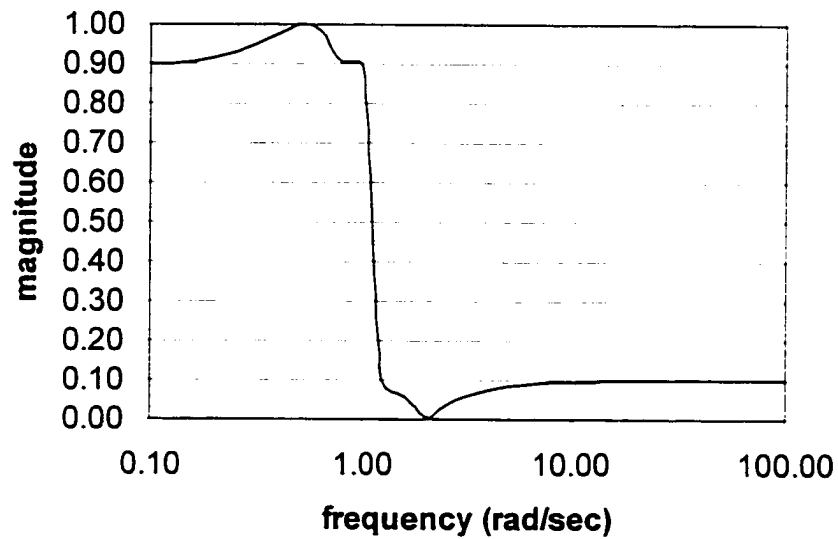
Figure 3-6 *Normalized Elliptic filter with the order of 4. The magnitude*

is larger than -3db when frequency < 1.0 rad/sec and less than -20 dB

when frequency > 1.2 rad/sec.

$$H_{NLF,elliptic}(s) = \frac{0.1s^4 + 0.54s^2 + 0.53}{s^4 + 0.90s^3 + 1.68s^2 + 0.87s + 0.59} \tag{3-6}$$

A low pass digital filter used to calculate LFP at different cutoff frequencies and different sampling intervals can be obtained by using the transformation of Equation 3-7 from the analog normalized low pass filter in Equation 3-6 (Proakis et al. 1996).

$$s \rightarrow \cot\left(\frac{w_c T_s}{2}\right)\left(\frac{z-1}{z+1}\right) \tag{3-7}$$

w_c is the cutoff frequency of the filter. It is chosen as 0.02 rad/sec in the algorithm; T_s is the sample time. It has units of seconds.

CHAPTER IV

THE IMPLEMENTATION OF THE NEW ALGORITHM

We have introduced the general procedure of the new algorithm in Chapter II (Figure 2-7). Then the calculation of LFP is explained in Chapter III (Figure 3-3). The entire procedure consists of combining these two parts. This chapter begins with a discussion of several technical problems. Then the procedure for using the new algorithm is listed step by step.

TECHNIQUES IN THE NEW ALGORITHM

There are several implementation problems that need to be solved before the step by step procedure is given.

1. The selection of sample rate and sample duration

We sample data at a rate of 0.1 Hz. During the normal operation, there are three inputs to the coil leaving air temperature: setpoint changes (when they occur) are a direct input; air flow rate change in the VAV system as a disturbance; coil input air temperature change as another disturbance. First, the setpoint normally changes less than 5°F a day based on outside air temperature. Secondly, changes in air flow rate and coil input air temperature are caused by changes in room load and outside temperature. The dominant frequency of outside air temperature change is $1/86,400$ sec^{-1}, or a period of 24 hours. The dominant room load changes normally occur when the workday begins and

ends. (Some rooms have significant solar load change, which has a dominant period of 24 hours.) For example, they may occur from 7:00am to 9:00am when people come to their offices; or, from 4:00pm to 6:00pm when people leave. The dominant frequency of the room load variation in these special hours is around $1/3600$ sec^{-1}, or a period of 1 hour. Combining above analysis, the coil discharge air temperature will possess a frequency content lower than $1/3600$ sec^{-1}, since the coil can be assumed to be a linear system. Based on the sampling theorem, the highest frequency that can be detected with a sample rate of 10 seconds is $1/20$ sec^{-1}. Therefore, no important information will be lost in the coil operation when the sample rate is 0.10 Hz. The discharge air temperature and its setpoint are sampled at this rate in the algorithm.

Sampling duration is chosen as 20 minutes. In Chapter II, the ISE, which is a criterion of the algorithm, is calculated from the beginning until infinity. Practically, the ISE is calculated only for a duration of 20 minutes. The average value of the difference between the coil discharge air temperature and its setpoint is less than 0.08 °F, if the ISE is less than $100°F^2$.sec when the ISE is calculated over 20 minutes. It can be assumed that the difference becomes zero after this 20 minutes. Meanwhile, this sampling duration will provide enough high frequency discretion, based on the relationship between the frequency discretion and the sampling duration, as described in Equation 4-1. The frequency discretion will be 0.001 sec^{-1} when the sampling duration is 20 min. This frequency discretion is high enough, since the filter used in the dissertation

presented here discerns frequency content lower than 0.02 rad/sec and higher than 0.02 rad/sec.

$$\Delta f = \frac{1}{T_d} = \frac{1}{NT_s} \qquad (4\text{-}1)$$

Δf is the discretion of the signal in frequency domain;

T_d is the sampling duration;

N is the sampling point;

T_s is the sampling time

2. How to calculate ISE

The ISE is calculated over a duration of 20 minutes and is calculated using Equation 4-2 instead of Equation 3-1, where the sampling rate was 10 sec.

$$ISE_T = 10 * \sum_{i=0}^{119} e(i)^2 = 10 * \sum_{i=0}^{119} (t_{ao}(i) - t_{ao.set}(i))^2 \qquad (4\text{-}2)$$

ISE_T is the ISE of the original temperature difference. We add a subscript "T" to distinguish the ISE of the original temperature difference from the filtered signal, which will be introduced later.

$t_{ao}(i)$ is the sampled value of the coil discharge air temperature.

$t_{ao,set}(i)$ is the sampled value of the coil discharge air temperature setpoint.

i is the sample number. A sampling set is completed when i changes from 0 to 119. In total, 120 points are sampled. The duration is 20 minutes since the sampling rate is 10 sec.

Equation 4-3 can be used to more efficiently calculate ISE in field application of the algorithm.

$$ISE_{i+1} = ISE_i + 10 * (t_{ao}(i) - t_{ao,set}(i))^2 \qquad (4\text{-}3)$$

where,

i=0, 1, 2...119.

ISE_i=0 when i=0. The final value of ISE_T is equal to ISE_i when i=119.

3. How to calculate LFP

LFP in Equation 3-7 is the indicator to determine whether we should increase or decrease P and I gains. As introduced in Chapter III, we can pass the discharge air temperature signal through an elliptic low pass filter, then divide the ISE of the signal in the low frequency range by the ISE of the original data to get LFP (Figure 3-3).

Based on the analysis of Chapter II, the cutoff frequency of the elliptic low pass filter is selected as 0.02 rad/sec. When the sampling interval is chosen as 10 seconds, the

filter can be obtained by using Equation 3-11 to transform Equation 3-10. This filter is expressed in the z-domain as Equation 4-4, in which z is the variable. It can also be described in the time domain as Equation 4-5 with i as the variable, in which e is the difference between the coil discharge air temperature and its setpoint; el is the difference after the filter. It only retains the low frequency content of the original signal. All high frequency components are blocked.

$$H(z) = \frac{el(z)}{e(z)} =$$

$$\frac{0.096556 - 0.381025z^{-1} + 0.568988z^{-2} - 0.381025z^{-3} + 0.096556z^{-4}}{1 - 3.897167z^{-1} + 5.708831z^{-2} - 3.725218z^{-3} + 0.913610z^{-4}}$$

(4-4)

$$el(i) = 0.096556e(i) - 0.381025e(i-1) + 0.568988e(i-2)$$
$$- 0.381025e(i-3) + 0.096556e(i-4) + 3.897167el(i-1)$$
$$- 5.708831el(i-2) + 3.725218el(i-3) - 0.913610el(i-4)$$

(4-5)

The ISE in the low frequency region can then be calculated using a similar approach to that used to obtain the total ISE.

$$ISE_{L,i+1} = ISE_{L,i} + 10 * el^2$$

(4-6)

where,

i=0, 1, 2...119.

$ISE_{L,i}$=0 when i=0. The final value of ISE_L is equal to $ISE_{L,i}$ when i=119.

Combining with the result from Equation 4-3,

$$LFP = \frac{ISE_L}{ISE_T} \tag{4-7}$$

THE PROCEDURE OF THE NEW ALGORITHM

The whole procedure of the new algorithm can be processed step by step based on the techniques described above and shown in Figure 4-1.

1. First, we sample the coil discharge air temperature and its setpoint at the sampling rate of 10 seconds.

2. Then we will calculate ISE of the original temperature difference based on Equation 4-3. The final value of ISE is obtained after 20 minutes. The P and I gains remain unchanged if the ISE is less than $100°F^2$.sec. P and I gains will need to be changed if the ISE is larger than $100°F^2$.sec.

3. The value of LFP needs to be calculated before the P and I gains are changed. The difference between the coil discharge air temperature and its setpoint passes through the low pass filter, which is described in Equation 4-5. The ISE of the filtered signal can be calculated as Equation 4-6. Thereafter, the LFP can be obtained by dividing the filtered ISE by the original ISE, which is described in Equation 4-7.

4. The P and I gains need to decrease if LFP is smaller than 0.5, while P and I gains need to increase if LFP is larger than 0.5.
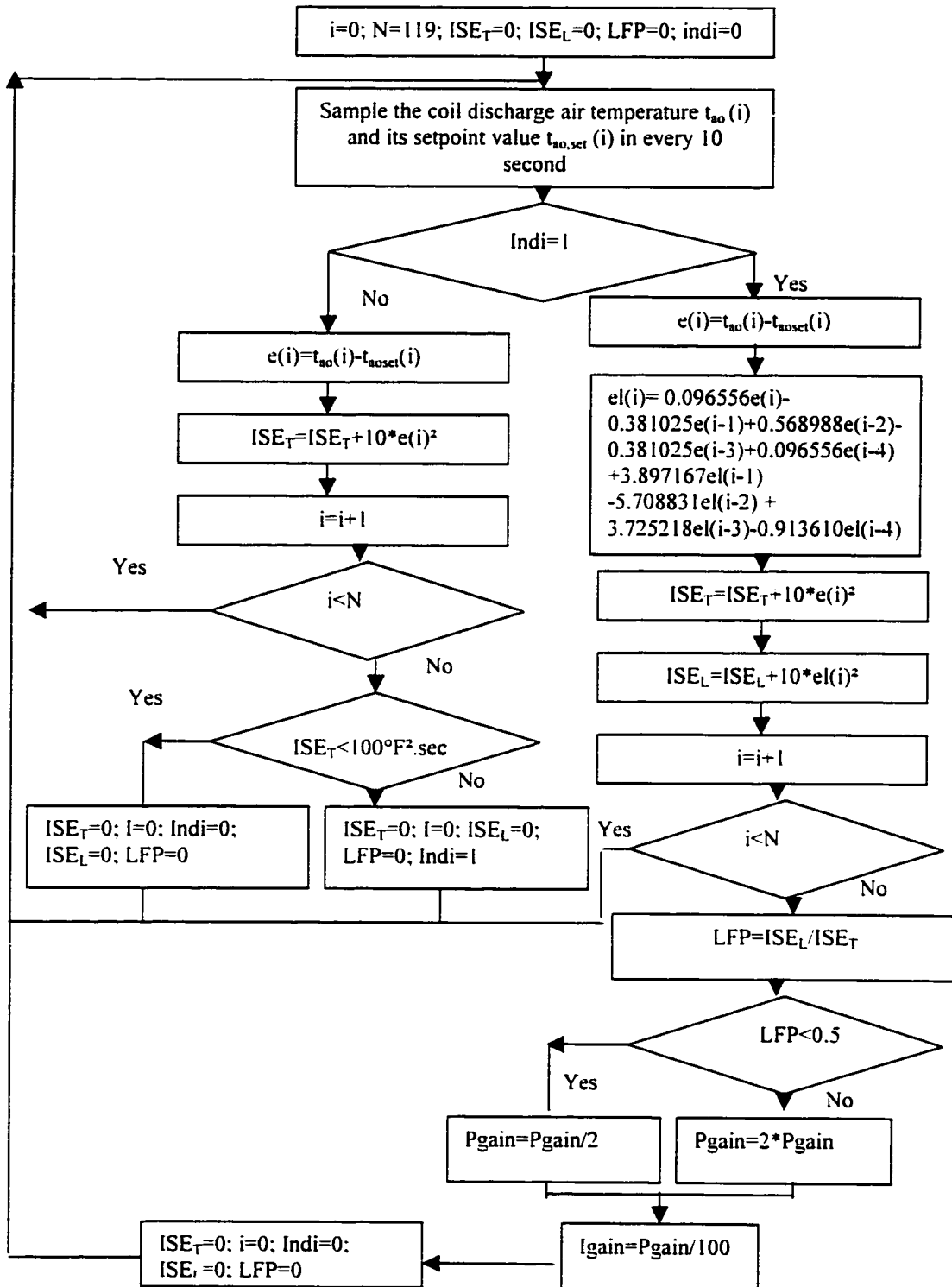
Figure 4-1 *The procedure of the new algorithm.*

5. The P and I gains keep the ratio of 100 when their values are changed. The P and I gains will be cut in half if they need to be decreased. The P and I gains will be doubled if they need to be increased.

CHAPTER V

APPLICATION OF THE NEW ALGORITHM

The algorithm is applied to a real case in this chapter. First, the tested system is introduced. Then the algorithm is written in a control language and combined into the original control program. Finally, the application of the algorithm is demonstrated and shown to function correctly for two test cases.

INTRODUCTION OF THE TESTED SYSTEM

The cooling coil of AHU#10 in the Zachry Engineering Center on the Texas A&M University campus was selected to test the algorithm. The air conditioning system in this building is a dual duct system (Figure 5-1). The system first mixes the return air and outside air together. The minimum fresh air requirement can be maintained, meanwhile the energy efficiency can be maximized by adjusting the ratio of the outside air and the return air which normally have different temperatures. Pneumatic dampers are used to control this process. The supply fan gives a preset pressure rise so that an adequate indoor air supply rate is maintained. A variable frequency drive (VFD) is used to control the fan speed. A part of the mixed air goes to the cold duct. It is cooled down to a preset temperature in the cooling coil using chilled water, which is circulated through the cooling coil. Meanwhile the rest of the air goes to the hot duct. It is heated to a preset temperature in the heating coil using hot water, which is circulated through the heating coil. Both cold air and hot air are sent throughout the building. Finally, the
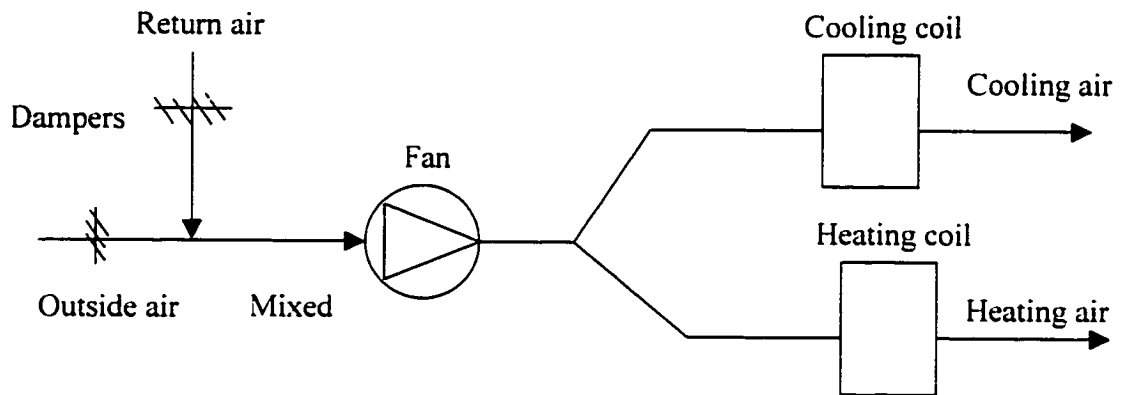
Figure 5-1 The schematic diagram of the tested dual duct system.

terminal mixing box for each room adjusts the ratio of cold air and hot air, and each room gets supply air at the temperature it requires.

Several preset values need to be determined for this air handling system. They are selected so that the energy efficiency is maximized and indoor comfort is maintained (Liu and Claridge 1998).

1. Static air pressure after the fan. A VFD controls the fan speed so that the lower of the cold duct static pressure and the hot duct static pressure is maintained at a setpoint. This setpoint is pre-calculated based on outside air temperature: The setpoint is 1 inch of water when the outside air temperature is lower than 55 °F. The setpoint is 2 inches of water when the outside air temperature is higher than 80 °F. The setpoint is linearly interpolated when the outside air temperature is between 55 °F and 80 °F. The control scheme is expressed in Equation 5-1.

$$P_{set} = \begin{cases} 1 & t_o < 55°F \\ \dfrac{t_o - 55}{80 - 55} + 1 & 55°F < t_o < 80°F \\ 2 & t_o > 80°F \end{cases} \qquad (5\text{-}1)$$

where

P_{set} is the pressure setpoint.

t_o is the outside air temperature.

2. The heating coil discharge air temperature setpoint. This setpoint is also pre-calculated based on outside air temperature: The setpoint is 90°F when the outside air temperature is lower than 55°F. The setpoint is 70°F when the outside air temperature is higher than 70°F. The setpoint is linearly interpolated when the outside air temperature is between 55°F and 70°F. The control scheme is expressed in Equation 5-2.

$$t_{ao\_set.h} = \begin{cases} 90 & t_o < 55°F \\ 90 - \dfrac{t_o - 55}{70 - 55}(90 - 70) & 55°F < t_o < 70°F \\ 70 & t_o > 70°F \end{cases} \qquad (5\text{-}2)$$

3. The cooling coil discharge air temperature setpoint. This setpoint is also pre-calculated based on outside air temperature: The setpoint is 60°F when the outside air temperature is lower than 55°F. The setpoint is 54°F when the outside air temperature is higher than 94°F. The setpoint is linearly interpolated when the outside air temperature is between 55°F and 94°F. The control scheme is expressed in Equation 5-3.

$$t_{ao\_set.c} = \begin{cases} 60 & t_o < 55°F \\ 60 - \dfrac{t_o - 55}{94 - 55}(60 - 54) & 55°F < t_o < 94°F \\ 54 & t_o > 94°F \end{cases} \qquad (5\text{-}3)$$

THE ORIGINAL CONTROL PROGRAM

The system is controlled by a Direct Digital Control (DDC) system, which was installed by Landis & Staefa, Inc. The control scheme is programmed in a high level language designed by the company. Then the program is downloaded to the Field Control Units (FCU) in the office. Usually, there are several FCUs in a building, and each FCU controls at least one AHU. Among these FCUs, FCU #5 controls AHUs #9, 10, and 11. The original control scheme for AHU #10 is shown in Figure 5-2 from lines 170 to 330. The flow chart is shown in Figure 5-3.

Two commands in the program are different from common high level languages. The first one is *TABLE (X1, X2, Y1, Y2, Z1, Z2)*: this command means the value of X2 is determined by X1. X2 is equal to Y2 if X1 is less than Y1. X2 is equal to Z2 if X1 is larger than Z1. X2 will be linearly interpolated when X1 is between Y1 and Z1. The second command is *LOOP (DIRECTION,MEASUREMENT,CONTROL, SETPOINT, PGAIN, IGAIN, DGAIN, SAMPLING, INITIAL, MIN, MAX,X)*: This statement functions as a PI controller. There are a total of 12 parameters in the statement: DIRECTION is a parameter to determine the direction of the control signal. It can be selected as either '128' or '0'. The control signal will increase when the measurement is larger than the setpoint if DIRECTION is selected as 0, while the control signal will decrease when the measurement is larger than the setpoint if DIRECTION is selected as 128; MEASUREMENT is the signal sent into the PI controller from a sensor. It can be temperature, pressure etc. The objective of the PI controller is to maintain this parameter

170   IF (B10FRZ .EQ. OFF) THEN GOTO 220

180   OFF (B10SS)

190   SET (1.0,B10OAD,B10CDV,B10SPD)

200   SET (1.0,B10HDV)

210   GOTO 391

220   IF (B10PR .EQ. ON) THEN GOTO 260

230   SET (1.0,B10OAD)

240   SET (18.0,B10CDV,B10HDV)

250   GOTO 391

260   TABLE (OADBT,B10STA,55,1,80,2)

270   TABLE (OADBT,B10HSP,55.0,90.0,70.0,70.0)

280   TABLE (OADBT,B10CSP,55,60,90,54)

290   LOOP (0,B10MAT,B10OAD,55.0,70,2,4000,3,11.0,7.0,14.0,0)

300   MIN ($LOC3 ,B10CDS,B10HDS)

310   LOOP (128,$LOC3 ,B10SPD,B10STA,100,5,0,1,8.0,3.0,15.0,0)

320   LOOP (0,B10HDT,B10HDV,B10HSP,750,15,0,1,8.0,4.0,18.0,0)

330   LOOP (128,B10CDT,B10CDV,B10CSP,ZPGAIN,ZIGAIN,0,1,8.5,5.0,12.0,0)

Figure 5-2 *The original program for AHU #10 (lines 170 -330) followed by the implementation of the new algorithm.*

350   IF (ZK .EQ. 1) THEN GOTO 380

360   SAMPLE (10) GOSUB 2000 B10CDT,B10CSP,ZK,ZN,ZM

370   GOTO 391

380   SAMPLE (10) GOSUB 4000 ZPGAIN,ZIGAIN, B10CDT,B10CSP,ZK,ZN,ZM

1000 GOTO 5010

2000 ZEN=ZEN+($ARG1-$ARG2)*($ARG1 - $ARG2)

2050 $ARG5 = $ARG5 + 1

2060 IF ($ARG5 .LT. $ARG4) THEN GOTO 3000

2065 $ARG5 = 0

2070 IF (ZEN .GT. 10.0) THEN GOTO 2075

2071 $ARG3 = 0

2072 GOTO 2080

2075 $ARG3 = 1

2080 ZEN=0

3000 RETURN

4000 ZY5 = $ARG3 - $ARG4+10

4010 ZYH1=0.096556*ZY5+0.568988*ZY3+0.096556*ZY1+3.897167*ZYL4

+3.725218*ZYL3

4020 ZYH2=0.381025*ZY4+0.381025*ZY2+5.708831*ZYL3+0.913610*ZYL1

4030 ZYL5=ZYH1-ZYH2

4031 4170 ZYL1 = ZYL2

Figure 5-2 continued

```
4180  ZYL2 = ZYL3

4190  ZYL3 = ZYL4

4120  ZYL4=ZYL5

4210  ZY1 = ZY2

4220  ZY2 = ZY3

4230  ZY3 = ZY4

4240  ZY4=ZY5

4270  $ARG7 = $ARG7 + 1

4300  ZEL = ZEL + (ZYL4 -10) *( ZYL4 - 10)

4300  ZEN = ZEN + (ZY4 - 10) * (ZY4 - 10)

4330  IF ($ARG7 .LT. $ARG6 ) THEN GOTO 5000

4340  LFP=ZEL/ZEN

4440  IF (LFP .GT. 0.5) THEN GOTO 4500

4450  $ARG1=2*$ARG1

4460  GOTO 4600

4500  $ARG1=$ARG1/2

4600   $ARG2=$ARG1/100

4610  SET(0,$ARG7, ZEL,ZEN, ZYL1, ZYL2, ZYL3, ZYL4,ZYL5, ZY1, ZY2, ZY3, ZY4)

4620  $ARG5=0

5000  RETURN

5010  GOTO 10
```

Figure 5-2 *continued*
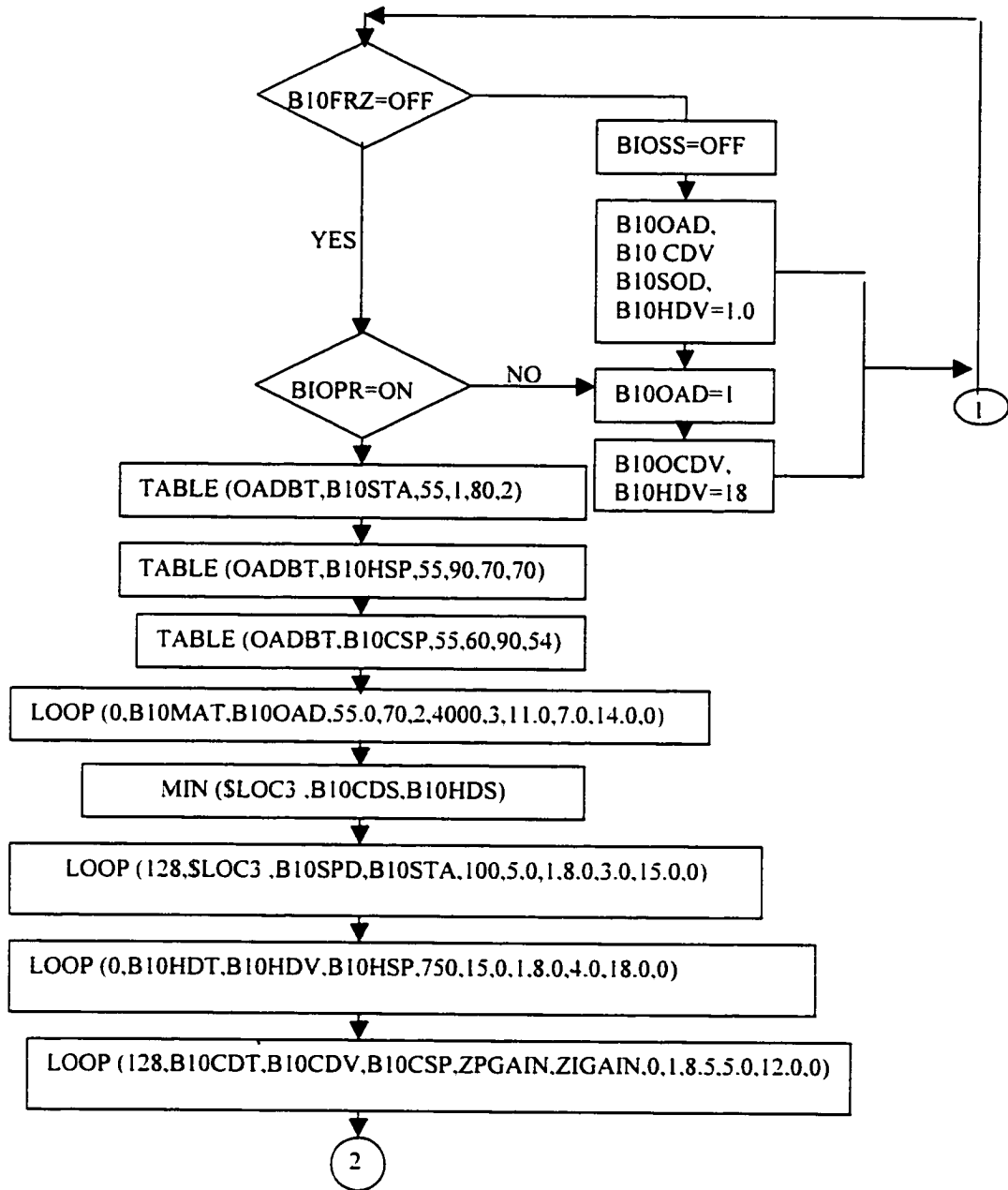
Figure 5-3 *The flow chart for the original control program.*

at its setpoint; CONTROL is the signal sent out to the actuator. The setpoint is supposed to be maintained when the signal is correct; SETPOINT is the value the measurement needs to maintain. It is pre-defined; PGAIN is the proportional gain of the PI controller. IGAIN is the integral gain of the PI controller; DGAIN is the derivative gain of the PID controller if it is not equal to zero. The controller will become a PI controller if the DGAIN is selected as zero; SAMPLING is the sampling rate of the PI controller; INITIAL is the initial value the PI controller will send out; MIN is the minimum value the PI controller will send out; MAX is the maximum value the PI controller will send out; X is not used and is entered as 0.

Variables in the program of Figure 5-2 will keep their initial values in the process unless they are changed by sensors or by program statements. The parameter definitions of the program from lines 170 to 330 in Figure 5-2 are as follows:

B10CDS is the static pressure for the cold duct. This is a measurement from the pressure sensor installed in the system. It is sent to the corresponding FCU. The initial value is 1 inH$_2$O.

B10CDT is the cooling coil discharge air temperature. This is a measurement from the temperature sensor installed in the system. It is sent to the corresponding FCU. The initial value is 55 °F

B10CDV is the control signal to the cooling coil valve. The valve is normally open and the spring range is from 5 psi to 12 psi. Its initial value is 8 psi.

B10CSP is the temperature setpoint for the cooling coil discharge air. It is a temporary parameter in the FCUs. It is used for numerical calculation. We call it a 'soft point'. Its initial value is 55 °F.

B10FRZ is the indicator of freezing mixed air temperature. It is a sensor signal sent from the system to the FCU. It will be 1 if there is freezing air flowing inside. Otherwise it is 0. Its initial value is 0.

B10HDS is the static pressure for the hot duct. It is a measurement that comes from the pressure sensor. Its initial value is 1 inH$_2$O.

B10HDT is the heating coil discharge air temperature. It is a measurement that comes from the temperature sensor. Its initial value is 100°F.

B10HDV is the control signal to the heating coil valve. The valve is normally open. It has a spring range from 4 psi to 18 psi and its initial value is 13 psi.

B10HSP is the temperature setpoint for the heating coil discharge air. It is a soft point in the FCU with an initial value of 100°F.

B10MAT is the mixed air temperature. It is a measurement from the temperature sensor with an initial value of 70°F.

B10OAD is the outside air damper. It is a pneumatic damper. The input signal has a range of 7 psi to 14 psi and its initial value is 11 psi.

B10PR is the indicator of whether the fan is in "on" status. It is a signal which comes from the system. It will be 1 if the fan is on, while it will be 0 if the fan is off. Its initial value is 1.

B10SPD is the control signal to the VFD. The VFD has a range from 3 psi to 15 psi, with an initial value of 8 psi.

B10SS is the start signal for the AHU. The value will be 1 if the AHU is on; otherwise it will be 0. Its initial value is 1.

B10STA is the static pressure setpoint. It is calculated based on outside air temperature.

OADBT is the outside air temperature. It comes from the temperature sensor. Its initial value is 55°F.

ZPGAIN is the Proportional gain for the PI controller of the cooling coil. It is a soft point in the program with an initial value of 100.

ZIGAIN is the Integral gain for the PI controller of the cooling coil. It is a soft point in the program with an initial value of 1.

Lines 170-250 in Figure 5-2 are used to protect the air handling system under emergency conditions, such as when freezing air enters the system or the fan is manually or accidentally shut down.

Line 260 is used to calculate the static pressure setpoint (B10STA) based on outside air temperature (OADBT). It has the same function as Equation 5-1. Line 270 is used to calculate the discharge air temperature setpoint (B10HSP) for the heating coil based on outside air temperature. It has the same function as Equation 5-2. Line 280 is used to calculate the discharge air temperature setpoint (B10CSP) for the cooling coil based on outside air temperature. It has the same function as Equation 5-3.

Line 290 is used to control the dampers so that the mixed air temperature does not go below 55°F. This is done by sending a pneumatic signal to control the damper position (B10OAD). The "loop" statement functions as a PI controller. The P gain of this PI controller is 0.7. The I gain is 0.02. The sampling rate is 1 second. The initial value of the control signal is 11 psi. The minimum value of the control signal is 7 psi. The maximum value is 14 psi. These values are determined by hardware requirements.

Line 300 is used to select the lower value between the cold duct static pressure (B10CDS) and the hot duct static pressure (B10HDS). Then this value is put into the temporary variable $Loc3. Then line 310 functions as a PI controller to calculate the fan speed based on the setpoint (B10STA) and the value of $loc3. The P gain is 0.1 and the I gain is 0.05. The sampling rate is one second. The initial signal is eight psi. The minimum value of the signal is three psi and the maximum value is 15psi.

Line 320 is a PI controller to control the heating coil discharge air temperature at its setpoint (B10CSP). The P gain is 7.5 and the I gain is 0.15. The sampling rate is one second. The controller sends out a pneumatic signal (B10HDV) to the hot deck valve. The initial value is eight psi, while the minimum value is 4 psi and the maximum value is 18 psi.

Line 330 is a PI controller to control the cooling coil discharge air temperature at its setpoint (B10CSP). The P gain is ZPGAIN. The I gain is ZIGAIN. The sampling rate is one second. The controller sends out a pneumatic signal (B10CDV) to the cold deck valve. The initial value is eight psi. The minimum value is 5 psi and the maximum value is 12 psi.

The P gain (ZPGAIN) and I gain (ZIGAIN) of the PI controller for the cooling coils are fixed as 1 and 0.05 initially. However, we found that the controller performs well with these settings only during the summer. The discharge air temperature can never reach the setpoint in winter. The on-line self-tuning algorithm is required to make the cooling coil discharge air temperature match its setpoint quickly throughout the year.

PROGRAMMING OF THE NEW ALGORITHM

Lines 350 to 5010 in Figure 5-2 are combined with the original program to automatically tune up the P and I gains. The flow chart of the tune-up process is shown in Figure 5-4. All the parameters required in the added program lines are soft points. They need less memory than hard points, such as outside air temperature. The parameter definitions are as follows:

$ARGn is a pseudo variable. It represents the nth parameter that is passed from the main program to the subroutine. n can be chosen as an integer from 1 to 20.

LFP is the low frequency proportion. It is used to determine the search direction for P and I gains. Its initial value is 0.
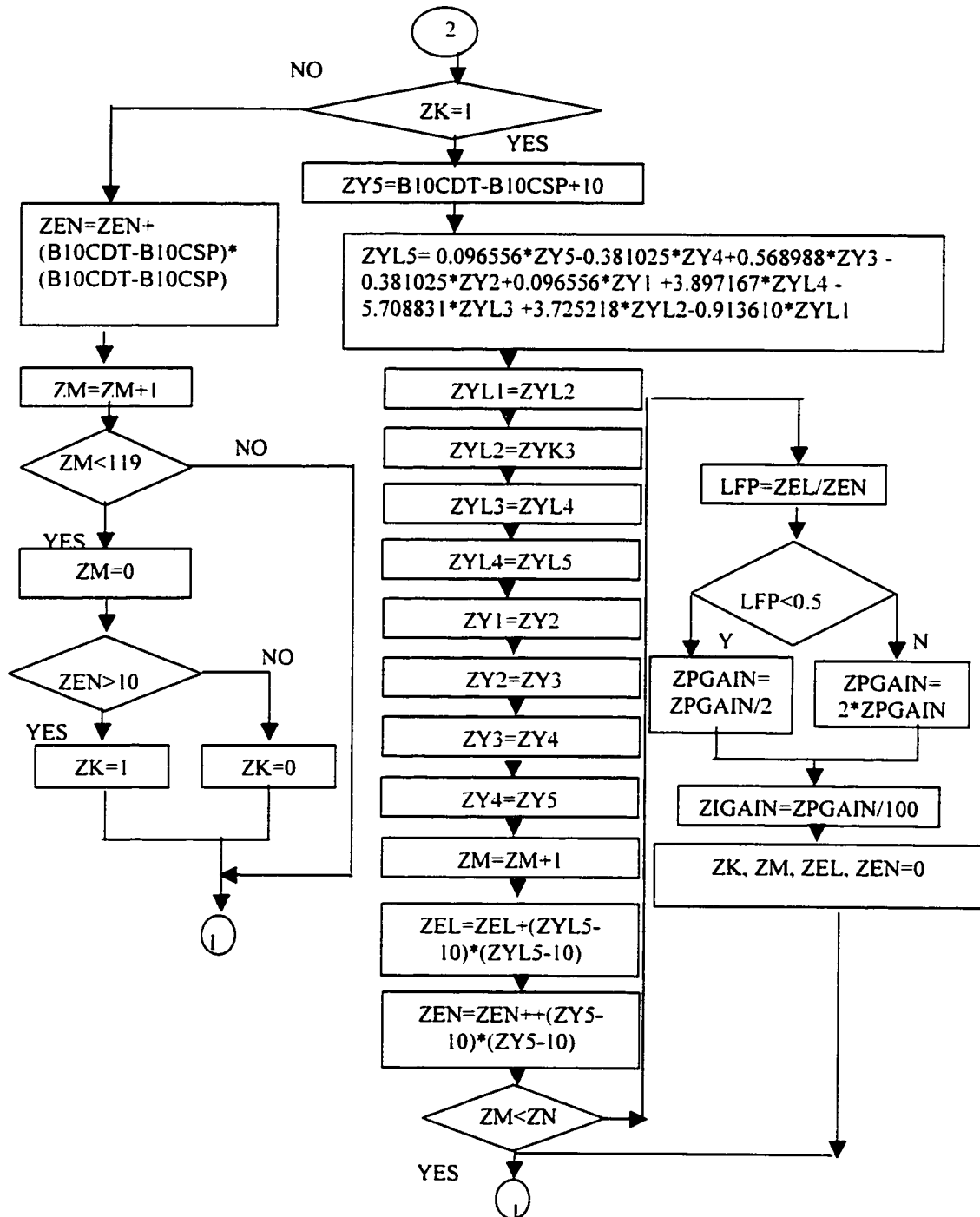
Figure 5-4 The flow chart for the newly added program.

$LOC3 is the smaller of the cold duct pressure and the hot duct pressure.

ZEL is the ISE for the signal in the low frequency band. Its initial value is 0.

ZEN is the ISE for the original signal. Its initial value is 0.

ZK is the indicator to determine whether P and I gains need to be adjusted. Its initial value is 0.

ZM is the counter. Its initial value is 0.

ZN is a fixed value. Its initial value is 119.

ZTD is the difference between the coil discharge air temperature and its setpoint. Its initial value is 0.

ZYL1 is from the fourth previous sampling time filtered signal. Its initial value is 10.

ZYL2 is from the third previous sampling time filtered signal. Its initial value is 10.

ZYL3 is from the second previous sampling time filtered signal. Its initial value is 10.

ZYL4 is the previous filtered signal. Its initial value is 10.

ZYL5 is the current filtered signal. Its initial value is 10.

ZY1 is from the fourth previous sampling time original signal. Its initial value is 10.

ZY2 is from the third previous sampling time original signal. Its initial value is 10.

ZY3 is from the second previous sampling time original signal. Its initial value is 10.

ZY4 is the previous original signal. Its initial value is 10.

ZY5 is the current signal. Its initial value is 10.

"ZK" in line 350 of Figure 5-2 is the indicator of whether the P and I gains need to be adjusted. It has a value of either 0 or 1. The P and I gains need to be adjusted if ZK is 0. P and I gains keep their original values if ZK is 1. ZK is set as 0 initially.

If ZK is 0, the program will go to the subroutine in lines 2000 to 3000. This subroutine is used to calculate ISE, as given by Equation 4-3. The subroutine will set ZK to 1 if ISE is larger than 100 while it will set ZK to 0 if ISE is less than 100. "SAMPLE (10)" in line 360 means the sampling rate of the subroutine is 10 seconds. B10CDT is the cooling coil discharge air temperature sent to the subroutine. B10CSP is the setpoint. ZK is the indicator of whether P and I gains need to be adjusted. ZN has the same function as N in Equation 4-3 and is set as 119 before hand. ZM is a counter. It is the same as "i" in Equation 4-3.

If ZK in line 350 is equal to 1, which means the P and I gains need to be adjusted, the program will go to a subroutine in lines 4000 to 5000. This subroutine is used to search for new P and I gains. First, the original difference signal (ZY4) between the coil discharge air temperature and its setpoint is passed through the low pass filter, as given in Equation 4-5. This is done in lines 4000 to 4230. Then the ISE of the low frequency difference (ZEL) (Equation 4-6) is calculated in line 4300. The ISE of the original difference (ZEN) (Equation 4-3) is calculated in line 4310. Finally, LFP (Equation 4-7) is calculated in line 4340. If LFP is larger than 0.5, the P gain is doubled (line 4450) and the I gain is set to 1% of the P gain (line 4600). If LFP is smaller than

0.5, the P gain is cut in half (line 4500) and the I gain is set to 1% of P gain (line 4600). Line 4610 is used to set the initial values of the program.

The new algorithm has been easily implemented. It needs a very small amount of memory in the FCU. 40 lines are added to the original program to implement the new algorithm and a total of 14 soft points are added to the control system.

These 40 lines are written in very basic commands. They can be modified to fit in the control languages for Johnson Control and Honeywell. In both subroutines, the pseudo variable $ARGn is used to represent the nth variable which is passed from the main program to subroutines. For example, $ARG1 in the first subroutine represents B10 CDT and $ARG1 in the second subroutine is used to present ZPGAIN. Therefore, the subroutines become more general. They can be easily modified to apply to other coils by simply changing the variables in line 360 and line 380.

THE APPLICATION RESULTS

Two tests were conducted to validate the algorithm. The results were recorded using the embedded function of the Energy Management System (EMS) software produced by Landis & Staefa, Inc.

The first test is shown in Figures 5-5 and -6. In the beginning, a high pair of P and I gains, which are 7.5 and 0.075 respectively, replaced the optimal values of 2 and 0.02. Oscillation occurred as soon as the high P and I gain values were used. The discharge air temperature oscillates with a period of three minutes and relatively constant amplitude for about six cycles (The process lasts for 20 minutes). The algorithm detected this poor performance, and decreased the P and I gains to 3.75 and 0.0375 respectively. The oscillation amplitude decreased and the period increased. After another 20 minutes, the P and I gains decreased to 1.88 and 0.0188 respectively. Consequently, the oscillation amplitude decreased more and the period increased more. The oscillation disappeared after 40 minutes and the setpoint was reached. It appears that this algorithm is capable of identifying the problem of high P and I gain values and correcting it automatically for this system.

The second test is shown in Figures 5-7 and -8. A low P and I gain pair (0.6 and 0.006) was assigned first. Drifting occurred when low P and I gain values were used. The period of the drifting is about 20 minutes. After 20 minutes, the algorithm increased the P and I gains to 1.2 and 0.012 respectively. Drifting was suppressed. Then the
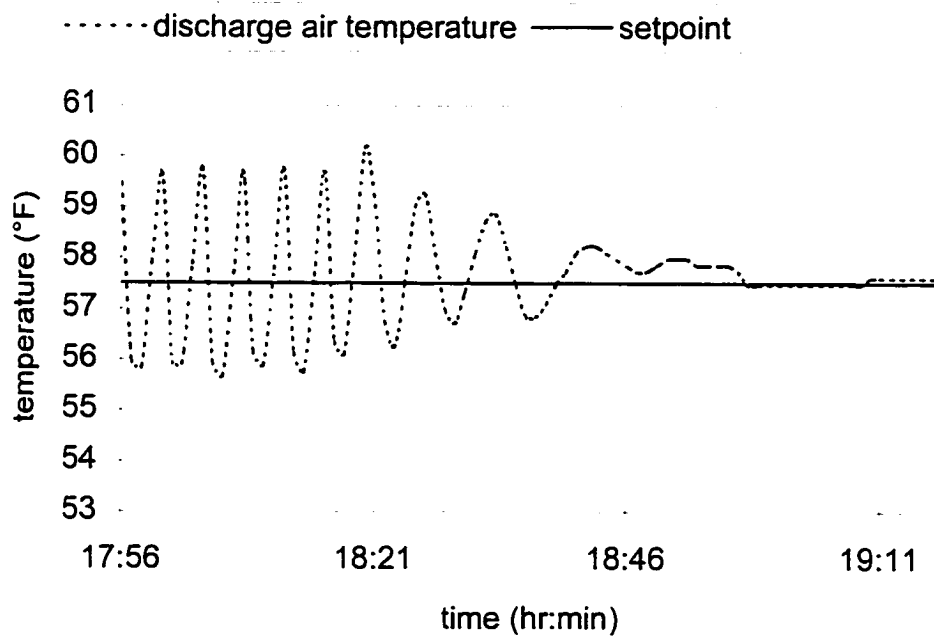
Figure 5-5 *The dynamic response of the coil under different P and I gains in test 1.*
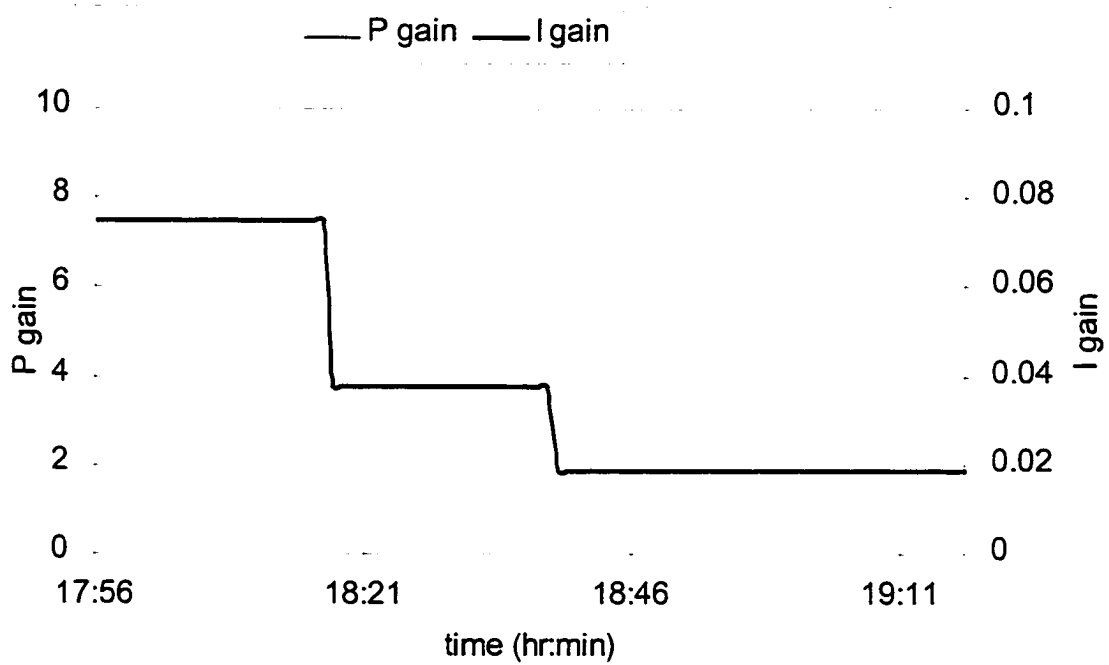
Figure 5-6 *The change of P gain and I gain in test 1. The P and I gains decreased*

continuously until an optimal set of P and I gains were reached.
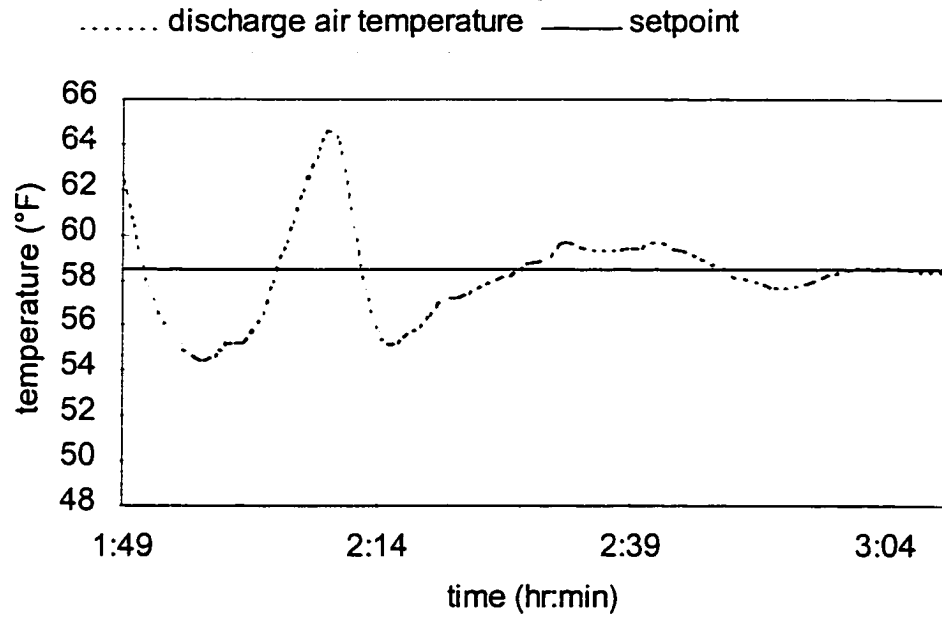
Figure 5-7 The dynamic response of the coil under different P and I gains in test 2.
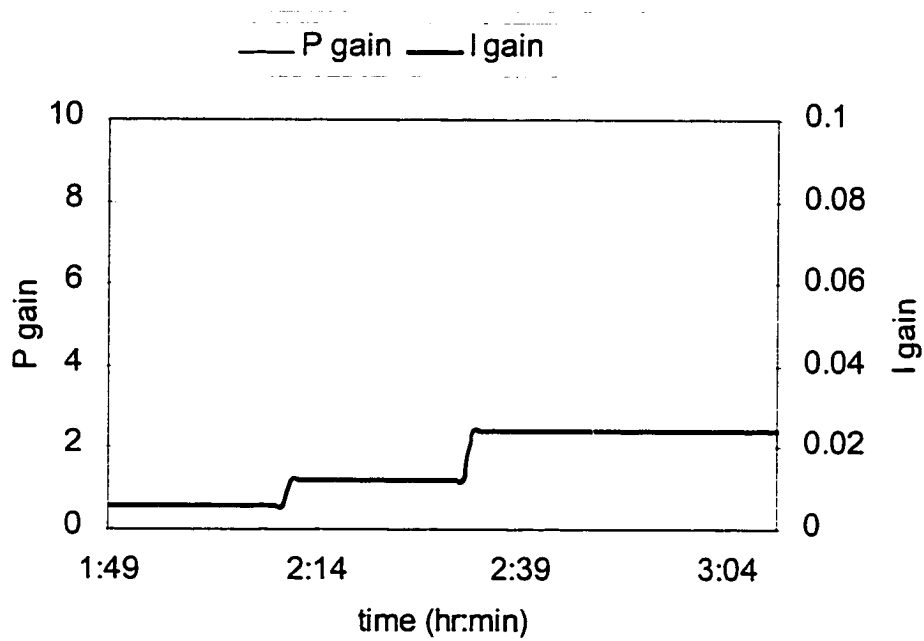
Figure 5-8 *The change of P gain and I gain in test 2. The P and I gains increased continuously until optimal set of P and I gains were reached.*

algorithm increased the P and I gains to 2.4 and 0.024 respectively. The drifting finally disappeared and the setpoint was reached. It appears that the algorithm can identify low P and I gains for this system and correct them as well.

Therefore, the algorithm has been shown to function correctly for these two cases.

CHAPTER VI

CONCLUSIONS AND FUTURE WORK

An on-line self-tuning algorithm for the heating and cooling system in buildings

has been developed. Several results have been obtained in this study:

1. The algorithm uses 'iteration' to search for the optimal P and I gains. It skips the

   model identification step, which is an indispensable step for common self-tuning

   methods in HVAC applications. Therefore, it will not interrupt normal coil operation

   and can be executed in real time.

2. The algorithm evaluates the controller performance by the integral square error (ISE)

   between the coil output signal and its setpoint. This criterion measures the long-term

   dynamic behavior of the coil. Indoor comfort and energy efficiency can be

   maintained as long as this criterion is within the allowed range.

3. Suitable P and I gains can be found by searching along the straight line $k_i = k_p/100$.

   This is a general criterion for practical coils in a building.

4. P and I gains are doubled when they are too small; P and I gains are cut in half when

   they are too large. The optimal P and I gains will not be missed under this iterative

   step change.

5. The direction of the correction needed by the P and I gains can be identified by

   calculating the low frequency proportion (LFP). The P and I gains need to be

   decreased when LFP is too small, which means that high frequencies dominate the

   ISE spectrum. The P and I gains need to be increased when LFP is too large. The low

   frequencies dominate ISE in this case.

6. Digital filters were used instead of using Fourier transforms to calculate the LFP. Fourier transforms would require more CPU time and memory. This is not practical for field applications. The digital filter method is much easier to implement. It takes less CPU time and memory, and this makes the algorithm simple and practical.

7. The algorithm has been tested in the field, and its feasibility has been illustrated.

This dissertation does not answer all questions within this specific research area. Several areas, which may benefit from further investigation:

1. The coil dynamic model needs to be developed further for future study. Two of the three coil dynamic characteristics, time constant and DC gain, are discussed thoroughly. However, the solution for the other characteristic, time delay, still needs investigation.

2. Suitable P and I gains are obtained along the straight line of $k_i=k_p/100$ in the algorithm. However, this search route may not be the optimal one. We may find a more efficient route in the shape of a quadratic curve or even nonlinear curve.

3. The new algorithm has been compared with other common self-tuning methods in HVAC applications, and its advantage has been pointed out. More comparison can be done with advanced adaptive control methods, such as the MIT rule (Astrom and Wittenmark 1989).

4. The new algorithm needs to be evaluated over a wide range of operating conditions such as, experience in an entire year. Then, more definitive conclusions can be drawn.

REFERENCES

Astrom, K. J., and T. Hagglund. 1984. Automatic tuning of simple regulators with specifications on phase and amplitude margins. *Automatica* 20 (5): 645-651.

Astrom, K. J., and T. Hagglund. 1988. A new auto-tuning design. *IFAC International Symposium on Adaptive Control of Chemical Processes*, Copenhagen, Denmark. pp.135-148.

Astrom, K. J., and B. Wittenmark. 1989. *Adaptive Control*, Reading, Mass.: Addison-Wesley Publishing Company, Inc.

Bak, Joseph, and Donald J. Newman. 1982. *Complex Analysis*, New York: Springer-Verlag Inc.

Bekker, J.E., P.H. Meckl, and D.C. Hittle. 1992. A tuning method for first-order processes with PI controllers. *ASHRAE Transactions* 99 (2): 19-23.

Chantre, P., B.M. Maschke, and B. Barthelemy. 1994. Physical modeling and parameter identification of a heat exchanger. *Proceedings of IECON'94 - 20th Annual Conference of IEEE Industrial Electronics*, Bologna, Italy. Vol. 3, pp. 1965 - 1970.

Clark, D. R. 1985. *HVACSIM+ Building Systems and Equipment Simulation Program - Users Guide*, Gaithersburg, Md.: U.S. Dept. of Commerce, National Bureau of Standards.

Corripio, A.B. 1990. *Tuning of Industrial Control Systems*, Research Triangle Park, N.C.: Instrument Society of America.

Dexter, A. L., and F.G. Jota. 1985. Multi-loop self-tuning control of an air-conditioning plant. *Proceedings of Int. Symposium on Recent Advances in Control and Operation of Building HVAC Systems,* Trondheim, Norway, 113-123.

Donoghue, J.F. 1977. Review of control design approaches for transport delay processes. *ISA Transactions,* 16 (2): 27-34.

Federspiel, C.C., and J.E. Seem. 1996. Temperature control in large buildings. *The Control Handbook,* William S. Levine, ed., pp. 1191-1204. Boca Raton, Fla.: CRC/IEEE Press.

Franklin, Gene F., J. David Powell, and Abbas Emami-Naeini. 1995. *Feedback Control of Dynamic Systems,* Reading, Mass.: Addison-Wesley Publishing Company, Inc.

Haines, R.W. 1988. *HVAC Systems Design Handbook,* Blue Ridge Summit, Pa.: TAB Professional and Reference Books.

Jota, F. G., and A.L. Dexter. 1988. Self-tuning control of an air-handling plant. *Proceedings of IEE International Conference on Control,* Oxford, UK, pp.41-46.

Liu, M., and D.E. Claridge. 1998. Use of calibrated HVAC system models to optimize system. *ASME Journal of Solar Energy Engineering,* 120: 131-138.

MacArthur, J.W., E.W. Grald, and A.F. Konar. 1989. An effective approach for dynamically compensated adaptive control. *ASHRAE Transactions* 95 (2): 411-423.

Marshall, J.E. 1979. *Control of Time-delay Systems,* New York: P. Peregrinus on behalf of the Institution of Electrical Engineers.

Marshall, J.E. 1992. *Time-delay Systems,* New York: Ellis Horwood LTD.

Mayr, O. 1970. *The Origins of Feedback Control*, Cambridge Mass.: MIT Press.

Pinella, M.J. 1986. Self-tuning digital integral control. *ASHRAE Transactions* 92 (2B): 202-209.

Proakis, John G., and Dimitris G. Manolakis. 1996. *Digital Signal Processing*, Englewood Cliffs, N.J.: Prentice-Hall, Inc.

Seborg, D.E., T.F. Edgar, and D.A. Mellichamp. 1989. *Process Dynamics and Control*. New York: John Wiley &Sons.

Seem, John E. 1997. Implementation of a new pattern recognition adaptive controller developed through optimization. *ASHRAE Transactions* 103 (1): 494-506.

Wallenborg, A. O. 1992. A new self-tuning controller for HVAC systems. *ASHRAE Transactions* 98(1): 19-25.

Xia, L., J. A. D. Abreu-Garcia, and Tom T. Hartley. 1991. Modeling and simulation of a heat exchanger. *IEEE International Conference on Systems Engineering*, Akron, Oh., pp. 453-456.

Zhang, Zhihui. 1992. *Thermodynamic Measurement and Automatic Control*. Chinese Architecture Industrial Publishing Co. Beijing, China.

Zhou, Q., and M. Liu. 1998. An on-line self-tuning algorithm of PI controller for the heating and cooling coil in buildings. *Proceedings of 11th Symposium on Improving Building Systems in Hot and Humid Climates*, Fort Worth, Tex., pp. 285-293.

Ziegler, J. G., and N. B. Nichols. 1942. Optimum settings for automatic controllers. *Trans. ASME*, 64: 759-768.

Ziegler, J. G., and N. B. Nichols. 1943. Process lags in automatic control circuits. *Trans.*

ASME, 65: 433-444.

APPENDIX A

TIME CONSTANT AND DC GAIN OF COILS

Two characteristics of the coil dynamics, time constant and DC gain, are studied in this Appendix.

First of all, it is assumed that the heat exchange rate of the coil is proportional to the difference between the average air temperature and average water temperature. The heat exchange rate is then calculated as:

$$Q = UA\left(\frac{t_{ao} + t_{ai}}{2} - \frac{t_{wi} + t_{wo}}{2} \right) \qquad (A-1)$$

where,

Q is the coil heat exchange rate;

UA is the coil heat transfer coefficient;

t_{ao} is the coil output air temperature;

t_{ai} is the coil input air temperature;

t_{wo} is the coil output air temperature; and

t_{wi} is the coil input air temperture

Then it is assumed that the first order of system dynamics is the only term taken into account in the coil heat transfer process. The dynamic heat exchange equations

under a step change in the water flow rate, water flow rate changes from W_0 to W_1, are obtained as:

$$UA_1\left(\frac{t_{ao}+t_{ai}}{2}-\frac{t_{wi}+t_{wo}}{2}\right)=C_{pa}G(t_{ai}-t_{ao})-\frac{C_{pa}V_a\rho_a}{2}\frac{dt_{ao}}{d\tau} \qquad (A-2)$$

$$C_{pw}W_1(t_{wo}-t_{wi})+\frac{C_{pw}\rho_w V_w}{2}\frac{dt_{wo}}{d\tau}=C_{pa}G(t_{ai}-t_{ao})-\frac{C_{pa}\rho_a V_a}{2}\frac{dt_{ao}}{d\tau} \qquad (A-3)$$

where,

C_{pa} is air heat capacity;

C_{pw} is water heat capacity;

G is the air flow rate;

UA_1 is the heat transfer coefficient when water flow rate is W_1;

V_a is air volume inside the coil;

V_w is water volume inside the coil;

W_1 is current water flow rate;

ρ_a is air density;

ρ_w is water density; and

τ is time.

The heat balance equations when the coil is in initial status are:

$$UA_0 \left(\frac{t_{ao}^{0} + t_{ai}}{2} - \frac{t_{wi} + t_{wo}}{2} \right) = C_{pa}G(t_{ai} - t_{ao}^{0})$$

(A-4)

$$C_{pw}W_0(t_{wo}^{0} - t_{wi}) = C_{pa}G(t_{ai} - t_{ao}^{0})$$

(A-5)

where,

t_{ao}^{0} is the initial output air temperature;

t_{wo}^{0} is the initial output water temperature;

UA_0 is the coil heat transfer coefficient when water flow rate is W_0; and

W_0 is the initial water flow rate.

Combining Equations A-2 and -4,

$$\frac{\rho_a C_{pa} V_a}{2} \frac{d\Delta t_{ao}}{d\tau} + (C_{pa}G + \frac{UA_1}{2})\Delta t_{ao} - \frac{UA_1}{2}\Delta t_{wo}$$
$$+ (UA_1 - UA_0)(\frac{t_{ao}^{0} + t_{ai}}{2} - \frac{t_{wi} + t_{wo}^{0}}{2}) = 0$$

(A-6)

Combining Equations A-3 and -5,

$$\frac{\rho_w C_{p_w} V_w}{2} \frac{d\Delta t_{wo}}{d\tau} + \frac{\rho_a C_{pa} V_a}{2} \frac{d\Delta t_{ao}}{d\tau} + C_{pa} G \Delta t_{ao} + \Delta t_{wo}$$

$$+ C_{pw}(W_1 - W_0)(t_{wo}^0 - t_{wi}) = 0 \qquad \text{(A-7)}$$

where,

$$\Delta t_{ao} = t_{ao} - t_{ao}^0 \text{ ; and}$$

$$\Delta t_{wo} = t_{wo} - t_{wo}^0 \text{ .}$$

Put Equation A-7 into A-6:

$$\frac{\rho_w C_{pw} V_w \rho_a C_{pa} V_a}{2UA_1} \frac{d^2 \Delta t_{ao}}{d\tau^2}$$

$$+ \left[\frac{\rho_a C_{pa} V_a}{2} + \frac{C_{pw} W_1 \rho_a C_{pa} V_a}{UA_1} + \frac{\rho_w C_{pw} V_w}{2} + \frac{G C_{pa} \rho_w C_{pw} V_w}{UA_1} \right] \frac{d\Delta t_{ao}}{d\tau}$$

$$+ \left[C_{pa} G + C_{pw} W_1 + \frac{2 G C_{pa} C_{pw} W_1}{UA_1} \right] \Delta t_{ao} \qquad \text{(A-8)}$$

$$+ C_{pw} W_1 \frac{(UA_1 - UA_0)(\frac{t_{ao}^0 + t_{ai}}{2} - \frac{t_{wi} + t_{wo}^0}{2})}{\frac{UA_1}{2}} + C_{pw}(W_1 - W_0)(t_{wo}^0 - t_{wi}) = 0$$

Equation A-8 is equivalent to Equation A-9,

$$
\frac{\dfrac{\rho_w C_{pw} V_w \rho_a C_{pa} V_a}{2 U A_1}}{C_{pa}G + C_{pw}W_1 + \dfrac{2 G C_{pa} C_{pw} W_1}{U A_1}} \frac{d^2 \Delta t_{ao}}{d\tau^2}
$$

$$
+ \frac{\dfrac{\rho_a C_{pa} V_a}{2} + \dfrac{C_{pw}W_1 \rho_a C_{pa} V_a}{U A_1} + \dfrac{\rho_w C_{pw} V_w}{2} + \dfrac{G C_{pa} \rho_w C_{pw} V_w}{U A_1}}{C_{pa}G + C_{pw}W_1 + \dfrac{2 G C_{pa} C_{pw} W_1}{U A_1}} \frac{d\Delta t_{ao}}{d\tau}
$$

$$
+ \Delta t_{ao}
$$
\hfill (A-9)

$$
+ \frac{C_{pw}W_1 \dfrac{(UA_1 - UA_0)(\dfrac{t_{ao}^0 + t_{ai}}{2} - \dfrac{t_{wi} + t_{wo}^0}{2})}{UA_1} + C_{pw}(W_1 - W_0)(t_{wo}^0 - t_{wi})}{2}}{C_{pa}G + C_{pw}W_1 + \dfrac{2 G C_{pa} C_{pw} W_1}{U A_1}} = 0
$$

So far, a simplified dynamic model of the coil is developed. Practical numbers are put into the equation to physically understand it. A coil in Brooke army hospital in San Antonio is measured. The input air flow rate is 16.245 lbm/s; the input water flow rate is 7.783 lbm/s, the input air temperature is 80 °F; the output air temperature is 55 °F; the input water temperature is 45 °F; the output water temperature is 57 °F; the air volume inside the coil is 70.63 ft^3 and water volume inside the coil is 35.31 ft^3. Then the heat transfer coefficient, UA, is calculated based on heat balance equation as 20,580 Btu/h.°F. The step change of water flow rate is from 7.783 lbm/s to 8.820 lbm/s. The

changes in the heat transfer coefficient in this case are very small and are ignored. The coefficients of the second order term and the first order term, respectively, in Equation A-9 are calculated, when the parameters are equal to above numbers. (The air density is 0.0749 lbm/ft^3. The water density is 62.430 lbm/ft^3. The heat capacity of water is 1 Btu/lbm.°F. The heat capacity of air is 0.24 Btu/lbm.°F.)

$$\frac{\dfrac{\rho_w C_{pw} V_w \rho_a C_{pa} V_a}{2UA_1}}{C_{pa}G + C_{pw}W_1 + \dfrac{2GC_{pa}C_{pw}W_1}{UA_1}} = 9.88 \sec^2 \qquad \text{(A-10)}$$

$$\frac{\dfrac{\rho_a C_{pa} V_a}{2} + \dfrac{C_{pw}W_1 \rho_a C_{pa} V_a}{UA_1} + \dfrac{\rho_w C_{pw} V_w}{2} + \dfrac{GC_{pa}\rho_w C_{pw} V_w}{UA_1}}{C_{pa}G + C_{pw}W_1 + \dfrac{2GC_{pa}C_{pw}W_1}{UA_1}} = 105.47 \sec \qquad \text{(A-11)}$$

The coefficient of the first order term is much larger than the coefficient of the second order term. The impact of the second order term can be ignored. Furthermore, the first two terms in the nominator of Equation A-11 are very small compared with the other two and they can be ignored as well. Then Equation A-9 is simplified to Equation A-12,

$$\frac{\dfrac{\rho_w C_{pw} V_w}{2} + \dfrac{GC_{pa}\rho_w C_{pw} V_w}{UA_1}}{C_{pa}G + C_{pw}W_1 + \dfrac{2GC_{pa}C_{pw}W_1}{UA_1}} \frac{d\Delta t_{ao}}{d\tau} + \Delta t_{ao}$$

$$+ \frac{C_{pw}(W_1 - W_0)(t_{wo}^{\ 0} - t_{wi})}{C_{pa}G + C_{pw}W_1 + \dfrac{2GC_{pa}C_{pw}W_1}{UA_1}} = 0 \qquad \text{(A-12)}$$

And the time constant of the system is,

$$T = \frac{\dfrac{\rho_w C_{pw} V_w}{2} + \dfrac{GC_{pa}\rho_w C_{pw} V_w}{UA_1}}{C_{pa}G + C_{pw}W_1 + \dfrac{2GC_{pa}C_{pw}W_1}{UA_1}} \qquad \text{(A-13)}$$

The Equation A-13 indicates that the time constant of the system is influenced by water volume in the coil, air flow rate, water flow rate, and coil heat transfer coefficient.

Meanwhile, it is noticed from Equation A-12 that the DC gain between the water flow rate and the discharge air temperature depends on water flow rate, air flow rate, and

heat transfer coefficient. The relationship between the water flow rate and valve position change depends on the differential pressure across the water side of the coil and the valve characteristic. Therefore, the overall DC gain of the coil system, including the coil and valve, depends on water flow rate, air flow rate, coil heat transfer coefficient, differential pressure across the water side of the coil, and the valve characteristic.

APPENDIX B

RISE TIME, PEAK TIME, SETTLING TIME AND OVERSHOOT

Rise time, peak time, settling time, and overshoot are standard quantities used to evaluate the control system behavior. The definitions of these criteria are shown in Figure B-1. For the closed-loop system of the coil, the rise time is the time it takes the coil discharge air temperature to reach the vicinity of its new set point. Practically, the rise time is defined as the time elapsed from when the coil discharge air temperature has changed by 10% of the difference between its initial value and the new setpoint, to when the temperature has changed by 90% of the amount needed to reach the setpoint. The settling time is the time it takes for the transients of the coil discharge air temperature to decay. The transients can be considered as decayed when the oscillation amplitude of the coil discharge air temperature is less than 1% of the initial offset. The overshoot is the maximum amount by which the coil discharge air temperature overshoots its final value divided by the initial offset value (which is often expressed as a percentage). The peak time is the time it takes the coil with a PI controller to reach the maximum overshoot point. This criterion indicates how quickly the close loop system will react to a step change in setpoint.

The PI controller in this study needs to be designed such that the room temperature has small fluctuation. The time constant between the room temperature change and the coil discharge air temperature change is large and depends on the air
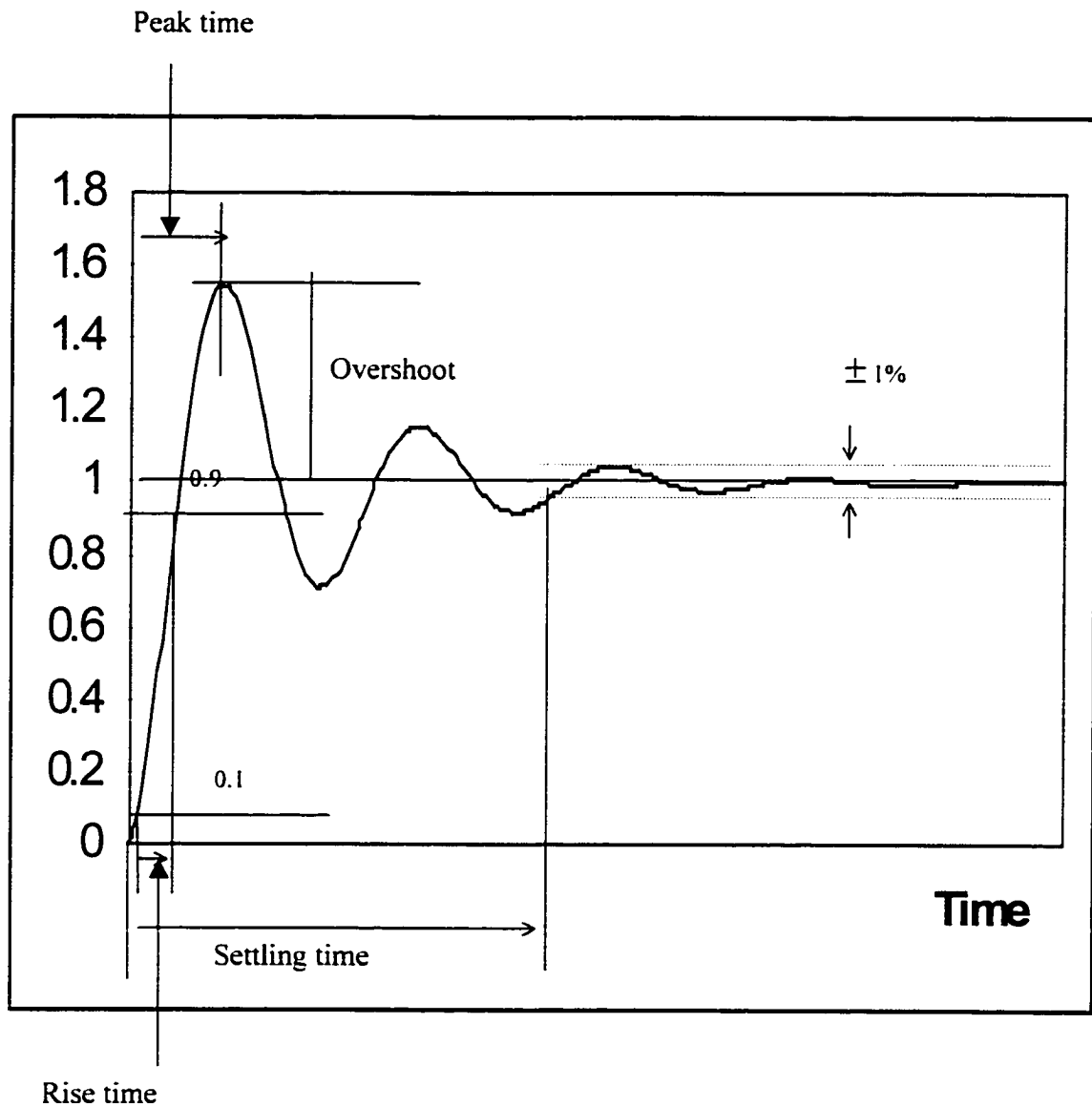
Peak time

Figure B-1 *Definition of the rise time, settling time, peak time and*

overshoot. These are the traditional criteria used to evaluate the dynamic

performance of the controller.

exchange rate of the room. Normally, it is around 30 minutes and acts like a low pass filter. Therefore, the settling time is the most important factor among above four criteria since it contains the lowest frequency information. It is the objective of the PI controller to keep the settling time small so that the HVAC system will stabilize at the setpoint in a relatively short time.

APPENDIX C

THE STABILITY OF COILS BASED ON NYQUIST CRITERION

Harry Nyquist of the Bell telephone laboratories proposed a criterion to evaluate the stability of the closed loop system in 1932. The Nyquist stability criterion relates the open-loop frequency response to the number of closed-loop pole of the system in the Right Half Plane (RHP). It turns out being very useful in dealing with systems with pure delays.

The Nyquist stability criterion is based on a result from complex variables theory known as the argument principle (Bak and Donald 1982). A contour map of a complex function will only encircle the origin if the contour contains a singularity (pole or zero) of the function.

Take a system of: $F(s)=s-s_0$ for example. We want to determine whether s_0 is inside a contour C or outside. The result can be obtained by evaluating $F(s)$ as s moves on the contour C. The contours of C when s_0 is located inside and outside are shown as examples in Figure C-1 and -2, respectively. It is shown that the image of C encircles the origin under the mapping F, when s_0 is inside the contour of C. Meanwhile, it is shown that the image does not encircle the origin, when s_0 is outside the contour of C.
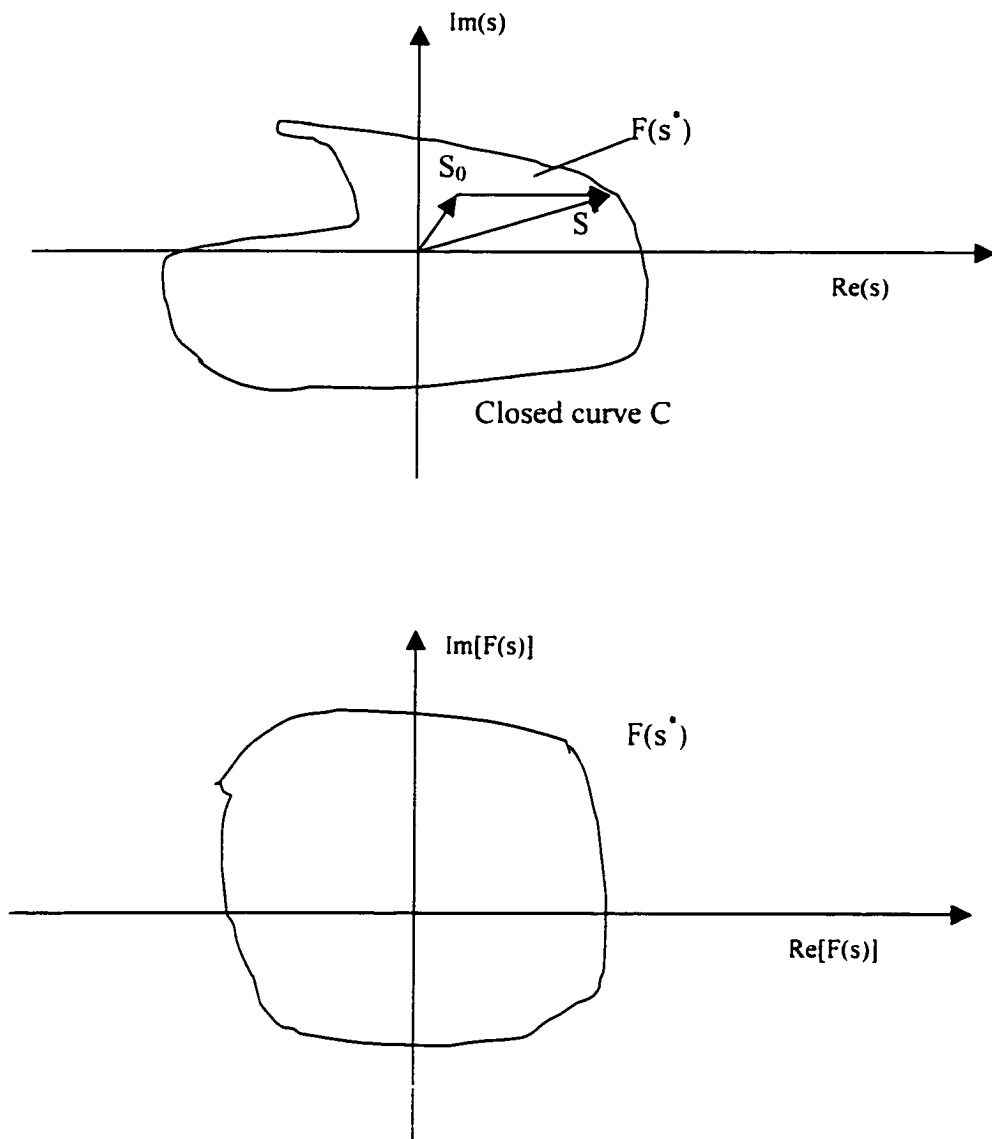
Figure C-1 *The image of C under the mapping F when s_0 is inside the contour of C. We can see the image F(s*) encircle the origin.*
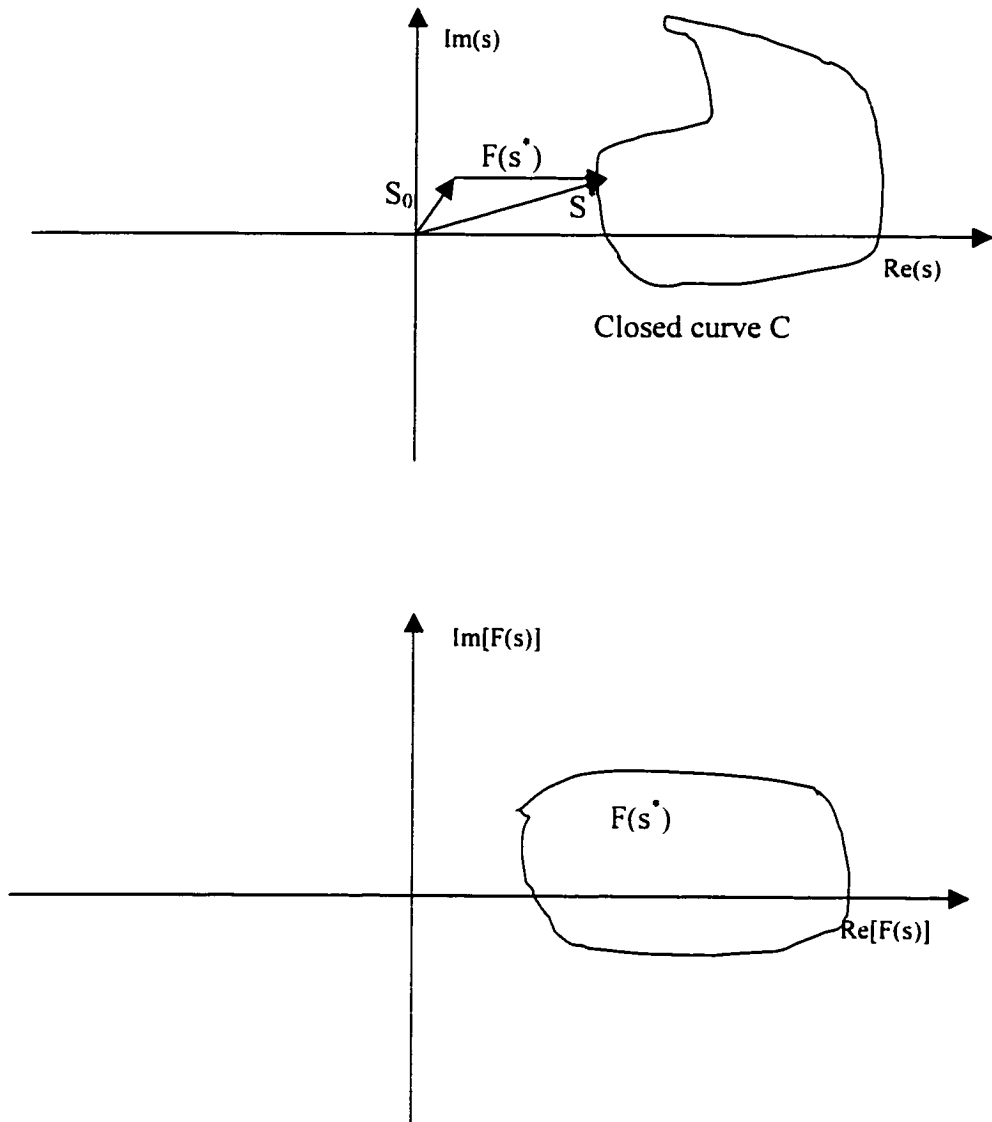
Figure C-2 *The image of C under the mapping F when s_o is outside the contour of C. We can see the image F(s*) does not encircle the origin.*

To apply this principle to control design, we let the C contour in the S plane encircle the entire RHP (Figure C-3). The resulting evaluation of F(s) will only encircle the origin if F(s) has a RHP pole or zero. We call this special contour as C_1 and the resulting evaluation plot as Nyquist plot.

The contour behavior becomes useful when it is applied into a contour evaluation of closed-loop system, specifically for the system in Figure C-4. The closed-loop transfer function is

$$\frac{Y(s)}{R(s)} = T(s) = \frac{KG(s)}{1 + KG(s)} \tag{C-1}$$

Therefore, the closed-loop roots are the solutions of 1+KG(s)=0. If the evaluation contour of s enclosing the entire RHP contains a zero or pole of 1+KG(s), then the evaluated contour of 1+KG(s) will encircle the origin. Notice that 1+KG(s) is simply KG(s) shifted to the right one unit (Figure C-5), and we can plot KG(s). Therefore, if the plot of 1+KG(s) encircles the origin, the plot of KG(s) will encircle −1 on the real axis. −1 is the critical point at this case.
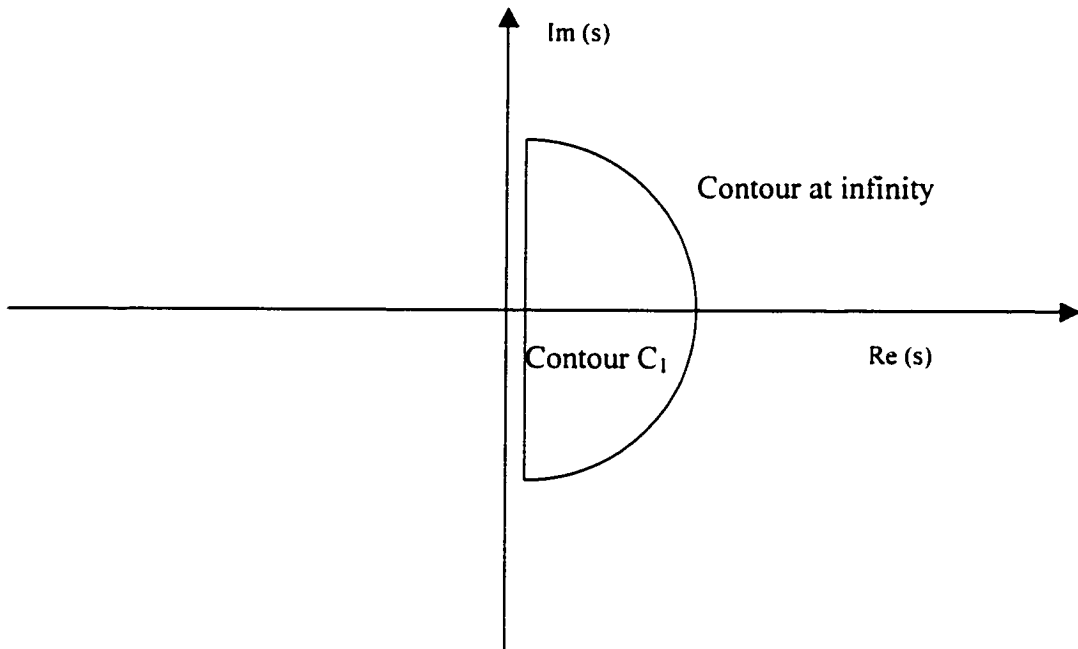
Figure C-3 *A s-plane plot of a contour C_1, which encircles the entire RHP.*

Whether F(s) has a RHP pole or zero can be determined by drawing the image of
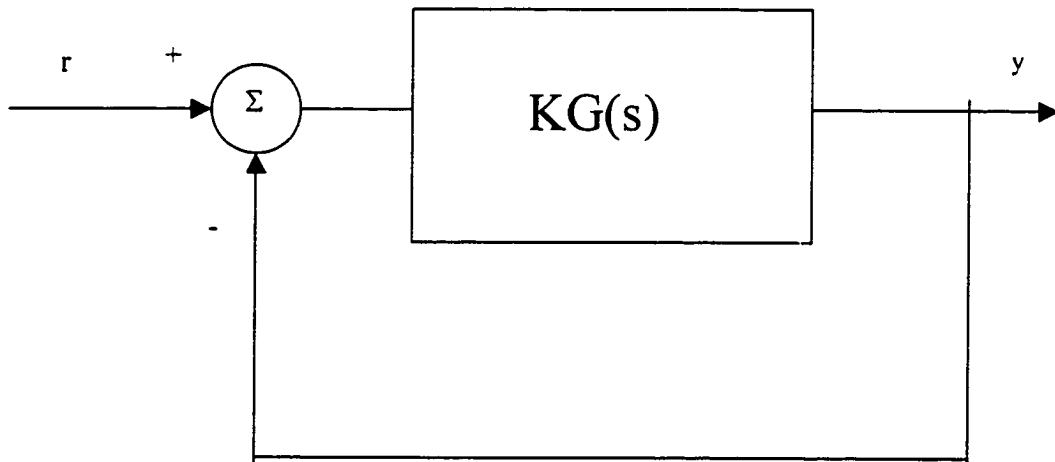
$$C_1.$$

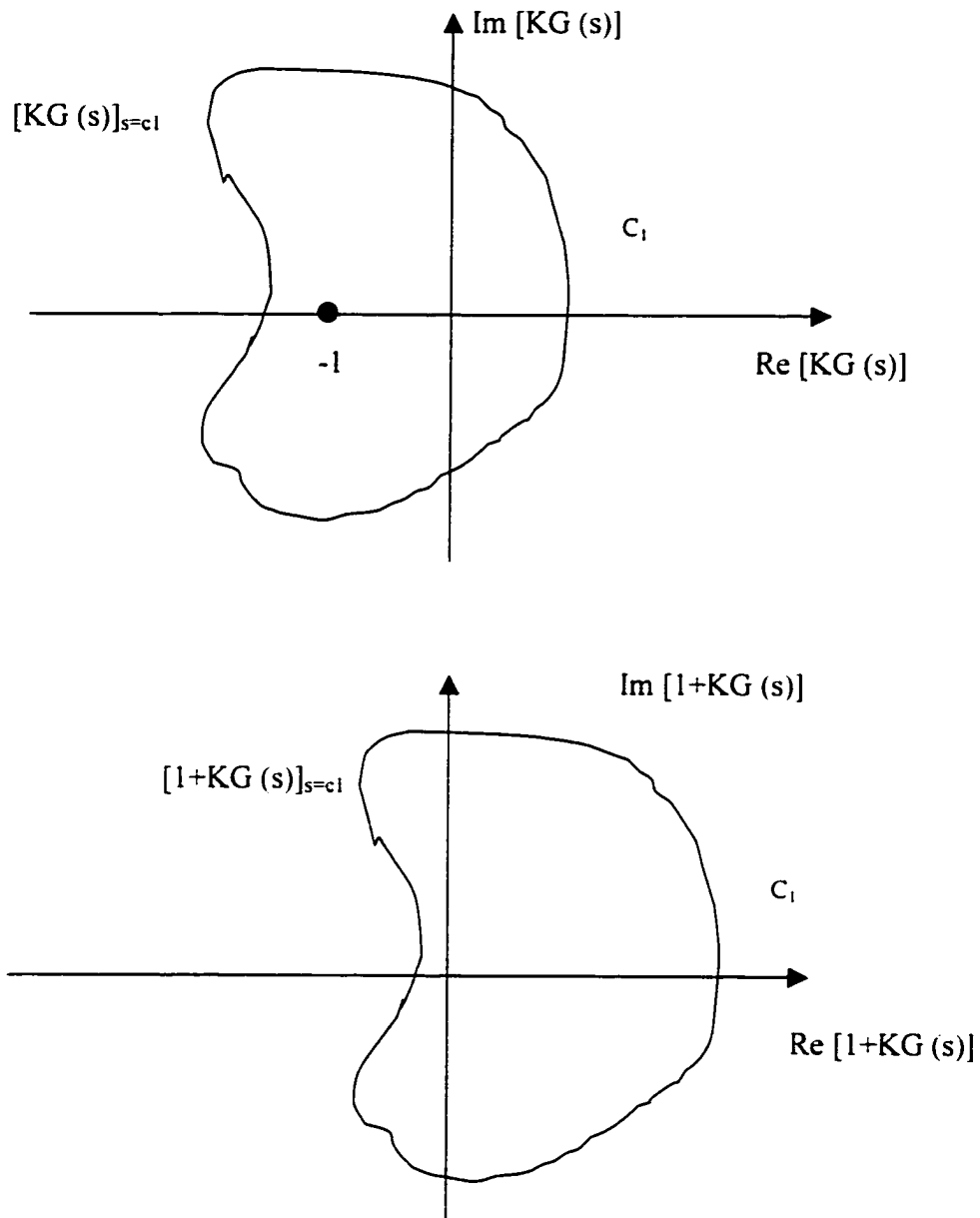*Figure C-4* Block diagram for $Y(s)/R(s) = KG(s)/[1 + KG(s)]$.

Figure C-5 Evaluation of KG(s) and 1+KG(s): Nyquist plots.

To determine whether the encirclement is due to a pole or zero, we write

1+KG(s) in terms of poles and zeros of KG(s):

$$1 + KG(s) = 1 + K\frac{b(s)}{a(s)} = \frac{a(s) + Kb(s)}{a(s)} \qquad (C\text{-}2)$$

Equation C-2 shows that the poles of 1+KG(s) are also the poles of G(s). Assuming there are no poles of G(s) in RHP, which is the case in HVAC application, an encirclement of –1 by KG(s) indicates a zero of 1+KG(s) in the RHP and thus an unstable root of the closed-loop system.

Take a system with a transfer function of Equation C-3 for example.

$$G(s) = \frac{1}{s+1} \qquad (C\text{-}3)$$

The image of C_1 under the mapping of G(s) can be calculated as Figure C-6. The result is expressed as Equation C-4 and it is drawn as Figure C-7.

$$G(s^*) = \frac{1}{\ell e^{j\varphi}} = \frac{1}{\ell}e^{j(-\varphi)} \qquad (C\text{-}4)$$
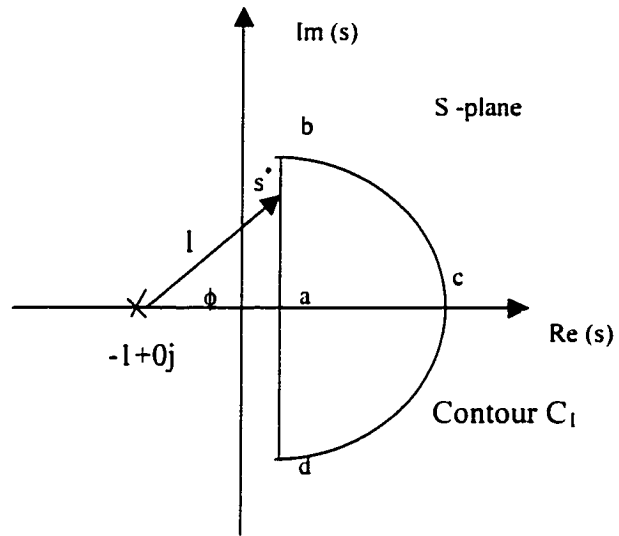
Figure C-6 The calculating of image of C_1 under the mapping of $G(s)$.
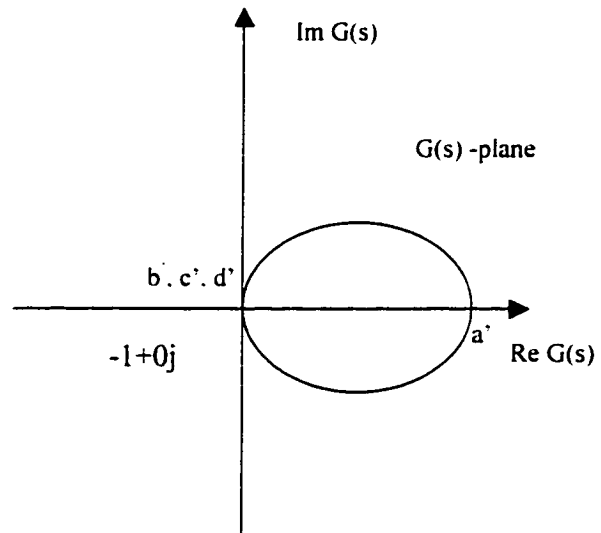
Figure C-7 Nyquist plot for $G(s)$.

It can be seen that the contour does not encircle the point of $-1+j0$. Therefore, there is no pole in RHP for the closed loop system of $G(s)=1/(s+1)$.

The open loop system for the coil with a PI controller can be expressed as Equation C-5.

$$G(s) = \left(k_p + \frac{k_i}{s} \right)\left(\frac{k_s}{Ts+1} \right)e^{-r_d s} \qquad (C-5)$$

We can first draw the Nyquist plot for a part of system without pure delay as Equation C-6.

$$G'(s) = \left(k_p + \frac{k_i}{s} \right)\left(\frac{k_s}{Ts+1} \right) \qquad (C-6)$$

The image of C_1 under the mapping of G'(s) can be calculated as Figure C-8 and it is expressed in Equation C-7.

$$G'(s') = \frac{k_s k_p}{T} \frac{l_3}{l_1 l_2} e^{j(\phi_3 - \phi_1 - \phi_2)} \qquad (C-7)$$

Figure C-8 The calculating of image of C_1 for the coil with a PI controller (w/o pure delay).

Figure C-9 Nyquist plot for the coil with a PI controller (w/o pure delay).
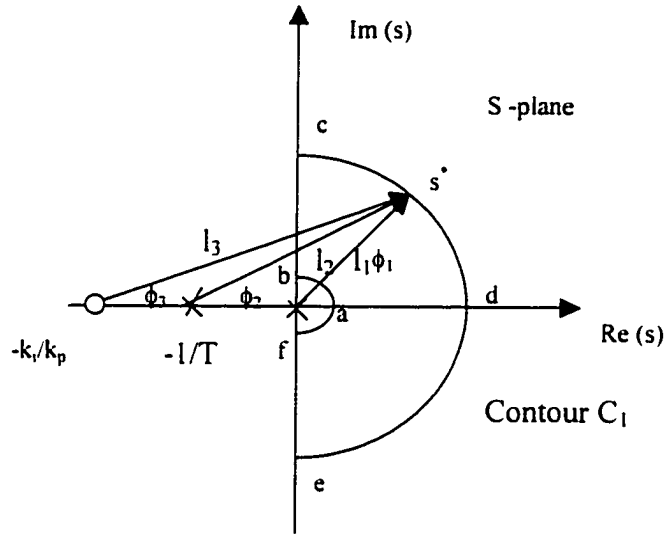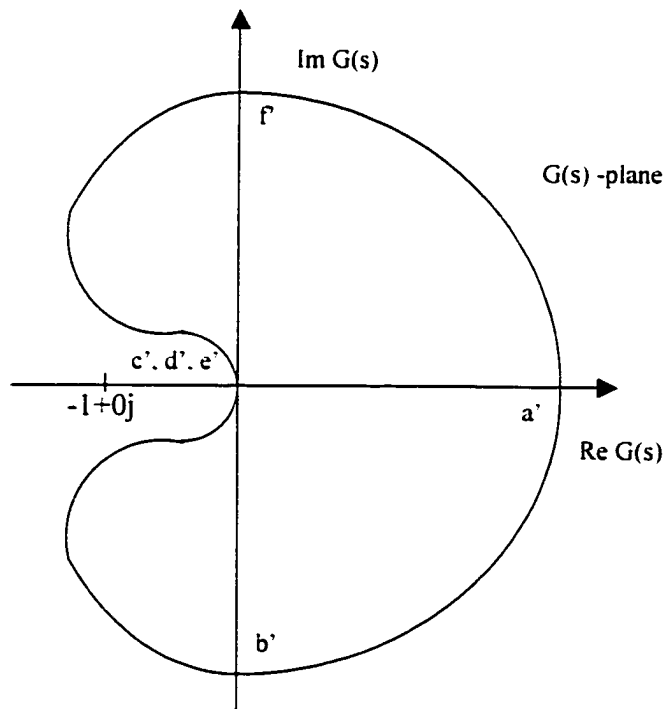
The time constant and DC gain of the typical coil, T, and k_s, are larger than zero. The k_p and k_i are normally chosen larger than zero for a PI controller in HVAC application. The image of C_1 under the mapping of G'(s) does not encircle the point of $-1+j0$ at these cases (shown in Figure C-9). Therefore, the system is stable.

For the system with delay time larger than zero, the equation to calculate the image of contour C_1 (shown in Figure C-7) is modified to Equation C-8.

$$G(s^*) = \frac{k_s k_p}{T} \frac{l_3}{l_1 l_2} e^{j(\phi_3 - \phi_1 - \phi_2 - \tau_d w)}$$ (C-8)

Then, the image in Figure C-9 is evolved to Figure C-10. The Nyquist plot of the system revolves an angle of $\theta = \tau_d W$. For example, the point of A' is now transformed to the point of A. The system is not stable if the magnitude of A' is larger than 1. The image will encircle the point of $-1+j0$ after the revolving. A threshold can be found for the stability of the system. First, we found the critical frequency where the magnitude of the G'(s*) is equal to one. This is obtained by Equation C-9, which comes from Equation C-6.

$$\left| G'(j w_g) \right| = 1$$ (C-9)

w_g is the critical frequency.
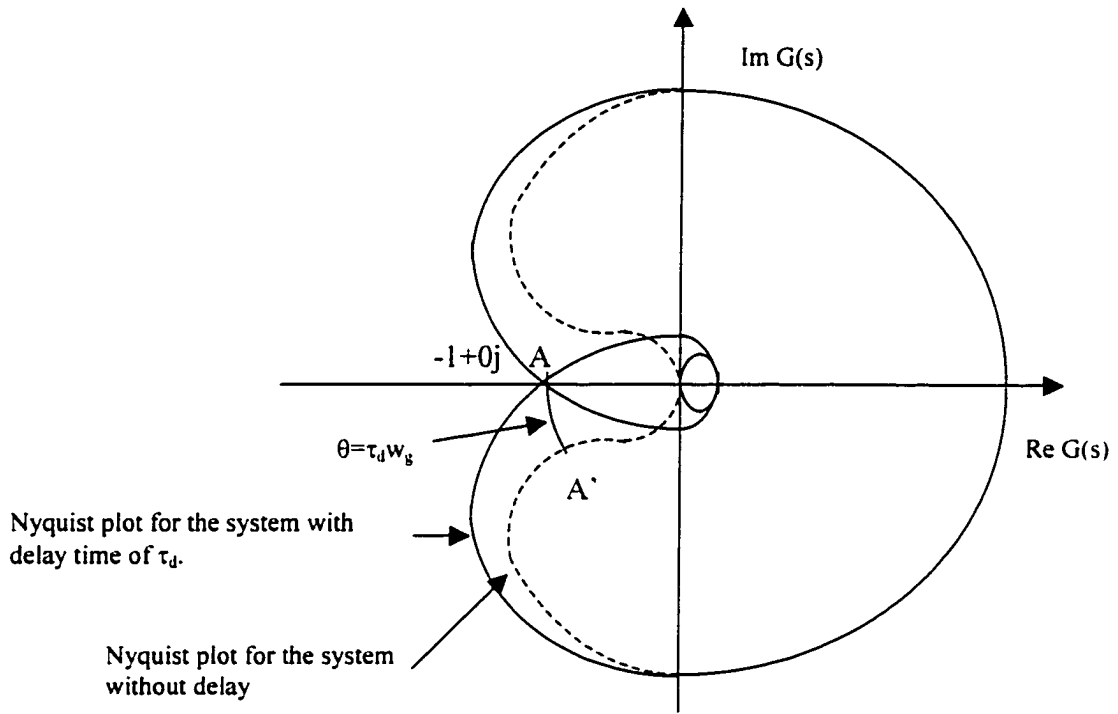
Figure C-10 *The Nyquist plot for the system with delay*

time larger than zero.

The figure shows Nyquist plots with the following labels: "Im G(s)" on the vertical axis, "Re G(s)" on the horizontal axis, "-1+0j" and "A" near the left intersection, "θ=τ_dw_g" with arrow, "A'" below, "Nyquist plot for the system with delay time of τ_d." and "Nyquist plot for the system without delay".

Then,

$$
w_g{}^2 = \frac{\sqrt{\left[\left(\frac{k_s k_p}{T}\right)^2 - \left(\frac{1}{T}\right)^2\right]^2 + 4\left(\frac{k_s k_i}{T}\right)^2} + \left(\frac{k_s k_p}{T}\right)^2 - \left(\frac{1}{T}\right)^2}{2}
\tag{C-10}
$$

The system is stable, if the angle of G'(s) at the critical frequency plus the angle brought by the delay time is larger than π. This is shown in Equation C-11:

$$
\angle G'(j\,w_g) - \tau_d\,w_g > \pi
\tag{C-11}
$$

Put Equations C-6 and -10 to Equation C-11, we get Equation C-12. Further, Equation C-12 can be written in the form of Equation C-13. Finally, Equation C-13, combined with the assumption of the k_p and k_i are chosen to be larger than zero, consists of the stability conditions for the coil with an PI controller. The conditions are rewritten in Equations 2-6, -7, and -8.

$$\tau_d \sqrt{\dfrac{\sqrt{\left(\left(\dfrac{k_s k_p}{T}\right)^2 - \left(\dfrac{1}{T}\right)^2\right)^2 + 4\left(\dfrac{k_s k_i}{T}\right)^2} - \left(\dfrac{1}{T}\right)^2 + \left(\dfrac{k_s k_p}{T}\right)^2}{2}}$$

$$< \arccos \dfrac{\dfrac{k_s k_i}{T} - \dfrac{1}{T}\dfrac{k_s k_p}{T}}{\sqrt{\left(\dfrac{k_s k_p}{T}\right)^2\left(\dfrac{1}{T}\right)^2 + \left(\dfrac{k_s k_i}{T}\right)^2 + \left(\dfrac{k_s k_p}{T}\right)^2 \dfrac{\sqrt{\left(\left(\dfrac{k_s k_p}{T}\right)^2 - \left(\dfrac{1}{T}\right)^2\right)^2 + 4\left(\dfrac{k_s k_i}{T}\right)^2} - \left(\dfrac{1}{T}\right)^2 + \left(\dfrac{k_s k_p}{T}\right)^2}{2} + \dfrac{\left(\dfrac{1}{T}\right)^2\left(\dfrac{k_s k_i}{T}\right)^2}{\dfrac{\sqrt{\left(\left(\dfrac{k_s k_p}{T}\right)^2 - \left(\dfrac{1}{T}\right)^2\right)^2 + 4\left(\dfrac{k_s k_i}{T}\right)^2} - \left(\dfrac{1}{T}\right)^2 + \left(\dfrac{k_s k_p}{T}\right)^2}{2}}}} \qquad \text{(C-12)}$$

$$\tau_d \sqrt{\dfrac{\sqrt{\left(\left(\dfrac{k_s k_p}{T}\right)^2 - \left(\dfrac{1}{T}\right)^2\right)^2 + 4\left(\dfrac{k_s k_i}{T}\right)^2} - \left(\dfrac{1}{T}\right)^2 + \left(\dfrac{k_s k_p}{T}\right)^2}{2}}$$

$$< \arccos \dfrac{\dfrac{k_s k_i}{T} - \dfrac{1}{T}\dfrac{k_s k_p}{T}}{\left(\dfrac{1}{T}\right)^2 + \sqrt{\dfrac{(\left(\dfrac{k_s k_p}{T}\right)^2 - \left(\dfrac{1}{T}\right)^2)^2 + 4\left(\dfrac{k_s k_i}{T}\right)^2} - \left(\dfrac{1}{T}\right)^2 + \left(\dfrac{k_s k_p}{T}\right)^2}{2}}} \qquad \text{(C-13)}$$

APPENDIX D

CALCULATION OF THE ISE

The integral of square error in Equation D-1 is used to evaluate the performance of PI controller.

$$ISE = \int_0^\infty e(t)^2 \, dt = \int_0^\infty (t_{ao}(t) - t_{ao,set}(t))^2 \, dt \tag{D-1}$$

t_{ao} is the coil discharge air temperature and it is a function of time.

$t_{ao,set}$ is the coil discharge air temperature setpoint and it is also a function of time.

$e(t)$ is the difference between the coil discharge air temperature and its setpoint under unit step change.

The equation is easier to solve in the phase domain, since there exists a time delay term in the coil model (Equation 2-1). We can use Parseval's theorem and write the cost functional ISE, in the form

$$ISE = \frac{1}{2\pi i} \int_{-i\infty}^{i\infty} E(s)E(-s) \, ds \tag{D-2}$$

$E(s)$ is the representation of $e(t)$ in phase domain.

We know from Equation 2-8 in Chapter II that E(s) can be expressed as Equation D-3

$$E(s) = \frac{Ts + 1}{Ts^2 + s + (k_p s + k_i)k_s e^{-\tau_d s}}$$ (D-3)

Put it into Equation D-2,

$$ISE = \frac{1}{2\pi i} \int_{-i\infty}^{i\infty} \left(\frac{s + \dfrac{1}{T}}{s^2 + \dfrac{1}{T}s + (\dfrac{k_p k_s}{T}s + \dfrac{k_i k_s}{T})e^{-\tau_d s}} \cdot \frac{-s + \dfrac{1}{T}}{s^2 - \dfrac{1}{T}s + (-\dfrac{k_p k_s}{T}s + \dfrac{k_i k_s}{T})e^{\tau_d s}} \right) ds$$ (D-4)

It is hard to solve Equation D-4 directly, since there are infinite poles in the integrand. However, all poles of E(s), or equivalently all the zeros of

$$s^2 + \frac{1}{T}s + (\frac{k_p k_s}{T}s + \frac{k_i k_s}{T})e^{-\tau_d s}$$ lie in the left half of the complex s-plane, as long as

the close loop system is stable (The stability condition is expressed in Equation 2-6, 7, 8.). We can separate the integrand into two parts, and then close the contour for one part on the right and the other part on the left. One way to achieve such a separation is to consider the poles of E(s). At such a point,

$$e^{-\tau_d s} = -\frac{s^2 + \dfrac{1}{T}s}{\dfrac{k_p k_s}{T}s + \dfrac{k_i k_s}{T}} \qquad (D\text{-}5)$$

and consequently

$$E(-s) = \frac{-s + \dfrac{1}{T}}{s^2 - \dfrac{1}{T}s + \left(-\dfrac{k_p k_s}{T}s + \dfrac{k_i k_s}{T}\right)e^{\tau_d s}}$$

$$= \frac{\left(s^2 + \dfrac{1}{T}s\right)\left(-s + \dfrac{1}{T}\right)}{s^4 + \left[\left(\dfrac{k_p k_s}{T}\right)^2 - \left(\dfrac{1}{T}\right)^2\right]s^2 - \left(\dfrac{k_i k_s}{T}\right)^2} \qquad (D\text{-}6)$$

Subtracting this term and adding it in yields

$$ISE = \frac{1}{2\pi i}\int_{-i\infty}^{i\infty}\left\{\frac{s+\frac{1}{T}}{s^2+\frac{1}{T}s+(\frac{k_pk_s}{T}s+\frac{k_ik_s}{T})e^{-\tau_d s}}\left[\frac{-s+\frac{1}{T}}{s^2-\frac{1}{T}s+(-\frac{k_pk_s}{T}s+\frac{k_ik_s}{T})e^{\tau_d s}}-\frac{(s^2+\frac{1}{T}s)\left(-s+\frac{1}{T}\right)}{s^4+\left[\left(\frac{k_pk_s}{T}\right)^2-\left(\frac{1}{T}\right)^2\right]s^2-\frac{k_ik_s}{T}^2}\right]\right.$$
$$\left.+\frac{s+\frac{1}{T}}{s^2+\frac{s}{T}+(\frac{k_pk_s}{T}s+\frac{k_ik_s}{T})e^{-\tau_d s}}\frac{(s^2+\frac{1}{T}s)\left(-s+\frac{1}{T}\right)}{s^4+\left[\frac{k_pk_s}{T}^2-\left(\frac{1}{T}\right)^2\right]s^2-\frac{k_ik_s}{T}^2}\right\}ds \qquad (D\text{-}7)$$

The required separation is then obtained by rewriting the integral for the cost functional in the manner demonstrated in D-8. Since the term in square brackets has been formed in such a manner that it is always zero when

$$s^2+\frac{1}{T}s+(\frac{k_pk_s}{T}s+\frac{k_ik_s}{T})e^{-\tau_d s}$$ is zero, it follows that this term will cancel as is demonstrated by D-8. Thus the desired separation has been obtained, in the sense that the first term in the integrand contains no poles of E(s) whereas the second term contains no poles of E(-s).

$$ISE = \frac{1}{2\pi i}\int_{-i\infty}^{i\infty}\left\{\frac{(\frac{k_p k_s}{T}s - \frac{k_i k_s}{T})\left(-s + \frac{1}{T}\right)e^{\tau_d s}}{\left(s^2 - \frac{1}{T}s + (-\frac{k_p k_s}{T}s + \frac{k_i k_s}{T})e^{\tau_d s}\right)\left\{s^4 + \left[\frac{k_p k_s}{T}^2 - \left(\frac{1}{T}\right)^2\right]s^2 - \frac{k_i k_s}{T}^2\right\}} + \frac{\left(s + \frac{1}{T}\right)(s^2 + \frac{1}{T}s)\left(-s + \frac{1}{T}\right)}{\left(s^2 + \frac{1}{T}s + (\frac{k_p k_s}{T}s + \frac{k_i k_s}{T})e^{-\tau_d s}\right)\left\{s^4 + \left[\frac{k_p k_s}{T}^2 - \left(\frac{1}{T}\right)^2\right]s^2 - \frac{k_i k_s}{T}^2\right\}}\right\}ds \qquad \text{(D-8)}$$

Since all the zeros of $s^2 + \frac{1}{T}s + (\frac{k_p k_s}{T}s + \frac{k_i k_s}{T})e^{-\tau_d s}$ lie in the left half of

the complex s-plane and all those of $s^2 - \frac{1}{T}s + (-\frac{k_p k_s}{T}s + \frac{k_i k_s}{T})e^{\tau_d s}$ lie in the

right half, it should now be possible to close the contour on the left for the first part of

the integrand, and on the right for the second part. In this way, it is then possible to avoid

the infinite number of poles of either E(s) or E(-s) that would otherwise occur. However,

before doing this, consideration must be given to the solution of Equation D-9, which is

a term in the denominator of Equation D-8.

$$s^4 + \left[\frac{k_p k_s}{T}^2 - \left(\frac{1}{T}\right)^2\right]s^2 - \frac{k_i k_s}{T}^2 = 0 \qquad \text{(D-9)}$$

The solution of Equation D-9 is,

$$
s_{1,2,3,4} = \pm \sqrt{ \frac{\left(\frac{1}{T}\right)^2 - \left(\frac{k_p k_s}{T}\right)^2 \pm \sqrt{\left(\left(\frac{1}{T}\right)^2 - \left(\frac{k_p k_s}{T}\right)^2\right)^2 + 4\left(\frac{k_i k_s}{T}\right)^2}}{2} }
\qquad (\text{D-10})
$$

Although these are not poles of the combined integrand, they are poles of the separate parts. Consequently before separating the integral and closing the contours, the contour form $-i\infty$ to $i\infty$ is first deformed in order to avoid passing through these points. Without loss of generality, this is achieved by indenting it to the left of zeros of Equation D-9 (Figure D-1). The contours are then closed, and it is noted that the contributions from the semi-circles at infinity are indeed zero. Moreover, the first integral contains no enclosed poles and, consequently, is identically zero. On the other hand,
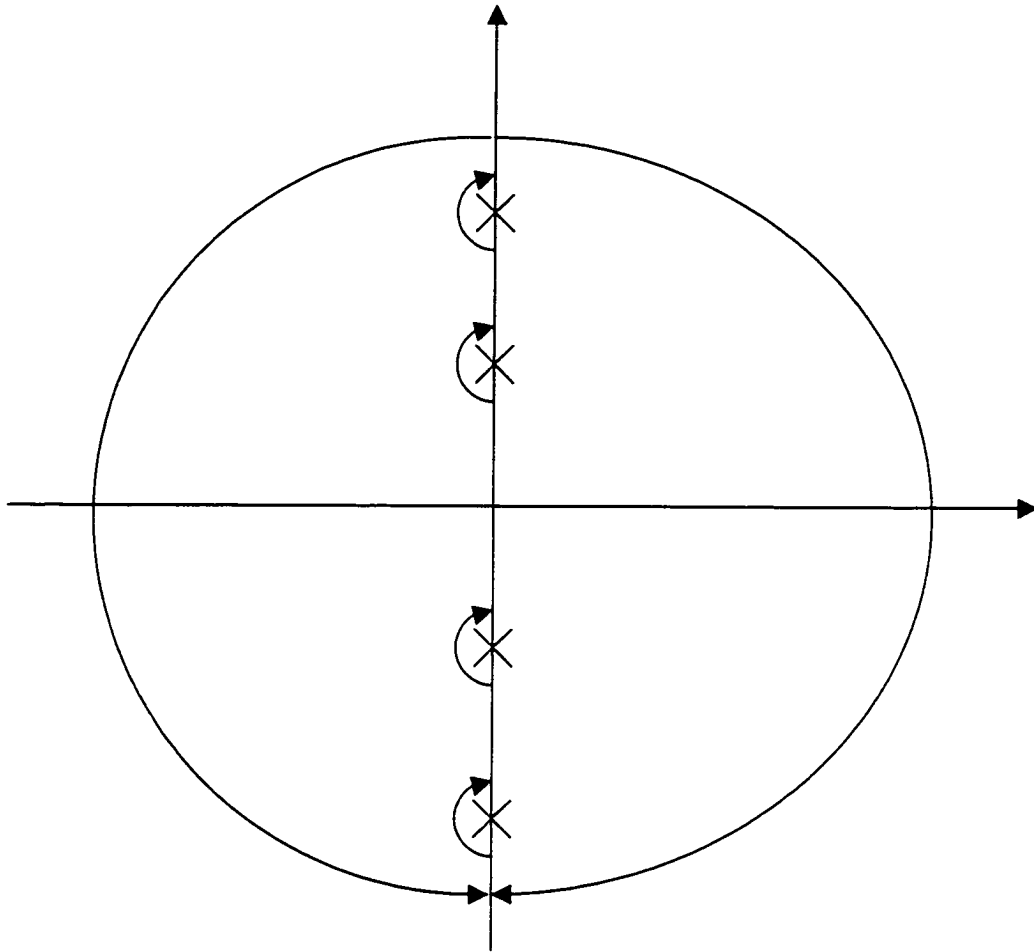
Figure D-1 *The separation techniques to calculate the cost function. The original integrand is separated into two parts. The contour for one part is on the right and the other part is on the left. The calculation of the cost functional is then reduced to evaluate the residues in four poles.*

the only enclosed poles of the second integral are those at zeros of Equation D-9.

Consequently, using the theory of residues

$$ISE = \sum_{r} \underset{s=s_r}{res} \left[\left(\frac{s + \frac{1}{T}}{s^2 + \frac{1}{T}s + (\frac{k_p k_s}{T}s + \frac{k_i k_s}{T})e^{-\tau_d s}} \right) \left(\frac{(s^2 + \frac{1}{T}s)\left(-s + \frac{1}{T}\right)}{s^4 + \left[\left(\frac{k_p k_s}{T}\right)^2 - \left(\frac{1}{T}\right)^2\right]s^2 - \left(\frac{k_i k_s}{T}\right)^2} \right) \right] \tag{D-11}$$

in which s=s$_r$, r=1, 2, 3, 4, is expressed in Equation D-10. Thus the problem has been reduced to evaluating residues at these four points.

The final solution of the cost functional is obtained after the calculation of D-10,

$$ISE = \begin{cases} \cfrac{1}{2\sqrt{\left(\left(\frac{k_s k_p}{T}\right)^2 - \left(\frac{1}{T}\right)^2\right)^2 + 4\left(\frac{k_s k_i}{T}\right)^2}} \\ \left[\left(\left(\frac{1}{T}\right)^2 - \rho^2\right)\cfrac{\frac{k_s k_i}{T} - \frac{1}{T}\frac{k_s k_p}{T} + \left(\left(\frac{1}{T}\right)^2 - \rho^2\right)\cosh(\rho\,\tau_d)}{\frac{k_s k_p}{T}\rho^2 - \frac{1}{T}\frac{k_s k_i}{T} - \rho\left(\left(\frac{1}{T}\right)^2 - \rho^2\right)\sinh(\rho\,\tau_d)} \\ \qquad + \left(\left(\frac{1}{T}\right)^2 + \sigma^2\right)\cfrac{\frac{k_s k_i}{T} - \frac{1}{T}\frac{k_s k_p}{T} + \left(\left(\frac{1}{T}\right)^2 + \sigma^2\right)\cos(\sigma\,\tau_d)}{\frac{k_s k_p}{T}\sigma^2 + \frac{1}{T}\frac{k_s k_i}{T} - \sigma\left(\left(\frac{1}{T}\right)^2 + \sigma^2\right)\sin(\sigma\,\tau_d)}\right] & when\,k_p \neq T\,k_i \\[2em] \cfrac{1}{2\sigma}\cfrac{1+\sin(\sigma\,\tau_d)}{\cos(\sigma\,\tau_d)} & when\,k_p = T\,k_i \end{cases}$$

(D-12)

where

$$\rho = \sqrt{\cfrac{\sqrt{\left(\left(\frac{k_s k_p}{T}\right)^2 - \left(\frac{1}{T}\right)^2\right)^2 + 4\left(\frac{k_s k_i}{T}\right)^2} + \left(\frac{1}{T}\right)^2 - \left(\frac{k_s k_p}{T}\right)^2}{2}}$$

$$\sigma = \sqrt{\cfrac{\sqrt{\left(\left(\frac{k_s k_p}{T}\right)^2 - \left(\frac{1}{T}\right)^2\right)^2 + 4\left(\frac{k_s k_i}{T}\right)^2} - \left(\frac{1}{T}\right)^2 + \left(\frac{k_s k_p}{T}\right)^2}{2}}$$

This Equation is same as Equation 2-6 in Chapter II.

VITA

Qianghua Zhou was born and brought up in Hunan, China. He finished high school in 1988. Then Hunan University enrolled him without examination due to his academic excellence. He got his B.S. degree in 1992 with the major of Heating, Ventilation and Air Conditioning (HVAC). He was selected to continue his graduate study in the HVAC major at Tsinghua University in the same year. This selection is based on a highly competitive examination. He got his M.S. Degree in 1995. He stayed at Tsinghua University to continue his research for the International Energy Agency Annex 25 (fault detection and diagnosis) after his graduation. He came to Texas A&M University in 1996. He worked for the Energy System Laboratory and obtained a Doctor of Philosophy in the Department of Mechanical Engineering in August 1999.

His permanent mailing address is:

Qianghua Zhou

Apt #704 in Maple BLD. #2

Changsha, Hunan 410082

P. R. China